

University College London

The use of matrix attachment regions to enhance the in-vivo potency of rAAV vectors

PhD Thesis

Joanna Evette Hanley

DECLARATION

I, Joanna Evette Hanley, confirm that the work presented in this thesis is my own. Where information has been derived from other sources, I confirm that this has been indicated in this thesis.

Signed: Joanna Hanley

Date: 06/03/2014

ABSTRACT

Adeno-associated virus vector encoding codon optimised human factor IX (AAV-LP1-hFIXco) has demonstrated great promise for the treatment of patients with severe haemophilia B. However, in some patients treated with a high vector dose, hepatocellular toxicity was observed. To improve AAV vector potency, various scaffold/matrix attachment regions (S/MARs) were cloned at the 3' end of a modified single-stranded (ss) AAV-LP1-hFIXco expression cassette. In a head to head comparison, a vector containing a S/MAR element from the human hypoxanthine-guanine phosphoribosyl-transferase gene in the forward orientation (ssAAV-LP1-hFIXco-HPRT-F) was found to mediate the highest levels of hFIX expression in mice. In comparison to animals transduced with a control vector containing no S/MAR, the ssAAV-LP1-hFIXco-HPRT-F transduced cohort expressed hFIX at 28-fold higher levels. This trend was reproducible in rhesus macaques where 10-fold higher FIX levels were observed following transduction with ssAAV-LP1-hFIXco-HPRT-F as compared to delivery of ssAAV-LP1-hFIXco-control vector. Through a deletion analysis, short regions from the IFN β and HPRT S/MARs with potent enhancer activity were identified. This allowed for the *in-silico* elicitation of motifs with a potential role in S/MAR function and also minimised the space occupied by S/MARs within our AAV expression cassette. When cloned into a self-complementary (sc) AAV-LP1-hFIXco expression cassette, the 130bp region from the HPRT S/MAR (fragment 2b) was sufficient to enhance FIX levels in mice by 35-fold over that observed with a control self-complementary vector. Mechanistic studies showed that S/MAR elements enhanced AAV transgene expression by reducing heterochromatin marks (H3K9me2 and HP1 α) in the promoter region, resulting in an increase in FIX mRNA levels by up to 20-fold. S/MARs therefore provide a novel inbuilt process for enhancing AAV mediated transgene expression by preventing epigenetic silencing of the provirus. As such, S/MARs offer the possibility to improve gene transfer to humans through using lower and potentially safer doses of AAV.

ACKNOWLEDGMENTS

I would like to thank my supervisor, Professor Amit Nathwani, for giving me the opportunity to carry out my PhD in his research group and for his expert guidance and help towards this thesis. I have learnt so much over the past four years and this would not have been possible without the advice of such a brilliant mentor. A special thank you must also go to Cecilia Rosales and Jenny McIntosh for their constant support and contribution towards my research. I would also like to thank my colleagues and good friends Marco Della Peruta, Gordon Cheung, Maria Virgilio, Christopher Allen, Marc Davies, Pollyanna Goh, Doyoung Lee, Arnold Pizzey, Deepak Raj, Allison Dane and Gabrielle To for their help and for making my PhD studies such a pleasant experience. Thank you also to Allison Dane, Deepak Raj and Marc Davies for all the proof reading. Last but most definitely not least, I would like to thank my family for their love and support through the more stressful times. To my late father, John Eric Hanley, I would like to say thank you for encouraging me to always believe in my abilities.

TABLE OF CONTENTS

TITLE PAGE.....	1
DECLARATION	2
ABSTRACT.....	3
ACKNOWLEDGMENTS.....	4
TABLE OF CONTENTS.....	5
TABLE OF FIGURES	9
LIST OF TABLES.....	11
COMMONLY USED ABBREVIATIONS	12
CHAPTER 1 INTRODUCTION	15
1.1 Haemophilia B.....	15
1.2 Gene therapy using adeno-associated virus.....	16
1.3 Improving vector potency.....	24
1.3.1 The AAV transduction pathway	24
1.3.2 Capsid modifications.....	28
1.3.2.1 Changing serotype/transcapsidation	28
1.3.2.2 Hybrid capsids	29
1.3.2.3 Epitope tagging	29
1.3.2.4 Immune escape capsids	29
1.3.2.5 Empty capsid decoys.....	30
1.3.2.6 Capsids that bypass cellular blocks.....	31
1.3.2.7 Critique of capsid modifications	32
1.3.3 Cassette optimisation	32
1.3.3.1 Self complementary vectors	32
1.3.3.2 Promoter selection	33
1.3.3.3 Codon-optimisation	34
1.4 Repeat induced gene silencing	35
1.5 Scaffold/Matrix Attachment Regions.....	38
1.6 Research aim.....	43
1.7 Brief outline of strategy:	43
CHAPTER 2 MATERIALS AND METHODS	46
2.1 Molecular biology	46
2.1.1 Reagents.....	46

2.1.2 Polymerase chain reaction (PCR)	47
2.1.3 Restriction enzyme digests	47
2.1.4 Agarose gel electrophoresis.....	48
2.1.5 Klenow fill-in	49
2.1.6 Alkaline phosphatase treatment.....	49
2.1.7 Ligations	49
2.1.8 Bacterial Transformation and expansion of Colonies	50
2.2 Vector production.....	51
2.2.1 Reagents.....	51
2.2.2 Triple transfection of HEK293T cells	52
2.2.3 Virus purification by affinity chromatography.....	53
2.2.4 Vector titration by Q-PCR.....	56
2.2.5 Vector titration by alkaline gel.....	56
2.2.6 Coomassie Stain of Capsid Proteins	58
2.3 Animal studies.....	61
2.4 Assessment of human factor IX (hFIX) antigen levels	61
2.4.1 Reagents.....	61
2.4.2 Transfection of HuH7 cells	63
2.4.3 Transduction of HuH7 cells with AAV2/8 vectors	63
2.4.4 Human Factor IX enzyme-linked immunosorbent assay (ELISA).....	64
2.4.5 Factor IX immunoprecipitation	67
2.4.6 Western blotting	67
2.4.7 Proviral copy number correction	69
2.5 Assessment of S/MAR function.....	70
2.5.1 Reagents.....	70
2.5.2 Determination of hFIX mRNA levels.....	70
2.5.3 Chromatin immunoprecipitation	71
CHAPTER 3 SCAFFOLD/MATRIX ATTACHMENT REGIONS ENHANCE THE <i>IN-VIVO</i> POTENCY OF AAV VECTORS	74
3.1 Introduction	74
3.1.1 AAV genomes are maintained as episomal chromatin	74
3.1.2 Histone deacetylase inhibitors (HDAC inhibitors) enhance AAV mediated transgene expression.....	75
3.1.3 The use of matrix attachment regions in gene transfer	76

3.1.4 Preliminary results	77
3.1.5 Chapter aim.....	80
3.2 Materials and methods	80
3.2.1 AAV-hFIX vector production and purification	80
3.2.2 Animal studies.....	81
3.2.3 HuH7 cell culture and transduction	82
3.2.4 Determination of FIX levels.....	82
3.2.5 Molecular studies.....	82
3.3 Results.....	83
3.3.1 <i>In-vitro</i> transduction analysis.....	83
3.3.2 Incorporation of HPRT and ApoB S/MARs in AAV expression cassettes enhances transgene expression <i>in-vivo</i>	84
3.3.3 hFIX mRNA analysis.....	89
3.3.4 HPRT S/MAR element enhances transgene expression at lower vector doses	89
3.3.5 Higher transgene expression with ssAAV8-LP1-hFIXco-HPRT-F and ssAAV8-LP1-hFIXco-IFN-R in nonhuman primates.....	93
3.4 Discussion.....	95
CHAPTER 4 MATRIX ATTACHMENT REGION DELETION ANALYSIS.....	99
4.1 Introduction	99
4.1.1 Recombinant AAV packaging capacity.....	99
4.1.2 Identifying regulatory sequences in S/MARs.....	103
4.2 Materials and methods	104
4.2.1 AAV-hFIX vector production and purification	104
4.2.2 Animal studies.....	106
4.2.3 HuH7 cell culture and transduction	107
4.2.4 Determination of FIX levels.....	107
4.2.5 Molecular studies.....	107
4.3 Results.....	108
4.3.1 Deletion analysis of IFN- β S/MAR identifies a smaller region with potent enhancer activity.....	108
4.3.2 Deletion analysis of HPRT S/MAR identifies a smaller region containing core enhancer activity.....	114
4.3.3 HPRT Fragment 2b enhances transgene expression in self-complementary vectors.....	120
4.4 Discussion.....	124

CHAPTER 5 THE FUNCTION OF MATRIX ATTACHMENT REGIONS IN AAV EXPRESSION CASSETTES.....	127
5.1 Introduction	127
5.1.1 The role of S/MARs in preventing transcriptional gene silencing.....	127
5.1.2 Polycomb group (PcG) complexes are recruited during RNAi based silencing...	129
5.1.3 S/MAR binding proteins are involved in chromatin remodelling	130
5.2 Materials and methods	131
5.2.1 Chromatin immunoprecipitation	131
5.3 Results.....	131
5.3.1 S/MARs confer higher transgene expression through epigenetic modification of the ssAAV-LP1-hFIXco genome	131
5.3.2 Preliminary mechanistic data.....	134
.....	137
5.4 Discussion.....	138
CHAPTER 6 CONCLUSIONS AND FUTURE DIRECTIONS	141
Bibliography	152

TABLE OF FIGURES

Figure 1.1: Schematic of the AAV transduction pathway.	27
Figure 1.2: Silencing of inverted repeat arrays through RNA interference (RNAi).	37
Figure 1.3: Cruciform formation.	42
Figure 1.4: Schematic of the single stranded rAAV cassette.	45
Figure 2.1: A typical AAV8 purification chromatogram.	55
Figure 2.2: Typical QPCR traces and standard.	59
Figure 2.3: Gel based titration of AAV8.	60
Figure 2.4: A typical hFIX ELISA standard curve.	66
Figure 3.1: Construction of single stranded AAV-hFIXco containing IFN β S/MAR: Schematic of vectors.	78
Figure 3.2: FIX expression in C57BL/6 mice.	79
Figure 3.3: Construction of single stranded AAV-hFIXco vectors containing S/MAR elements.	85
Figure 3.4: Transgene expression in HuH7 cells.	86
Figure 3.5: Transgene expression in C57BL/6 mice.	87
Figure 3.6: Proviral copy number correction.	88
Figure 3.7: FIX mRNA levels in liver.	90
Figure 3.8: FIX expression in male C57BL/6 mice: low dose analysis.	91
Figure 3.9: Proviral copy number correction.	92
Figure 3.10: Higher potency of S/MAR containing vector in nonhuman primates.	94
Figure 4.1: Split AAV Vector Strategies.	101
Figure 4.2: Schematic of a self-complementary AAV vector.	102
Figure 4.3: Construction of single stranded AAV-hFIXco vectors containing truncated IFN β S/MAR fragments.	110
Figure 4.4: Transgene expression in HuH7 cells.	111
Figure 4.5: Transgene expression in C57BL/6 mice.	112
Figure 4.6: Proviral copy number correction.	113
Figure 4.7: Construction of single stranded AAV-hFIXco vectors containing truncated HPRT S/MAR fragments.	116
Figure 4.8: Transgene expression in HuH7 cells.	117
Figure 4.9: Transgene expression in C57BL/6 mice.	118

Figure 4.10: Proviral copy number correction.	119
Figure 4.11: Transgene expression in HuH7 cells.	121
Figure 4.12: HFIX levels in C57BL/6 mice.	122
Figure 4.13: Proviral copy number correction.	123
Figure 5.1: Cytosine methylation profiles of the AAV LP1 promoter revealed by bisulphite sequencing.	128
Figure 5.2: Epigenetic modification of ssAAV-LP1-hFIXco proviral DNA.....	133
Figure 5.3: ChIP analysis on ssAAV-LP1-hFIXco-Control and ssAAV-LP1-hFIXco-HPRT-F chromatin.	134
Figure 5.4 Preliminary nucleolin ChIP analyses.	136
Figure 5.5: Preliminary EZH2 ChIP analyses.	137
Figure 6.1: Schematic of the GENECAPP protocol.	145
Figure 6.2: Schematic of conditional Dicer knockouts.....	146
Figure 6.3: Schematic of protein binding microarrays (PBMs).	149
Figure 6.4: Generation of incremental truncation libraries.....	150

LIST OF TABLES

Table 1: Summary of tissue tropism for AAV serotypes 1-9	21
Table 2: Summary of AAV transduction limitations and solutions.	25
Table 3: Summary of cell surface receptors for AAV serotypes 1-9	26
Table 4: Summary of the role of S/MAR elements.	41

COMMONLY USED ABBREVIATIONS

AAV	Adeno-associated Virus
ApoB	Apolipoprotein B
ApoE	Apolipoprotein E
BUR	Base unpairing region
bp	Base pair
cDNA	Complementary deoxyribose nucleic acid
ChIP	Chromatin immunoprecipitation
CMV	Cytomegalovirus
CNS	Central nervous system
CUE	Core unwinding element
DMEM	Dulbecco's modified eagle medium
DNA	Deoxyribose nucleic acid
dsRNA	Double stranded ribose nucleic acid
ELISA	Enzyme-linked immunosorbent assay
EZH2	Enhancer of zeste homolog 2
FIX	Coagulation factor nine
GFP	Green fluorescent protein
GO	Gene ontology
GOMO	Gene ontology for motifs
hAAT	Human α -antitrypsin
HCR	Hepatic control region
HDAC	Histone deacetylase
hFIX	Human coagulation factor nine
HMG	High mobility group
HPRT	Hypoxanthine-guanine phosphotidylribosyl-transferase
HSC	Haematopoietic stem cell

HSPG	Heparin sulphate proteoglycan
IFNβ	Interferon β
ITR	Inverted terminal repeat
Kb	Kilobase
KDa	Kilodalton
Kg	Kilogram
KSHV	Kaposi sarcoma herpes virus
LCA	Leber's congenital amaurosis
MCS	Multiple cloning site
MEME	Multiple expectation maximisation for motif elicitation
MOI	Multiplicity of infection
mRNA	Messenger ribose nucleic acid
MVM	Minute virus of mice
NAbs	Neutralising antibodies
NHP	Nonhuman primate
NM	Nuclear matrix
nm	Nanometer
nt	Nucleotide
ORF	Open reading frame
PBM	Protein binding microarray
PcG	Polycomb group
PCR	Polymerase chain reaction
PTGS	Post transcriptional gene silencing
PWM	Position weight matrix
rAAV	Recombinant adeno-associated virus
QPCR	Quantitative polymerase chain reaction
RIGS	Repeat induced gene silencing

RISC	RNA induced silencing complex
RITS	RNA induced initiation of transcriptional gene silencing complex
RNA	Ribose nucleic acid
RNAi	Ribose nucleic acid interference
RT-PCR	Reverse transcription polymerase chain reaction
RU	Relative units
SAF-A	Scaffold attachment factor-A
SAHA	Suberoylanilide hydroxamic acid
SATB1	Special AT-rich sequence binding protein 1
SCID	Severe combined immunodeficiency
SEM	Standard error of the mean
SIDD	Stress induced duplex destabilisation
siRNA	Small interfering ribose nucleic acid
S/MARS	Scaffold/matrix attachment regions
SWI/SNF	SWItch Sucrose NonFermentable complex
TGS	Transcriptional gene silencing
trs	Terminal resolution site
UTR	Untranslated region
vg	Vector genomes
wt	Wild type

CHAPTER 1 INTRODUCTION

1.1 Haemophilia B

Haemophilia B is a genetic bleeding disorder characterised by the absence of a functional plasma protein known as coagulation Factor IX (FIX). The disease is transmitted as an X-linked recessive disorder, due to mutation at Xq27.1, with an incidence of 1 in 25000 male births (Ljung *et al*, 1990). Due to non-random X chromosome inactivation, females can occasionally demonstrate markedly low FIX levels but are typically carriers of the disorder only (Kasper & Buzin, 2009).

Factor IX plays a central role in the coagulation cascade and is required for the activation of Factor X in partnership with activated Factor VIII. In the absence of active Factor X, thrombin formation is significantly impaired. As thrombin is required for platelet activation and the generation of fibrin, deficiency of FIX results in aberrant blood clot formation which subsequently allows for haemorrhage after only minimal trauma (Cancio *et al*, 2013). In Haemophilia patients, excessive deep bleeding into the joints and muscle is characteristic and can eventually lead to debilitating arthropathy.

Based on the quantity of active FIX present in patient plasma, the bleeding phenotype can be classified as mild, moderate or severe. Those with a severe phenotype demonstrate active FIX levels of $\leq 1\%$ of normal physiological levels whilst moderate and mild phenotypes corresponds to FIX levels of 1-5% and 5-40% of normal values respectively. A severe phenotype is apparent at infancy with haemorrhage often occurring spontaneously irrespective of prophylactic use of FIX protein concentrates. In contrast, for excessive bleeding to occur, those with a mild or moderate phenotype must usually be challenged by severe or mild trauma respectively (Cancio *et al*, 2013).

In the early 1980s the first cloning of the human FIX gene led to the generation of recombinant FIX concentrates that later received US Food and Drug Administration (FDA) approval (Kurachi & Davie, 1982). This development has crucially enabled prophylactic administration of FIX protein to patients. As a result, the health and life expectancy of those with haemophilia B has significantly improved. However, as patients with a severe phenotype typically require multiple infusions per week and bleeding is still known to occur in spite of prophylactic therapy, current treatment is not without limitation.

To improve upon this matter, several gene therapy strategies have been designed with the aim of providing correct FIX gene copies to patients for long term correction of the disorder (Herzog *et al*, 1997; High *et al*, 2004b; High, 2011; Palmer *et al*, 1989). Most recently, patients with a severe phenotype have been successfully treated following transduction of the liver with a self-complementary adeno-associated virus (AAV) expressing human factor IX (Nathwani *et al*, 2011). However, in this trial, whilst patients treated with a high vector dose (2×10^{11} vector genomes (vg)/Kg) demonstrated the greatest improvement in FIX levels; they also showed a transient elevation in levels of serum aminotransferase which is indicative of liver toxicity. This transaminitis was believed to occur through immune mediated clearance of hepatocytes presenting AAV capsid antigens. As such, it has been recognised that vector potency must be increased to minimise the dose required for therapeutic effect and subsequently improve safety. This thesis herein describes a study designed to improve AAV vector potency in the context of the human FIX expression cassette previously used in the clinic.

1.2 Gene therapy using adeno-associated virus

Genetic disease represents a significant problem in human health and a substantial burden on the health care system. However, for many of the more common inherited disorders including sickle cell anaemia and cystic fibrosis, treatment options remain limited. The most obvious solution for the long term treatment of genetic diseases is gene therapy. This refers to the transfer of normal gene copies to an individual with a mutation in the gene being provided (High, 2011). Approximately 23 years ago, clinical gene therapy commenced in a trial for the treatment of children diagnosed with adenosine deaminase deficient severe combined immunodeficiency (ADA-SCID) (Blaese *et al*, 1995). Due to the safety demonstrated in these early trials, in recent years many gene therapy products have entered late phase testing and true gene therapeutics are beginning to materialise (Yla-Herttuala, 2012).

The main goal of gene therapy is to achieve sustained transgene expression at levels that are considered to be therapeutic. To accomplish this goal, current gene therapy appears to be focusing on two major approaches. In the first strategy, viral vectors that integrate their genomes into host DNA, such as lentiviruses and retroviruses, are used for the *ex-vivo* delivery of therapeutic genes to host cells (Bank, 1996). As vector genomes are maintained in the cells via integration, long term transgene expression can be achieved upon re-

infusion of transduced cells into patients. This strategy has been used for the successful treatment of ADA-SCID and X-linked adrenoleukodystrophy by transducing patient haematopoietic stem cells (HSCs) with retroviral or lentiviral vectors carrying the gene of interest (ADA and ABCD1 respectively) (Aiuti *et al*, 2009; Cartier *et al*, 2009). More recently, by transducing patient HSCs with a lentiviral vector expressing the arylsulfatase gene (ARSA), Luigi Naldini's group demonstrated the ability to safely and effectively treat patients with late infantile metachromatic leukodystrophy (MLD): a lysosomal storage disorder characterised by mass demyelination and neurodegeneration due to accumulation of the arylsulfatase substrate (sulfatide) in cells of the nervous system (Biffi *et al*, 2013). After re-infusion of treated cells, therapeutically relevant myeloid cells (enzyme-proficient CD14+ and CD15+ cells that are able to migrate to the CNS and scavenge stored sulfatide) taken from patient peripheral blood demonstrated greater than normal generation of ARSA as compared to cells taken from healthy donors. In contrast to older un-treated siblings, at 18 to 24 months follow up, the neurodegenerative disorder was not found to progress in any of the three patients who all demonstrated continuous motor and cognitive development and normal brain MRI. Using this strategy, the same group also demonstrated the ability to effectively treat patients with Wiskott-Aldrich syndrome (WAS) (Aiuti *et al*, 2013). Following re-infusion of patient HSCs transduced with a lentiviral vector expressing WAS protein (WASP), all three patients enrolled in this phase I/II trial demonstrated improved platelet counts and protection from the severe infection, bleeding and eczema that characterises this primary X-linked immunodeficiency.

In the second strategy, post mitotic tissues such as skeletal muscle, central nervous system (CNS) and liver are transduced with non integrating vectors such as adenovirus and adeno-associated virus (AAV) (Ehrhardt *et al*, 2008). As these tissues do not divide rapidly episomal/non-integrated vector genomes are stabilised and transgene expression can be maintained long term. One of the greatest success stories for this strategy includes the use of AAV vectors expressing the RPE65 gene to transduce the retina of patients diagnosed with Leber's congenital amaurosis (Bainbridge *et al*, 2008; Maguire *et al*, 2008). For example, in a 2009 trial, subretinal injection of an AAV-RPE65 vector at a dose range of 1.5×10^{10} to 1.5×10^{11} vector genomes (vg) was well tolerated in all patients with the greatest improvements observed in children who all gained ambulatory vision (Maguire *et al*, 2009). More recently, rAAV has been used to successfully treat patients with advanced heart failure (HF) through delivery of the SERCA2a gene involved in myocyte contraction (Jessup *et al*, 2011). In the Calcium Up-regulation by Percutaneous Administration of Gene Therapy

in Cardiac Disease (CUPID) trial, HF patients received a serotype one rAAV vector expressing the SERCA2a gene at either a high (1×10^{13} vg) intermediate (3×10^{12} vg) or low (6×10^{11} vg) dose via intracoronary infusion. At 12 months follow up, patients in the high dose group met the criteria for clinical efficacy in terms of maximal rate of oxygen consumption (VO_2 -max), reduced N-terminal prohormone brain natriuretic peptide levels (a HF biomarker), left ventricular end-systolic volume and decreased frequency of cardiovascular events. As a result of this success, a further 200 patients will be recruited to a CUPID 2 phase 2b trial. All patients will be treated at the high vector dose that was previously shown to be efficacious (Sikkel *et al*, 2014).

Although substantial progress has been made in the field of gene therapy, vectors commonly used for gene transfer are not without their drawbacks. For instance, integration of vector genomes is associated with the risk of insertional mutagenesis. This was clearly demonstrated when X-linked SCID patients receiving HSCs transduced with retroviral vectors developed leukaemia (Cole, 2008; Hacein-Bey-Abina *et al*, 2003a; Hacein-Bey-Abina *et al*, 2003b). Non-integrating vectors also have their disadvantages, such as adenoviral vectors, which are highly immunogenic. The issues associated with such immunogenicity were clearly evident in pre-clinical studies for the treatment of Haemophilia B whereby rhesus macaques transduced with adenoviral vectors expressing coagulation factor IX (FIX) showed signs of hepatotoxicity due to destruction of transduced hepatocytes that was mediated by the cellular immunity (Lozier *et al*, 1999). In contrast, the adeno-associated virus demonstrates an improved safety profile.

Wild type AAV is a small, non-pathogenic, human parvovirus that depends on co-infection of a helper virus (e.g. adenovirus, papillomavirus or herpesvirus) for the completion of replication (Conway *et al*, 1997; Hoggan *et al*, 1966; Mueller & Flotte, 2008). The single stranded DNA genome of AAV is approximately 4.7kb in size and consists of two large open reading frames (*rep* and *cap*) flanked by 145bp t-shaped hairpin structures known as inverted terminal repeats (ITRs). The ITRs provide free 3' hydroxyl groups that prime second strand DNA synthesis and contain terminal resolution sites (*trs*) involved in the regulation of viral gene expression and genome encapsidation (Goncalves, 2005; Koczot *et al*, 1973). The 5' open reading frame (ORF) *rep* encodes four regulatory proteins (Rep78, Rep68, Rep52 and Rep40) that control replication and site specific integration of wild type viral genomes whilst the 3' ORF *cap* encodes the three structural proteins VP1 (90kDa),

VP2 (72kDa) and VP3 (60kDa) that form the multiple subunits of icosahedral AAV capsids in a 1:1:20 ratio (Berns & Linden, 1995; Rose *et al*, 1971).

Amongst vectors of viral origin, recombinant AAV (rAAV) vectors have several attributes that make them attractive for gene therapy:

- As ITR sequences are typically the only viral DNA elements retained in rAAV genomes, the absence of regulatory genes renders recombinant vectors replication defective and minimises the risk of host genome integration, with viral genomes persisting predominantly as concatemeric episomes (Smith, 2008).
- AAV vectors are regarded as non-pathogenic and are not associated with any known human diseases (Daya & Berns, 2008).
- AAV vectors can transduce both dividing and quiescent cells (Alexander *et al*, 1996).
- Multiple serotypes of AAV have been discovered and characterised in terms of capsid antigenicity (with the most well characterised designated AAV1-12) (Atchison *et al*, 1965; Bantel-Schaal & zur Hausen, 1984; Gao *et al*, 2004; Gao *et al*, 2002; Hoggan *et al*, 1966; Mori *et al*, 2004; Rutledge *et al*, 1998). As each serotype has a distinct tissue tropism and immunologic profile, changes in serotype can be exploited to avoid neutralising immune responses arising due to previous AAV exposure whilst also enabling some control over vector biodistribution (Table 1). For instance AAV8 and AAV1 efficiently transduce hepatocytes and muscle cells respectively (Nathwani *et al*, 2011; Stroes *et al*, 2008) while AAV2 has been used to transduce retinal cells for the successful treatment of Lebers congenital amaurosis (LCA)(Bainbridge *et al*, 2008; Maguire *et al*, 2009).
- In several animal models, the ability to achieve long term transgene expression in post mitotic tissues (including muscle, liver, brain and retina) has been established following a single infusion of rAAV. A broad range of disorders have now been targeted with rAAV including Duchene muscular dystrophy, Parkinson's disease, α -1-antitrypsin deficiency, LCA and Haemophilia B (Bainbridge *et al*, 2008; Flotte *et al*, 2004; Flotte *et al*, 2011; Kaplitt *et al*, 2007; Manno *et al*, 2006; Stedman *et al*, 2000).
- The successful use of rAAV in pre-clinical models has allowed for the transition of rAAV to many phase I/II clinical studies (Bainbridge *et al*, 2008; Flotte *et al*, 2004; Flotte *et al*, 2011; High *et al*, 2004a; Maguire *et al*, 2008; Nathwani *et al*, 2011;

Stroes *et al*, 2008). This includes trials for the treatment of patients with severe haemophilia B, which will be discussed in the following paragraphs.

Table 1: Summary of tissue tropism for AAV serotypes 1-9.

AAV Serotype	Tissue tropism
1	Skeletal muscle (Stroes <i>et al</i> , 2008), CNS (Wang <i>et al</i> , 2003), pancreas (Loiler <i>et al</i> , 2005)
2	Skeletal muscle(Manno <i>et al</i> , 2003), CNS (Bartlett <i>et al</i> , 1998), liver (Koeberl <i>et al</i> , 1997), kidney (Takeda <i>et al</i> , 2004)
3	Skeletal muscle (Chao <i>et al</i> , 2000)
4	CNS (Davidson <i>et al</i> , 2000), retina (Weber <i>et al</i> , 2003)
5	Skeletal muscle(Chao <i>et al</i> , 2000), CNS (Davidson <i>et al</i> , 2000), retina (Maguire <i>et al</i> , 2009), liver (Nathwani <i>et al</i> , 2007)
6	Skeletal muscle (Blankinship <i>et al</i> , 2004), heart (Zincarelli <i>et al</i> , 2010), lung (Halbert <i>et al</i> , 2001)
7	Skeletal muscle (Gao <i>et al</i> , 2002), CNS (Taymans <i>et al</i> , 2007), retina (Allocca <i>et al</i> , 2007)
8	Liver (Nakai <i>et al</i> , 2005), skeletal muscle (Wang <i>et al</i> , 2005), retina (Allocca <i>et al</i> , 2007), pancreas (Nakai <i>et al</i> , 2005), heart (Wang <i>et al</i> , 2005), CNS (Taymans <i>et al</i> , 2007)
9	Skeletal muscle (Yue <i>et al</i> , 2011), liver (Vandendriessche <i>et al</i> , 2007), heart (Inagaki <i>et al</i> , 2006), CNS (Foust <i>et al</i> , 2009), lung (Bostick <i>et al</i> , 2007), kidney (Bostick <i>et al</i> , 2007)

Haemophilia B has long been one of the most extensively studied diseases in terms of gene therapy. This is because an increase in factor IX to only 1% of normal physiological levels is enough to convert a patient's phenotype from severe to mild (Ljung, 1999). In addition to this modest target, well defined coagulation assays and small and large animal models of the disease exist for ease of preclinical testing (Murphy & High, 2008). Using immunodeficient mice and a canine model of Haemophilia B, long term stable expression of coagulation factor IX (FIX) following intramuscular delivery of an AAV2-FIX vector was demonstrated. In this study stable FIX expression levels of 5-7% and 1-2% of normal were observed in mice and dogs respectively (Herzog *et al*, 1997; Herzog *et al*, 1999). However, as anti-hFIX neutralising antibodies were detected in dogs treated with higher vector doses, subsequent clinical investigation was limited to a dose of 1.5×10^{12} vg/injection site (Herzog *et al*, 2002; Manno *et al*, 2003). In addition to this limitation, the expression of collagen IV in human muscle prevents the release of FIX into the plasma (Schuettrumpf *et al*, 2005). This resulted in sub-therapeutic increments of human factor IX (hFIX) observed in each participant. Nonetheless, this study successfully demonstrated the safety of AAV mediated gene transfer to haemophilia B patients (with vector administration well tolerated in all participants at doses of up to 1.8×10^{12} vg/kg); thus a foundation for further clinical investigation was established.

Given the issues associated with FIX release from skeletal muscle, subsequent haemophilia B gene transfer trials have focused on transduction of the liver (Mount *et al*, 2002; Nathwani *et al*, 2011). Indeed, the liver is known to secrete FIX more efficiently than the muscle. Moreover, by pre-clinical evaluation in the haemophilic dog model, this approach was shown to promote FIX immune tolerance (Mingozzi *et al*, 2003). This work led to the clinical trial utilising a single stranded AAV2 vector expressing hFIX delivered via the hepatic artery (High *et al*, 2004a; Manno *et al*, 2006). Vector infusion of doses up to 2×10^{12} vg/kg was well tolerated in all patients and therapeutic hFIX levels of 3% to 11% were observed in patients receiving the high vector dose. However, hFIX expression was transient (lasting approximately 8 weeks) and began to decline in conjunction with a period of transaminitis. As greater than 70% of humans are AAV2 positive, liver injury was found to be mediated by memory T cell responses against hepatocytes presenting AAV2 capsid antigens (High *et al*, 2004a; High *et al*, 2004b). Thus the need to use alternative serotypes of vector or to implement an immunomodulatory regimen was recognised (Manno *et al*, 2006).

As previously described, improved tropism to the liver has been well documented with capsid serotype 8 (Nakai *et al*, 2005; Nathwani *et al*, 2011). Furthermore, there is a lower seroprevalence of antibodies to this capsid in the human population as compared to AAV2 (Boutin *et al*, 2010). Preclinical studies in nonhuman primates using serotype 8 vectors demonstrated great promise with stable FIX levels of 22% to 26% of normal achieved following liver transduction at a dose of 1×10^{12} vg/kg (Nathwani *et al*, 2007). Crucially this success was achieved in the clinical setting, with four out of six participants able to discontinue FIX prophylaxis while the other two received prophylactic injections at greater intervals (Nathwani *et al*, 2011). Such clinical success has been attributed to three important advances in vector design. Firstly, a codon-optimised Factor IX (FIXco) expression cassette was generated for improved transgene expression. Secondly, the self complementary format of the AAV genome allowed complementary positive and negative DNA strands to be packaged within the same virion, circumventing the inefficient process of second strand synthesis (McCarty *et al*, 2003; McCarty *et al*, 2001). Finally, vectors were pseudotyped with serotype 8 capsids in order to evade an immune response against capsid proteins previously reported with AAV2 (Mingozzi *et al*, 2007; Pien *et al*, 2009; Vandenberghe *et al*, 2006). As AAV8 is liver-tropic, non-invasive infusion of the vector via the peripheral vein was also made possible by the switch in capsid serotype. However, as observed in other previous trials, to achieve therapeutically relevant transgene expression high vector doses were required (High *et al*, 2004a; Nathwani *et al*, 2011).

In addition to putting pressure on vector production, the need for high MOIs (multiplicity of infection) of rAAV is associated with an increased risk of toxicity (Manno *et al*, 2006; Mingozzi *et al*, 2009). Indeed, whilst both participants that received the highest vector dose (2×10^{12} vg/kg) showed the greatest FIX expression (7-12% of normal), they also demonstrated elevated aminotransferase levels which is indicative of liver toxicity (Nathwani *et al*, 2011). In participant 5, aspartate aminotransferase and alanine aminotransferase reached levels of 143 and 202 IU per litre respectively by day 58 (maximum of normal range 37 and 41 IU per litre respectively) whilst in Participant 6, although liver enzyme levels remained within the normal range, aminotransferase levels approximately doubled by day 62 when compared to baseline. In both cases liver injury was suspected to be due to T-cell dependent immune-mediated clearance of hepatocytes in response to AAV8 capsid antigens.

In summary, rAAV vectors have demonstrated great promise in the field of clinical gene therapy. However, in some cases, high doses of vector are required to achieve therapeutic levels of gene expression. This is clearly demonstrated in clinical studies of factor IX gene transfer. The greater risk of toxicity associated with increased MOIs means that vector potency must be improved to render lower doses efficacious. Such improvements are achievable by first understanding the limitations of the AAV transduction pathway.

1.3 Improving vector potency

This next section will discuss the limitations imposed on AAV throughout the transduction pathway and will focus on capsid and expression cassette modifications that have been shown to overcome these limitations (summarised in table 2). As such modifications improve vector potency; they represent major steps towards AAV dose minimisation which is a focal point of this study.

1.3.1 The AAV transduction pathway

Major steps of the AAV cellular transduction pathway include: 1) binding to cell surface receptors (listed in Table 3), 2) virion internalisation by endocytosis, 3) intracellular trafficking, 4) uncoating and release of viral genome 5) single stranded to double stranded conversion of viral DNA and 6) concatemerisation of double stranded genomes (Choi *et al*, 2005; Nonnenmacher & Weber, 2012). Known rate limiting steps of AAV infection include the low abundance/absence of required cell surface receptors, inefficient escape of virions from the endosome (resulting in lysosomal/proteasomal degradation) and the slow conversion of genomes to transcriptionally active double stranded forms (Figure 1.1) (Choi *et al*, 2005). As previously mentioned, neutralising immune responses against capsid proteins also represent a formidable challenge to successful AAV gene transfer. With these barriers in mind a number of rationally modified rAAV capsids and genomes have been engineered with the overall aim of enhancing vector potency.

Table 2: Summary of AAV transduction limitations and solutions.

Transduction Limitation	Potential Solution
Pre-existing immunity to capsid antigens	Change serotype Immune escape capsid mutations/epitope tagging
Low abundance/ absence of required cell surface receptors in target tissues	Change serotype Hybrid capsids Capsid epitope tagging
Inefficient endosome escape	Hybrid capsids Capsid tyrosine mutations
Slow single strand to double strand genome conversion	Self-complementary vectors
Limited expression levels	Change promoter Include additional cis-regulatory elements Codon optimisation

Table 3: Summary of cell surface receptors for AAV serotypes 1-9. - = undefined, HSPG= heparin sulphate proteoglycan, FGFR= Fibroblast growth factor receptor, HGFR= Hepatocyte growth factor receptor, LamR= Laminin receptor, PDGFR= Platelet derived growth factor receptor, EGFR= Epidermal growth factor receptor.

AAV Serotype	Primary Receptor	Co-receptors
1	N-linked sialic acid (Wu <i>et al</i> , 2006)	-
2	HSPG (Summerford & Samulski, 1998)	FGFR (Qing <i>et al</i> , 1999), HGFR (Kashiwakura <i>et al</i> , 2005), LamR (Akache <i>et al</i> , 2006), $\alpha_v\beta_5$ (Summerford <i>et al</i> , 1999), $\alpha_5\beta_1$ (Akache <i>et al</i> , 2006)
3	HSPG (Rabinowitz <i>et al</i> , 2002)	FGFR (Blackburn <i>et al</i> , 2006), HGFR (Ling <i>et al</i> , 2010), LamR (Akache <i>et al</i> , 2006)
4	O-linked sialic acid (Kaludov <i>et al</i> , 2001)	-
5	N-linked sialic acid (Kaludov <i>et al</i> , 2001)	PDGFR (Di Pasquale <i>et al</i> , 2003)
6	HSPG (Ng <i>et al</i> , 2010), N-linked sialic acid (Wu <i>et al</i> , 2006)	EGFR (Weller <i>et al</i> , 2010)
7	-	-
8	-	LamR (Akache <i>et al</i> , 2006)
9	N-linked galactose (Shen <i>et al</i> , 2011)	LamR (Akache <i>et al</i> , 2006)

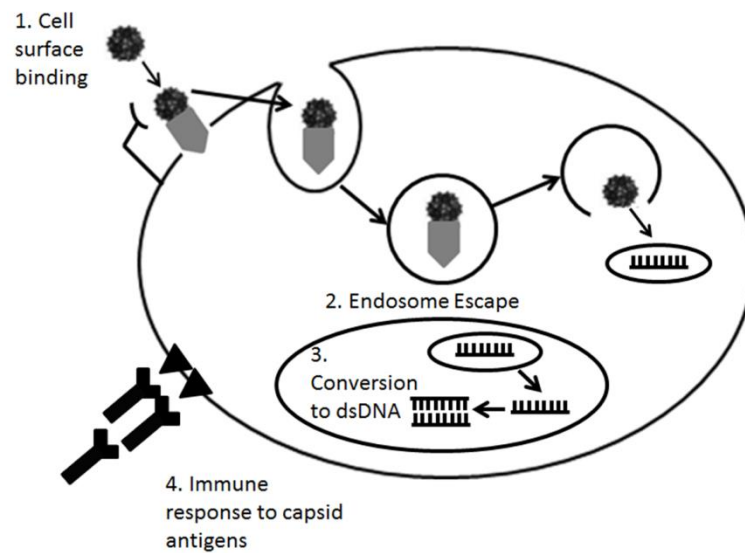


Figure 1.1: Schematic of the AAV transduction pathway. The major stages of AAV transduction are represented schematically including cell surface binding, endocytosis, endosome trafficking, nuclear transport, uncoating and double stranded conversion of vector genomes. Limiting stages of AAV gene transfer are highlighted with text. Adapted from: (Ding *et al*, 2005).

1.3.2 Capsid modifications

Multiple capsid modifications can be used to improve the potency of AAV vectors. This includes capsids that evade immune responses, improve the targeting of specific cell types or protect vectors from endosomal degradation. The use of such capsids and the ways in which they improve vector potency will be discussed in this section.

1.3.2.1 Changing serotype/transcapsidation

AAV2 was the first naturally occurring AAV isolate to be fully characterised (Hoggan *et al*, 1966). As a result, early AAV clinical trials focused heavily on the use of serotype 2 vectors. However, as previously described, in 2004 a phase I/II haemophilia B gene therapy study evaluating liver transduction with rAAV2 was closed due to unexpected toxicity (High *et al*, 2004a). These adverse events were believed to be due to pre-existing immunity against AAV2 capsid antigens (High *et al*, 2004b). Transcapsidation/pseudotyping refers to the packaging of AAV genomes containing ITRs from one serotype into the capsid of another serotype (Choi *et al*, 2005). As AAV2 ITRs are the most extensively studied they are frequently used for such cross-packaging whilst capsids alternative to serotype 2 are utilised to minimise the chances of invoking an immune response. Indeed in a study regarding the prevalence of total anti-AAV IgG for each serotype in a healthy human population, AAV2 and AAV1 antibodies were found to be most common (72 and 67% of the population respectively) with AAV9, 6, 5 and 8 antibodies demonstrating comparably lower seroprevalence (47, 46, 40 and 38% respectively) (Boutin *et al*, 2010). As such, the use of transcapsidation can improve AAV transduction efficiency by minimising the chances of neutralisation by pre-existing humoral immunity.

Additionally, changes in serotype can be exploited to selectively target tissues more effectively. For instance, vectors pseudotyped with AAV8 and rh.10 capsids have been found to transduce hepatocytes more effectively than AAV7 and 9 capsids at equivalent doses (Nathwani *et al*, 2009). This was determined by levels of hFIX transgene expression achieved following tail vein injection of each vector into 6-8 week old C57BL/6 mice. In these studies, at a dose of 4×10^{10} vg/kg, hFIX levels of $13 \pm 4 \mu\text{g/mL}$ and $12 \pm 2 \mu\text{g/mL}$ (approximately 250% of physiological levels) were observed 57 days after injection of AAV2/8 and 2/rh.10 cohorts respectively. These levels were substantially greater than that achieved with AAV2/9 and 2/7 vectors which gave hFIX levels of $7 \pm 3 \mu\text{g/mL}$ and $3 \pm 1 \mu\text{g/mL}$

respectively when administered at the same dose. Therefore, changes in serotype also allow for enhanced transduction efficiency by improving cell targeting.

1.3.2.2 Hybrid capsids

Further studies have demonstrated that AAV transduction can be improved by combining the attributes of two parental serotypes. Hybrid capsids can be produced by mixing plasmids encoding capsid proteins of different serotypes during vector production (Hauck *et al*, 2003). An example of the successful use of hybrid vectors was demonstrated by Jude Samulski's group through mixing of AAV1 and AAV2 capsid proteins (Rabinowitz *et al*, 2004). The resulting vector designated AAV1/2 was found to be capable of transducing the C2C12 mouse myoblast cell line which is known to be refractory to transduction with individual AAV1 or AAV2 vectors alone. The increased efficacy of transduction was believed to be due to the combined ability of AAV2 epitopes to bind heparin sulphate whilst AAV1 properties allowed for alternative trafficking of virions that prevented endosomal degradation. As such, hybrid capsids can improve the potency of AAV vectors by enhancing transduction of a target cell type whilst also preventing endosomal degradation.

1.3.2.3 Epitope tagging

By tagging rAAV capsids with specific epitopes, capsids can be engineered to target certain cell types more effectively. For example, by inserting a ligand derived from apolipoprotein E (ApoE) at the N-terminus of the VP2 protein, the resulting vector demonstrated 220-fold greater *ex vivo* transduction of low density lipoprotein receptor (LDL-R) expressing human islet cells as compared to unaltered rAAV2 (Loiler *et al*, 2003). Furthermore, as heparin sulphate proteoglycans (HSPGs) are present on all animal cell types, by carefully selecting the site of epitope insertion within the AAV2 capsid, HSPG binding can be ablated to improve tissue specificity: with prevention of HSPG binding known to be optimal by epitope insertion at positions 1 to 587 of the VP3 protein (Girod *et al*, 1999; Loiler *et al*, 2003; Nicklin *et al*, 2001; Opie *et al*, 2003).

1.3.2.4 Immune escape capsids

Through inserting peptides at capsid sites corresponding to known immunogenic epitopes, AAV vectors can be engineered to evade neutralising immune responses (Bartel *et al*, 2011). By screening AAV2 capsid mutants with a panel of polyclonal human sera, Hildegard

Büning's group observed that mutations at capsid position 534 or 573 significantly reduced antibody binding affinity (approximate 31% binding reduction in 42% of sera tested) (Huttner *et al*, 2003). Furthermore, by inserting a peptide that targets Mec1 cells at position 587, the same group demonstrated the ability of this mutant vector to effectively transduce target cells even in the presence of neutralising antisera. This observation suggests the possibility of simultaneously modulating cell tropism and immune neutralisation through a single peptide insertion (Huttner *et al*, 2003). Thus, epitope tagging can improve the potency of AAV vectors by enhancing specific cell targeting and by preventing immune responses.

1.3.2.5 Empty capsid decoys

It has recently been shown that the co-administration of empty AAV capsids, along with gene therapy vectors containing the transgene of interest, allows for neutralising anti-AAV antibodies (NAbs) to be titrated out in human serum in-vitro and in mice and nonhuman primate serum following intravascular delivery (Mingozzi *et al*, 2013). In this study, mouse models of anti-AAV response were immunised with human intravenous immunoglobulin (IVIg) 24 hours prior to administration of gene therapy vectors. AAV8 vectors expressing human FIX were injected intravenously at doses of 1×10^9 or 5×10^9 vg per animal with or without a 10X excess of empty AAV8 capsid. In naïve animals, FIX expression levels between groups receiving vector formulated in 10X empty capsids or PBS only were equivalent. However, in immunised animals, liver transduction was blocked when using gene therapy vector alone; whereas FIX expression was partially rescued in animals receiving vector combined with empty capsid (25% and 83% residual FIX expression at the low and high dose respectively). This approach was also successful in animals with higher AAV8 antibody titres of 1:10 and 1:100 when using a 50X and 100X excess of empty capsids respectively. Using an ELISA based assay to detect IgG-capsid immune complexes, this effect was shown to be implemented through absorption of NAbs by excess AAV capsid. As such, it was suggested that empty capsids act as decoys to protect AAV from neutralisation. This observation was recapitulated in rhesus macaques that are natural hosts of AAV8 and thus demonstrate neutralising activity. Following injection of 2×10^{12} vg/kg, monkeys receiving gene therapy vector only demonstrated undetectable or reduced levels of FIX (120-250ng/ml) when compared to animals receiving vector prepared in a 9X excess of empty capsid (300-450ng/ml).

By mutating the AAV2 capsid so that cell surface binding was disrupted, it was also demonstrated that empty; non-infective AAV capsids; which do not compete for cell entry and subsequently cannot cause antigen presentation; can be generated. However, the fact that professional antigen presenting cells are able to take up antigens without cell surface binding means that mutant empty capsids may indeed be immunogenic and, as a result, may enable immune mediated clearance of transduced cells. As such, this strategy may not overcome the limitation of T-cell responses to transduced hepatocytes that has been observed in humans. Furthermore, this approach was not found to be effective in mice with NAb titres exceeding 1:3000 even in the presence of 1000X excess empty capsids. As a result, this approach may not be beneficial in patients with higher antibody titres.

1.3.2.6 Capsids that bypass cellular blocks

As previously described, after entering the cell, AAV vector particles are processed through the endosomal compartment. By performing tyrosine-to-phenylalanine mutations of capsid residues, endosomal degradation of viral particles can be avoided by preventing capsid ubiquitination (Peters-Silva *et al*, 2009). Tyrosine mutants have indeed been accepted as viable tools for retinal gene therapy and have been shown to restore retinal function and visual behaviour in a mouse model of retinitis pigmentosa for at least 6 months after subretinal injection of AAV8 Y733F mutants expressing the PDE β gene (Pang *et al*, 2011).

Similar capsid mutations have also been utilised for liver transduction. In these studies, long term therapeutic gene expression of human coagulation factor IX (hFIX) was observed in a mouse model of Haemophilia B following administration of AAV2 Y730F and triple mutant AAV2 (Y444+500+730F) at doses previously reported to be subtherapeutic using non-mutant AAV2 vectors (Markusic *et al*, 2010). The use of capsid mutants in the liver crucially infers the feasibility of using these vectors in tissues that are less immune privileged than the eye. However, due to a lower seroprevalence in humans, AAV8 pseudotyped vectors still remain a stronger candidate for effective human liver transduction as compared to mutant AAV2. Indeed it is stated in the 2010 Markusic paper that tyrosine mutations are not thought to overcome the previously reported neutralizing immune responses to AAV2. Nonetheless tyrosine capsid mutations are a possible avenue of for improving vector potency by preventing degradation of viral particles.

1.3.2.7 Critique of capsid modifications

As demonstrated in previous literature, several modifications can be made to serotype 2 capsid proteins in order to enhance the potency of AAV2 vectors. This includes the insertion of epitopes to enhance binding to target cells or to avoid immune responses against capsid antigens. Although these modifications show great promise in AAV2, these results have not been reproduced in vectors of alternative serotypes, likely due to such modifications disrupting cell surface binding. For instance, in our unpublished data, we observed a decrease in liver transduction in mice when using an AAV8-FIX vector with mutated capsid tyrosine residues as compared to transduction using vectors with a wt AAV8 capsid. From these results one can speculate that these mutations resulted in the ablation of AAV8's natural liver tropism. Furthermore, due to a lower seroprevalence in humans, AAV8 pseudotyped vectors still remain a stronger candidate for effective human gene transfer as compared to mutant AAV2. In this study we aimed to test the potency of our AAV constructs by assessing expression of human factor IX following transduction of the liver. Serotype 8 was selected due to the strong liver tropism previously described. However, it should be noted that, contrary to previously mentioned literature reports, AAV9 has also been demonstrated as highly liver tropic (Vandendriessche *et al*, 2007). As capsid modifications have not been successfully used in serotype 8 vectors, mutant capsids were not used in this work. As such, we aimed to focus on expression cassette alterations.

1.3.3 Cassette optimisation

In addition to capsid modifications, vector potency can also be improved through alteration of the AAV expression cassette. This matter will be discussed in the following section with reference to the use of self-complementary vectors, cis-regulatory elements and codon-optimisation.

1.3.3.1 Self complementary vectors

As previously mentioned, single to double stranded conversion of AAV genomes is an essential step for generating transcriptionally active DNA forms. This complex process is

known to be a major rate limiting step for efficient gene expression. To overcome this limitation it is possible to generate a vector that delivers a duplex genome (McCarty *et al*, 2001). This is achievable by packaging complementary sense and antisense sequences within the same virion. The resulting so-called self-complementary genomes are single stranded inverted repeat sequences with a mutated ITR in the middle of the molecule. Deletion of a terminal resolution site (trs) from the central ITR means that the ITR can no longer act as a replication origin but is still capable of forming a hairpin structure. Thus upon uncoating, sense and antisense strands anneal by folding together at the hairpin to form transcriptionally active dimers (McCarty *et al*, 2003). With self-complementary vectors, stable hepatocyte transduction has been achieved at almost a log higher level than that observed with single stranded vectors at equivalent doses (Nathwani *et al*, 2009).

1.3.3.2 Promoter selection

Careful selection of promoters is important for obtaining high levels of transgene expression and for mediating tissue specific expression/preventing off target effects. In one example, to assess the potency of different promoters in the context of rAAV, Nathwani *et al* produced four vectors containing either the CMV (cytomegalovirus), MSCV (murine stem cell virus), CAGG (CMV enhancer/ β -actin promoter complex) or HBV (hepatitis B enhancer/core promoter complex) regulatory elements upstream of human factor IX (Nathwani *et al*, 2001). By portal vein injection, 1×10^{11} vg of each vector was administered to C57Bl/6 SCID mice. At 12 weeks post injection and thereafter FIX levels of approximately 10% of normal (506 ± 61 ng/mL) were observed in plasma samples from CAGG vector transduced mice. Expression from all other vectors was significantly lower (20-54 ng/mL) and southern blot analysis on genomic liver DNA showed that this difference was not due to variation in vector copy number. This suggests that careful selection of regulatory elements can enhance transgene expression. However, to restrict FIX expression to the liver, the use of a strong tissue specific promoter such as LP1 or HCR-hAAT is necessary.

A further example for the importance of cis-regulatory elements was provided by Mark Kay's group in 2000. In this study 20 μ g of retroviral hFIX plasmid constructs containing various regulatory sequences were delivered to C57BL/6 mice by tail vein injection (Miao *et al*, 2000b). By this analysis the ApoE-HCR-hAAT-FIXmg-bpA construct containing the ApoE hepatic locus control region, the human α antitrypsin promoter and the hFIX minigene (containing a portion of the first intron; the 3' untranslated region and the bovine growth

hormone polyA) demonstrated the highest serum hFIX levels of up to 18µg/ml one day after injection. This was a striking 68.9±27.5 fold increase in transgene expression as compared to basal levels obtained from animals receiving an equivalent dose of the hFIX cDNA construct without internal promoters. This construct has also demonstrated high levels of *in-vivo* transgene expression when cloned into a single stranded AAV expression cassette (vector designated AAV-hFIX16) (High *et al*, 2004a; Mingozzi *et al*, 2003). Thus, when designing AAV vectors with improved potency, it is worth considering the incorporation of intronic and UTR (untranslated region) sequences as well as exploring various promoter-enhancer combinations.

When optimising a sequence for use in a mammalian expression vector, it is also worth considering the use of an optimal Kozak sequence for efficient initiation of translation. The sequence GCCRCCAUG (where R is a purine and AUG is the initiation codon) is known to be the optimal Kozak sequence for expression of proteins in mammalian organisms and cell lines and is frequently used in gene therapy vectors (Xia, 2007).

1.3.3.3 Codon-optimisation

Codon optimisation has previously been shown to significantly enhance protein production and therefore must be considered as an option during vector optimisation (Haas *et al*, 1996; Nathwani *et al*, 2006). Analysis of the human FIX (hFIX) cDNA sequence has revealed several genetic elements that may limit hFIX expression in mammals. This includes a low GC content, an RNA instability motif, a high frequency of rare codons and a cryptic splice donor site (Wu *et al*, 2008). Using GeneOptimizer software Paul Monahan's group successfully engineered a codon- optimised hFIX (hFIXopt) sequence by removing negative cis-acting features, changing codon usage bias to *Homo sapiens*, and increasing GC content from 41 to 61% (Wu *et al*, 2008).

Using a self-complementary AAV2 format the optimised vector was delivered to C57BL/6 mice via portal vein injection at doses ranging from 3×10^9 to 1×10^{11} vg/mouse. At all doses tested non-optimised self-complementary vectors mediated a moderate increase in hFIX levels (1.5-2.6 fold) as compared to a single stranded vector. In contrast markedly higher levels of hFIX were observed with the hFIXopt vector (5.5-21.2 fold increase as compared with single stranded AAV). Notably at the lowest dose of 3×10^9 vg, hFIX levels remained in a therapeutic range when using scAAV2- hFIXopt. This suggests that codon-optimisation can be exploited to enhance the potency of AAV at lower doses.

In summary various modifications to AAV expression cassettes can be exploited to enhance viral transduction efficiency (summarised in Table 2). As such, vectors used in this study contained the improved codon-optimised hFIX expression cassette previously used in the clinic (Nathwani *et al*, 2011). To achieve liver specific expression, this cassette contained the LP1 promoter that consists of core domains from the human apolipoprotein hepatic control region and the human alpha-1-antitrypsin promoter (Nathwani *et al*, 2006). These cis-regulatory components prevented off target effects whilst also enhancing expression.

However, studies of rAAV proviral DNA structure suggest that there may be yet another avenue of AAV biology that can be altered to enhance vector potency. In previous studies, AAV concatemers have been found to form chromatin like structures *in-vitro* and *in-vivo* (Marcus-Sekura & Carter, 1983; Penaud-Budloo *et al*, 2008). This would infer that AAV genomes have the potential to undergo epigenetic silencing. Furthermore, in mice, enhanced AAV mediated transgene expression has been observed following co-administration of histone deacetylase (HDAC) inhibitors. This suggests that AAV genomes are subject to association with histone proteins that prevent transcription (Okada *et al*, 2006). Nonetheless, the effects of epigenetic silencing on AAV concatemers still remain to be explored as a potential route of vector improvement. This matter will be approached in the following sections.

1.4 Repeat induced gene silencing

The epigenetic silencing of exogenous DNA sequences is a phenomenon known to occur following gene transfer. This concept, known as repeat induced gene silencing, may represent an additional limitation of rAAV mediated gene expression. Repeat induced gene silencing and the impact that it may have on the potency of rAAV will be discussed in this section.

The theory of repeat induced gene silencing (RIGS) suggests that transgenes arranged in multicopy concatemeric arrays are subject to epigenetic silencing (Garrick *et al*, 1998; Selker, 1999). The first evidence for the silencing of multicopy transgenic loci was discovered in plants by Jorgensen and Mol through the introduction of extra pigment producing genes into petunias (Jorgensen *et al*, 1996; Napoli *et al*, 1990; van der Krol *et al*, 1990). Following gene transfer, mosaic pigmentation or even completely white flowers

were observed as opposed to the anticipated deep purple colouration. This suggests not only the silencing of transgene copies but also the silencing of homologous endogenous sequences.

Gene silencing events of this nature often occur at the post transcriptional level and are believed to operate through an 'abberant RNA' based mechanism (Sharp, 2001). In 1999 Hamilton and Baulcombe made the breakthrough discovery that short stretches of RNA (approximately 25nt) of both sense and antisense polarity are detectable in plants in stringent association with the occurrence of post transcriptional gene silencing (PTGS) (Hamilton & Baulcombe, 1999). The generation of such RNA species is now known to occur through the accumulation of double stranded RNA (dsRNA) which is later 'cut' by the ribonuclease Dicer in order to form the short sequences now designated small interfering RNAs (siRNAs) (Bernstein *et al*, 2001). As the dsRNA generated is derived from the transcription of exogenous sequences, siRNAs are able to bind to corresponding mRNAs and transgenes through base complementation. Thus, siRNAs demonstrate the ability to bring their associated protein complexes, RNA induced silencing complex (RISC) and RNA induced initiation of transcriptional gene silencing complex (RITS), into contact with complimentary sequences for the degradation of mRNA by ribonucleases and silencing of transgenic loci via histone modifications (transcriptional gene silencing (TGS)) respectively (Moazed, 2009). Although at present the RITS complex has only been identified in fission yeast, fungi and fruit flies, it is believed that analogous silencing events exist in higher species including mammals. However, the exact mechanism of silencing and composition of protein complexes involved in mammals remains undefined (Ahlenstiel *et al*, 2012).

So how does this theory relate to the silencing of rAAV genomes? Where transgenes are arranged in arrays that give rise to inverted repeat sequences, dsRNAs are more readily generated due to the direct provision of adjacent complementary sense and antisense transcripts (Figure 1.2). In this situation the silencing of transgene expression is known to be enhanced (Muskens *et al*, 2000; Wolffe & Matzke, 1999). Consequently, in the context of rAAV, one can envisage a state whereby viral genomes concatamerise in orientations that generate palindromes. This would potentiate the production of dsRNAs for subsequent silencing of transgene sequences. Furthermore, as 3' ITR and PolyA sequences are often deleted, the potential for read-through transcription of AAV inverted repeats and subsequent dsRNA generation is increased (McLaughlin *et al*, 1988; Rutledge & Russell, 1997; Yang *et al*, 1997).

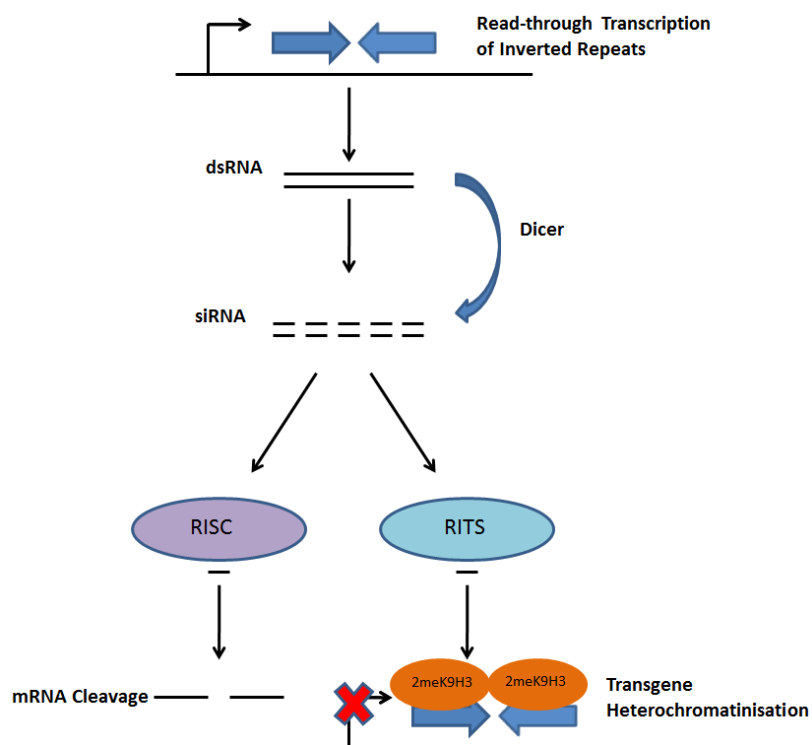


Figure 1.2: Silencing of inverted repeat arrays through RNA interference (RNAi). Through the direct provision of adjacent sense and antisense sequences, inverted repeats increase the potential for double stranded RNA formation. Double stranded RNAs are cut by the ribonuclease designated Dicer into small interfering RNAs (siRNAs). siRNAs then join with associated proteins to form complexes involved in mRNA cleavage and DNA heterochromatinisation of sequences complementary to the siRNA (RISC and RITS complexes respectively) with the overall effect of gene silencing.

Indeed this theory does serve to explain the nonlinear dose response and variagated/mosaic stable expression pattern observed in AAV transduced murine hepatocytes (Nakai *et al*, 2002). Furthermore, in non human primates, AAV vector genomes have been found to form chromatin like structures through assimilation with host DNA modifications (Leger *et al*, 2011). Concurrently in our group we have found that, following gene transfer, a proportion of exogenous sequences undergo heterochromatinisation (unpublished data).

The use of cis-regulatory elements that prevent gene silencing events may, therefore, improve the potency of rAAV vectors. For this reason we have developed single stranded AAV expression cassettes containing scaffold/matrix attachment regions (S/MARs).

1.5 Scaffold/Matrix Attachment Regions

The enhancer activity of S/MARs has been demonstrated in multiple gene transfer experiments using retroviruses, lentiviruses and plasmid DNA (Argyros *et al*, 2008; Dang *et al*, 2000; Kurre *et al*, 2003; Ramezani *et al*, 2003). As such, the incorporation of S/MAR elements into AAV expression cassettes may enhance vector potency and thus permit the use of lower doses. However, S/MARs have yet to be tested in the context of rAAV. The function of S/MARs in enhancing gene expression will be discussed in this section.

The nuclear matrix (NM) is defined as a network of proteinaceous filaments that constitute the framework of the cell nucleus (Berezney & Coffey, 1974). Branching filaments of the NM accommodate the formation of organised DNA domains as they provide a supporting structure for the attachment of chromatin loops (Mirkovitch *et al*, 1984). Furthermore, the NM acts as a hub of nuclear activity by tethering DNA into close proximity with proteins required for transcription, replication, RNA processing, RNA transport and recombination (Berezney *et al*, 1995).

Scaffold/matrix attachment regions play a fundamental role in genome organisation and co-ordination of expression from specific gene loci (summarised in table 4). They do so by serving as anchor points on DNA for the nuclear matrix and thereby place genes in close proximity to the aforementioned nuclear proteins required for gene expression (Ma *et al*, 1999). S/MARs generally consist of AT-rich regions found in the 5' or 3' flanking regions of genes, in introns, or at gene breakpoint cluster regions and, although S/MAR elements are

highly conserved across eukaryotic species, they do not contain any obvious consensus sequences. Instead S/MARs are defined by structural consensus as opposed to primary sequence (Argyros *et al*, 2011; Benham *et al*, 1997; Gluch *et al*, 2008).

For instance, a strong propensity to undergo DNA strand separation is a known property of S/MARs (Bode *et al*, 2006). Indeed S/MARs typically contain multiple base unpairing regions (BURs) that are readily detectable by chemical probing studies using reagents with a strong affinity for single stranded DNA (including potassium permanganate and chloroacetaldehyde) (Bode *et al*, 2000). The *In Silico* method known as Stress Induced Duplex Destabilisation (SIDD) also serves to map S/MARs through the prediction of the amount of energy (G) required to separate the DNA strand at any given base pair (X) under negative superhelical tension and in the context of the full sequence under analysis. Where less energy (G(X)) is required the probability of unpairing at that particular base position (P(X)) increases and so potent S/MAR sequences are identifiable as regions with low G(X) and high P(X) values (Benham *et al*, 1997; Bode *et al*, 2006).

Through such helix destabilization S/MARs are able to form their characteristic non-B DNA structures. For example, as S/MARs commonly contain palindromic sequences, DNA strand separation enables the formation of cruciform DNA (Figure 1.3) (Bode *et al*, 2000). Furthermore, S/MARs frequently contain sequences that allow for the formation of triple helical structures (including TG, TA, GC repeats and polypyrimidine/polypurine stretches) and DNA bending (oligod(A) stretches) (Boulikas, 1993).

It is these secondary structures that determine the association of S/MAR binding proteins. For instance, known S/MAR binding proteins include lamins (an NM component) and nucleolin (a histone chaperone protein), which recognise single-stranded DNA, and high mobility group proteins (HMG) that preferentially bind to cruciform structures (Kohwi-Shigematsu *et al*, 1998). The binding of proteins involved in histone distribution such as nucleolin and HMG-I/Y enables the associated DNA to be maintained in an open euchromatin state (Angelov *et al*, 2006; Bianchi & Agresti, 2005). As such, S/MAR sequences are thought to facilitate the initiation of transcription and thus enhance gene expression.

Additionally S/MARs can shield gene expression from position effects and/or block the action of distant enhancers thus serving as genetic insulators (Goetze *et al*, 2005). They also have origin of replication support functions which in the context of episomal vectors has

been shown to facilitate episome retention and replication in dividing mammalian cells (Baiker *et al*, 2000; Piechaczek *et al*, 1999; Schaarschmidt *et al*, 2004). For instance, the SV40 large T-antigen is a viral trans-acting factor required for replication of the SV40 episome. After deleting the large T-antigen gene from the SV40 genome and replacing it with a S/MAR element from the 5' region of the IFN β gene, rescue of SV40 episome replication has been demonstrated in-vitro with episomes retained at low copy numbers following successive cell divisions (Piechaczek *et al*, 1999).

Table 4: Summary of the role of S/MAR elements.

S/MAR Function	Mechanism
Prevention of silencing	<ul style="list-style-type: none">• Formation of partitioned looped domains• Insulation from positional effects
Increasing expression	<ul style="list-style-type: none">• High propensity for DNA strand separation facilitates access of proteins involved in transcription potentiation and chromatin remodelling
Stabilising expression	<ul style="list-style-type: none">• Anchoring chromatin to the nuclear matrix• Origin of replication complexes form at S/MAR regions

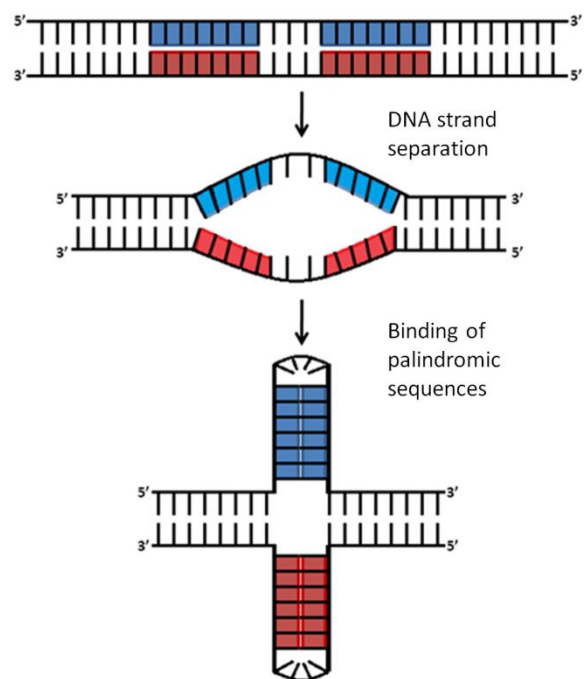


Figure 1.3: Cruciform formation. The ability for DNA strand separation to cause secondary structure formation is represented schematically. Strand separation at regions containing palindromic sequences enables binding of complementary sequences to form cruciform DNA.

1.6 Research aim

The aim of this project was to improve the potency of AAV vectors. As such, we hypothesised that the incorporation of matrix attachment regions into AAV expression cassettes would improve transgene expression by preventing epigenetic silencing. To address this matter we aimed to carry out a head to head comparison of multiple S/MARs in the single stranded AAV2/8 LP1-hFIXco format (Figure 1.4).

1.7 Brief outline of strategy:

S/MARs selected for head to head comparison in ssAAV8-LP1-hFIXco included regions from the human interferon- β (IFN- β), apolipoprotein B (apoB) and hypoxanthine-guanine phosphoribosyltransferase (HPRT) genes. Additionally, a region of the Kaposi sarcoma herpes virus (KSHV) genome known to promote autonomous replication was utilised as a non-S/MAR control element (Stedman *et al*, 2008). The IFN- β S/MAR has been shown to enhance transgene expression in multiple gene transfer vectors whilst the apoB S/MAR is well documented to have an insulatory role against positional chromatin effects (Namciu *et al*, 1998). Further to this, in the context of our AAV construct, the *in silico* approximation of energy required for unwinding (GX) is particularly low at the theoretical apoB S/MAR site. In contrast, the HPRT S/MAR has primarily been documented to have a role in autonomous replication (Sykes *et al*, 1988). In order to identify sequence regions required for enhancer activity and to minimise the space occupied by S/MARs within a given expression cassette, a deletion analysis was carried out on S/MAR sequences. The mechanism behind S/MAR activity was assessed by chromatin immunoprecipitation and RNA studies.

Strategy:

- S/MAR elements or fragments thereof were cloned into the pAV-LP1-hFIXco-SV40pA vector plasmid which was used for production of rAAV.
- The vectors were initially tested *in-vitro* prior to assessment *in-vivo* using the C57Bl/6 mouse model.
- HFIX expression levels were normalised for genome copy number in order to correct for discrepancy in transduction efficiency.
- This was followed by studies to establish the mechanisms responsible for augmentation of rAAV mediated transgene expression.

- To ascertain efficacy and safety across species promising vectors were tested in rhesus macaques.

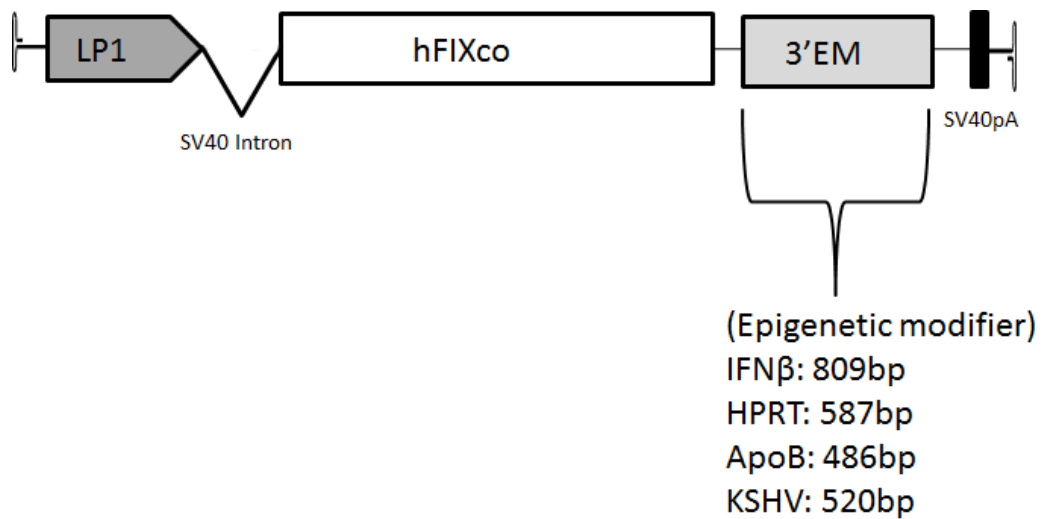


Figure1.4: Schematic of the single stranded rAAV cassette. All epigenetic modifiers (S/MAR elements) were cloned immediately 3' of codon optimised human Factor IX; upstream of a truncated SV40 poly A sequence. Expression was driven from the LP1 liver specific promoter.

CHAPTER 2 MATERIALS AND METHODS

Specific methods are discussed in the relevant results chapter

2.1 Molecular biology

2.1.1 Reagents

- HotStar Taq Plus DNA Polymerase (Qiagen, Crawley, UK)
- Phusion High-Fidelity DNA Polymerase (New England Biolabs UK Ltd, Hitchin, UK)
- Custom primers (Integrated DNA Technologies, Leuven, Belgium)
- Restriction enzymes (New England Biolabs UK Ltd, Hitchin, UK)
- NEBuffers 1-4 (New England Biolabs UK Ltd, Hitchin, UK)
- 100X BSA (New England Biolabs UK Ltd, Hitchin, UK)
- Molecular biology water (Sigma-Aldrich Company Ltd, Poole, UK)
- Agarose (Biolone, London, UK)
- Ethidium bromide (Sigma-Aldrich Company Ltd, Poole, UK)
- Tris base (VWR International Ltd, Lutterworth, UK)
- Boric acid (VWR International Ltd, Lutterworth, UK)
- Ethylenediaminetetraacetic acid (EDTA) (VWR International Ltd, Lutterworth, UK)
- Sucrose (Sigma-Aldrich Company Ltd, Poole, UK)
- Bromophenol blue (Sigma-Aldrich Company Ltd, Poole, UK)
- QIAquick Gel Extraction Kit (Qiagen, Crawley, UK)
- DNA Polymerase I, Large (Klenow) Fragment (New England Biolabs UK Ltd, Hitchin, UK)
- Calf Intestinal Phosphatase (New England Biolabs UK Ltd, Hitchin, UK)
- T4 DNA Ligase (New England Biolabs UK Ltd, Hitchin, UK)
- L-Broth capsules (MP Biomedicals, Cambridge, UK)
- Ampicillin (Melford Laboratories Ltd, Ipswich, UK)
- NEB 5-alpha Competent E.coli (High efficiency) (New England Biolabs UK Ltd, Hitchin, UK)
- pUC19 Vector (New England Biolabs UK Ltd, Hitchin, UK)
- SOC Outgrowth Medium (New England Biolabs UK Ltd, Hitchin, UK)
- NucleoSpin® Plasmid kit (Fisher Scientific, Loughborough, UK)

- Qiagen Plasmid Mega Kit (Qiagen, Crawley, UK)

2.1.2 Polymerase chain reaction (PCR)

Through amplification of specific plasmid DNA regions, PCR was used to generate short IFN β and HPRT S/MAR fragments. Using a Dyad[®] thermal cycler (BioRad Laboratories Ltd, Hemel Hempstead, UK) amplification was achieved by cycling between temperatures that enabled the denaturation of template DNA, annealing of sequence specific oligonucleotide primers, and extension of DNA polymerisation. All reactions were done in conjunction with a no template negative control to ensure no contaminating DNA was present. DNA polymerases used during this work included HotStar Taq DNA Polymerase (Qiagen, Crawley, UK) and Phusion High-Fidelity DNA Polymerase (New England Biolabs UK Ltd, Hitchin, UK).

The standard reaction mix for a 100 μ l PCR using HotStar Taq DNA Polymerase contained 10 μ l 10X PCR buffer (contains Tris.Cl, KCl, (NH₄)₂SO₄, 15 mM MgCl₂; pH 8.7), 0.5 μ M of each primer, 200 μ M of each dNTP, 2.5U HotStar Taq DNA Polymerase and 1 μ g DNA template. Standard cycling conditions used included an initial activation step of 95°C for 15 minutes followed by 35 cycles of denaturation at 94°C for 1 minute, annealing of primers for 1 minute and extension at 72°C for 1 minute. After the 35 cycles a final extension step was carried out at 72°C for 10 minutes.

The standard reaction mix for a 50 μ l PCR using Phusion High-Fidelity DNA Polymerase contained 10 μ l 5X Phusion HF buffer (containing 7.5 mM MgCl₂), 0.5 μ M of each primer, 200 μ M of each dNTP, 1U Phusion High-Fidelity DNA Polymerase and 250ng DNA template. Standard cycling conditions used included an initial denaturation step of 98°C for 30 seconds followed by 35 cycles of denaturation at 98°C for 5 seconds, annealing primers for 30 seconds and extension at 72°C for 15 seconds. After the 35 cycles a final extension step was carried out at 72°C for 10 minutes.

2.1.3 Restriction enzyme digests

Restriction enzyme digests were used to cut plasmid DNA at specific sites for subsequent molecular cloning experiments or to screen DNA extracted from transformed E.coli colonies

for the presence of desired plasmid constructs. All restriction enzymes and buffers used in this work were supplied by New England Biolabs UK Ltd (Hitchin, UK).

In addition to DNA the standard reaction mix for all restriction digests contained 10% 10X NEBuffer (buffer selection depended on the enzyme chosen) 1% 100X BSA (included only when required by the selected enzyme) and between 1% to 10% of the chosen restriction enzyme (depending on enzyme units and the amount of DNA to be digested). Final reaction volumes were made up with molecular biology water. Digests were carried out by heating the reaction mixes for 1 to 3 hours (dependent on the amount of DNA used) at 37°C using a Dyad® thermal cycler (BioRad Laboratories Ltd, Hemel Hempstead, UK).

Where subsequent purification of DNA fragments was required, samples were run on 1% to 2% weight/volume agarose gels. DNA bands were then visualised using a transilluminator and excised with a sharp scalpel. DNA was purified using the QIAquick Gel Extraction Kit (Qiagen, Crawley, UK) as per the manufacturer's instructions.

2.1.4 Agarose gel electrophoresis

Buffers

10X TBE: 108g Tris base, 55g boric acid, 9.3g EDTA in 1 litre ddH₂O

5X Loading buffer: 40% sucrose and 0.25% bromophenol blue in 10X TBE

Agarose gel electrophoresis was used to separate DNA fragments by size following restriction enzyme digests and to detect PCR products. Depending on the size of DNA fragments to be analysed, between 1% to 2% weight/volume agarose was dissolved in 100ml of 1X TBE by heating in a microwave oven. After a brief cooling period, 10µl of 500µg/ml ethidium bromide solution was added and the gel was poured into a mould. After setting the gel was placed in an electrophoresis tank filled with 1X TBE buffer. Samples were mixed with an appropriate volume of loading buffer immediately prior to loading into wells of the gel. The appropriate molecular size ladder was also loaded into one well to determine DNA fragment sizes. Samples were electrophoresed at 120V and fragments were detected by fluorescence of intercalated ethidium bromide under UV illumination.

2.1.5 Klenow fill-in

Klenow fill-in was used for the generation of blunt ended DNA where blunt end modification was required prior to DNA ligation. This was achieved using DNA Polymerase I, Large (Klenow) Fragment (New England Biolabs UK Ltd, Hitchin, UK). This proteolytic product of the E.coli DNA polymerase I enzyme retains 3' to 5' exonuclease and polymerisation activity and as such is able to fill in 5' overhangs and remove 3' overhangs.

In a standard Klenow fill-in, DNA with sticky ends was incubated with 1U/ μ g DNA large Klenow fragment, 1X NEBuffer 4 (contains 50mM Potassium Acetate, 20mM Tris-acetate, 10mM Magnesium Acetate, 1mM DTT, pH 7.9 at 25°C), and 33 μ M dNTP for 15 minutes at 25°C using a Dyad[®] thermal cycler (BioRad Laboratories Ltd, Hemel Hempstead, UK). To terminate the reaction EDTA was added to a final concentration of 10mM and samples were heated at 75°C for 20 minutes.

2.1.6 Alkaline phosphatase treatment

Alkaline phosphatase enzyme was used to remove 5' phosphate groups from vector backbone DNA in order to prevent self-ligation. The phosphatase enzyme used for this work was Calf Intestinal Phosphatase (CIP) (New England Biolabs UK Ltd, Hitchin, UK).

In addition to DNA, the standard reaction mix for a 50 μ l phosphatase treatment contained 5 μ l 10X NEBuffer 3 (contains 100mM NaCl, 50mM Tris-HCl, 10mM MgCl₂, 1mM Dithiothreitol, pH 7.9 at 25°C) and 5U CIP (stored in 10 mM Tris-HCl, 50 mM KCl, 1 mM MgCl₂, 50% Glycerol, 0.1 mM ZnCl₂, pH 8.2 at 25°C). Final reaction volumes were made up with molecular biology water. Standard reaction conditions entailed a 1 hour incubation at 37°C using a Dyad[®] thermal cycler (BioRad Laboratories Ltd, Hemel Hempstead, UK).

2.1.7 Ligations

Ligations were carried out for the insertion of DNA sequences into CIP treated linear vector backbone DNA. All reactions were done in conjunction with a backbone DNA only negative control to determine relative background levels of self-ligated vector DNA. All ligations in this work were carried out using T4 DNA ligase (New England Biolabs UK Ltd, Hitchin, UK).

On Ice, vector backbone DNA was mixed with an approximate 3-fold excess of insert DNA (as determined by the appearance of band intensity on a 1% agarose gel). In addition to DNA the standard reaction mix for a 20µl ligation contained 2µl 10X T4 DNA ligase buffer (containing 50mM Tris-HCl, 10mM MgCl₂, 1mM ATP, 10mM DTT, pH 7.5 at 25°C) and 800 U of T4 DNA ligase (stored in 10 mM Tris-HCl, 50 mM KCl, 1 mM DTT, 0.1 mM EDTA, 50% Glycerol, pH 7.4 at 25°C). Final reaction volumes were made up with molecular biology water. All reactions were carried out by overnight incubation at 4°C.

2.1.8 Bacterial Transformation and expansion of Colonies

Growth medium

L-Broth: 16 L-Broth capsules (MP Biomedicals, Cambridge, UK) dissolved in 1 litre ddH₂O; sterilised by heating at 121°C for 20 minutes in a bench top autoclave (Astell, Kent, UK). Ampicillin was added to a final concentration of 100µg/ml. 1litre of L-Broth contained 10g Tryptone, 5g yeast extract and 0.5g NaCl.

Bacterial transformations were carried out for the propagation of plasmid DNA. All reactions were carried out in conjunction with positive and negative control transformations (using pUC19 plasmid DNA and ligation mixture containing backbone DNA only respectively). DH5α chemically competent E.coli, pUC19 plasmid DNA and SOC outgrowth medium used in this study were supplied by New England Biolabs UK Ltd (Hitchin, UK).

For a standard transformation DH5α competent cells were thawed briefly on ice and divided into 25µl aliquots. 5µl of ligation mixture or 1µl pUC19 plasmid was added to one individual aliquot of competent cells and incubated on ice for 30 minutes. To allow for DNA uptake, all samples and controls were heat shocked at 42°C for 20 seconds and immediately placed on ice for a further 5 minutes. 475µl of SOC medium (containing 2% Vegetable Peptone, 0.5% Yeast Extract, 10 mM NaCl, 2.5 mM KCl, 10 mM MgCl₂, 10 mM MgSO₄, and 20 mM Glucose) was then added to each sample followed by a 1 hour incubation at 37°C with shaking. As all plasmid constructs contained an ampicillin resistance gene, samples were spread onto agar plates containing 100µg/ml ampicillin (Melford Laboratories Ltd, Ipswich, UK) under aseptic technique. Plates were incubated at 37°C overnight.

To determine whether ligations had been successful, plates were first checked to ensure that higher numbers of colonies were present for each construct in comparison to the negative control. The positive control plate was used to verify that transformation had occurred. Following these checks colonies were picked using pipette tips and placed in 5ml of LB medium. Samples were left in a 37°C shaking incubator overnight. The following day, DNA was extracted from 2ml of the cultures using the NucleoSpin® Plasmid kit (Fisher Scientific, Loughborough, UK) as per the manufacturer's instructions. 3 ml of each culture was reserved and stored at 4°C.

To ascertain whether the correct clones had been generated the extracted DNA was used in a diagnostic restriction digest whereby the enzymes selected would generate fragments of sizes that enabled correct plasmid constructs to be identified. Where positive digests were identified the corresponding 3ml of reserved bacterial culture was used to inoculate a further litre of LB medium. These cultures were incubated at 37°C overnight with shaking. The next day DNA was extracted from the cultures using the Mega Prep kit (Qiagen, Crawley, UK) as per the manufacturer's instructions.

2.2 Vector production

2.2.1 Reagents

- Sodium chloride (NaCl) (VWR International Ltd, Lutterworth, UK)
- Potassium chloride (KCl) (VWR International Ltd, Lutterworth, UK)
- Dipotassium phosphate (K_2HPO_4) (VWR International Ltd, Lutterworth, UK)
- Magnesium chloride (MgCl) (VWR International Ltd, Lutterworth, UK)
- Tris base (VWR International Ltd, Lutterworth, UK)
- Phosphate buffered saline (PBS) tablets (OXOID, Basingstoke, UK)
- Dulbecco's Modified Eagle Medium (DMEM) (PAA Laboratories Ltd, Yeovil, UK)
- PBS (PAA Laboratories Ltd, Yeovil, UK)
- Fetal bovine serum (FBS) (GIBCO, Paisley, UK)
- 10X Trypsin EDTA (PAA Laboratories Ltd, Yeovil, UK)
- Polyethylenimine (PEI) (Polysciences Inc, Northampton, UK)
- Deoxycholic acid (VWR International Ltd, Lutterworth, UK)
- Benzonase (Sigma-Aldrich Company Ltd, Poole, UK)
- Glycine (MP Biomedicals, Cambridge, UK)

- AVB Sepharose (GE Healthcare UK Ltd, Buckinghamshire, UK)
- Custom primers (Integrated DNA Technologies, Leuven, Belgium)
- Molecular biology water (Sigma-Aldrich Company Ltd, Poole, UK)
- 2 X QuantiFast SYBR Green Mastermix (Qiagen, Crawley, UK)
- Sodium hydroxide (NaOH) (VWR International Ltd, Lutterworth, UK)
- EDTA (VWR International Ltd, Lutterworth, UK)
- Glycerol (VWR International Ltd, Lutterworth, UK)
- Sodium dodecyl sulphate (SDS) (Sigma-Aldrich Company Ltd, Poole, UK)
- Xylene cyanol (Sigma-Aldrich Company Ltd, Poole, UK)
- 10000X Gel Red (Cambridge Bioscience, Cambridge, UK)
- Hyper Ladder I (Bioline, London, UK)
- 2-[4-(2-hydroxyethyl)piperazin-1-yl]ethanesulfonic acid (HEPES) (VWR International Ltd, Lutterworth, UK)
- Methanol (VWR International Ltd, Lutterworth, UK)
- Acetic acid (VWR International Ltd, Lutterworth, UK)
- Coomassie Brilliant blue R-250 (VWR International Ltd, Lutterworth, UK)
- Laemmli buffer (Sigma-Aldrich Company Ltd, Poole, UK)
- 10% Precise Tris-HEPES Gels (Thermo Scientific, Loughborough, UK)

2.2.2 Triple transfection of HEK293T cells

Buffers

1X TD buffer: 140mM NaCl, 5mM KCl, 0.7mM K₂HPO₄, 3.5mM MgCl₂, 25mM Tris, pH7.5 in 1L ddH₂O

PBS: 10 tables/litre ddH₂O (OXOID, Basingstoke, UK)

Triple transfections were carried out for AAV2/8 virus production. By transfecting cells with a transgene containing plasmid, a plasmid containing rep and cap genes and an adenoviral helper plasmid all genes required for the production and packaging of recombinant vector particles were expressed by the cells simultaneously (Nathwani *et al*, 2001). For each virus 40× 15cm plates of HEK293T cells were used at approximately 70% confluence on the day of transfection. Cells were cultured at 37°C, 5% CO₂ in DMEM (PAA Laboratories Ltd, Yeovil, UK) with 10% FBS (GIBCO, Paisley, UK) and enzymatically passaged with 1X trypsin EDTA (PAA Laboratories Ltd, Yeovil, UK) every 2-3 days.

For a standard 40 plate transfection, 6ml of 1mg/ml Polyethyleneimine (PEI) (Polysciences Inc, Northampton, UK) was added to 54ml serum free DMEM. In a separate tube 1.8mg of helper plasmid (containing essential genes from the adenoviral genome that support rescue and replication of AAV genomes), 0.6mg 2/8 plasmid (containing rep and cap genes), 0.6mg of transgene containing plasmid, and 40µg of PCL10.1-EF1α-GFP plasmid was added to serum free DMEM to a final volume of 62ml. The mixture containing DNA was then filtered into the PEI containing mixture through a 0.2µm syringe filter. The solution was mixed and incubated at room temperature for 15 minutes. 3ml of transfection solution was then added to each 15cm dish of HEK293T cells.

After 72 hours of incubation, cells were harvested using cell scrapers and transferred to 250ml conical tubes. A small fraction of each preparation was reserved for flow cytometry using a Beckman Coulter CyAn ADP Analyzer (Beckman Coulter UK Ltd, High Wycombe, UK) to determine transfection efficiency as a percentage of GFP positive cells. All tubes were centrifuged at 1500rpm for 10 minutes. Supernatants were discarded and cell pellets resuspended in 25ml 1×TD buffer. Cells were again spun for 10 minutes at 1500rpm and supernatants were discarded. Cell pellets were then collectively resuspended in 40ml 1×TD buffer. To lyse the cells and release viral particles freeze thaw cycles of 30 minutes at -80°C followed by 10 min at 37°C were repeated 5 times.

Prior to purification cells were incubated at 37°C for 30 minutes with 0.5% deoxycholic acid and 50units/ml Benzonase (Sigma-Aldrich Company Ltd, Poole, UK). Lysates were then spun at 4000×g for 30 minutes at 18°C, passed through a 0.45µm filter and diluted 1 in 3 in filtered PBS.

2.2.3 Virus purification by affinity chromatography

Buffers

1M Tris: 121.14g Tris base, pH 8.8 in 1 litre ddH₂O

Glycine buffer: 3.75g Glycine, pH 2.7 in 1 litre ddH₂O

PBS: 10 tables/litre ddH₂O, pH 7.5 (OXOID, Basingstoke, UK)

Affinity chromatography was carried out for the isolation of AAV vector particles from cell lysates using an ÄKTA Explorer FPLC system (GE Healthcare UK Ltd, Buckinghamshire, UK) and UNICORN 5.20 software. Purification of AAV2/8 was achieved using a 5ml AVB

Sepharose (GE Healthcare UK Ltd, Buckinghamshire, UK) packed column (Davidoff *et al*, 2004).

For a standard purification all lines were first washed with 20% ethanol followed by PBS (line A11 and A2) and 50mM glycine (line B1). After attaching the sepharose column, the affinity medium was equilibrated with filtered PBS pH 7.5 for 10-20 minutes (or until pH and absorbance readings were stable) at a flow rate of 2ml/min. The cell lysates obtained from 40 plate preparations were then loaded onto the column at 5ml/min through line A2 (traceable as an increase in absorbance at 260 and 280nm as unbound protein and DNA exit the column). Residual unbound protein and DNA was washed off the column in filtered PBS allowing for viral particles exclusively to be eluted in 50mM Glycine pH 2.7 (5ml/min). The eluate was collected in 1ml fractions into tubes containing 30µl 1M Tris pH 8.8 to neutralise the glycine. The virus containing fractions were identified by a peak in absorbance at 260 and 280nm. To remove glycine and restore pH, fractions were pooled together and dialysed overnight at 4°C in PBS using a 10KDa cut-off dialysis cassette (Slide-A-Lyzer Thermo Scientific, Loughborough, UK).

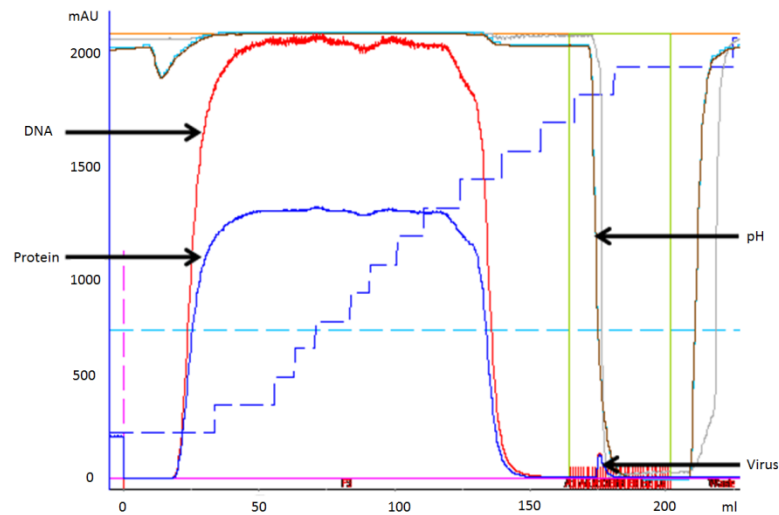


Figure 2.1: A typical AAV8 purification chromatogram. Red and Blue lines are indicative of DNA and protein respectively. The large increase in protein and DNA depicts loading of the virus onto the sepharose column. Elution of AAV particles coincides with a drop in pH (brown line). Fractions corresponding to the small peak in protein and DNA levels contained the purified virus. The amount of virus eluted is measured in milliabsorbance units (mAU).

2.2.4 Vector titration by Q-PCR

Quantitative-PCR was used to titrate vectors in terms of vector genome (vg) copies per ml (Fagone *et al*, 2011). Using primers designed against the LP1 promoter (5' primer, 5'-GGAGAGGAGCAGAGGTTGTC-3'; 3' primer, 5'-TGGTGGTGCCTGAAGCTGAG-3'), the titre of all AAV2/8 viruses was determined from a standard generated from serial dilutions of LP1 containing plasmid DNA.

In a standard Q-PCR 10µl of virus samples, negative control samples (Water) and standards were added to a 96 well plate in triplicate. Each virus was loaded in three different dilutions (1 in 100, 1 in 1000 and 1 in 10000). To each well the following master mix was added: 12.5µl 2× QuantiFast SYBR Green Mastermix (Qiagen, Crawley, UK), 1µl 5' primer, 1µl 3' primer (each 2.5µM) and 0.5µl molecular biology water (15µl master mix/well). Plates were then sealed, briefly spun by centrifugation and placed in a Realplex thermal cycler (Eppendorf, Stevenage, UK). After an initial heating period of 5 min at 95°C the following steps were carried out for 40 cycles: 95°C 10 sec and 60°C 30 sec. Copy number of viral genomes was calculated by Realplex software (Eppendorf, Stevenage, UK). To calculate viral genome copies per ml, copy number recorded per 10µl reaction was multiplied by the dilution factor and then by multiplied 100. As all standards used were double stranded DNA, values derived for single stranded viruses were multiplied by 2.

2.2.5 Vector titration by alkaline gel

Buffers

50X Alkaline electrophoresis buffer: 30g NaOH, 7.31g EDTA, pH 8.0 in 500ml ddH₂O

4X Sample loading buffer: 200µl Glycerol, 80µl 50X alkaline electrophoresis buffer, 60µl 20% w/v SDS, Xylene cyanol powder (arbitrary amount) in 1ml ddH₂O

1M Tris: 121.14g Tris base, pH 8.0 in 1 litre ddH₂O

0.1M NaCl: 5.84g NaCl in 1 litre ddH₂O, heated at 121°C for 20 minutes in a bench top autoclave (Astell, Kent, UK).

4X Gel red solution: 40µl 10000X Gel red (Cambridge Bioscience, Cambridge, UK) in 100ml 0.1M NaCl

To titre viruses more accurately by means of quantifying viral DNA, viruses were run on denaturing alkaline gels and band intensity was quantified by comparison against a standard (DNA ladder) (Fagone *et al*, 2011). To make the gels, 0.8g agarose was added to 98ml ddH₂O and heated in a microwave oven to dissolve the agarose. 2ml of 50X alkaline electrophoresis buffer was then added and the solution was cooled to below 50°C before pouring into a mould. 8.5µl of alkaline sample loading buffer was added to each 25µl aliquot of virus to be titred. Samples were mixed well and placed on ice. Samples were then run at 20V on the gel overnight at 4°C with 5µl Hyperladder I (Bioline, London, UK) loaded in a separate lane. The next day gels were washed for one hour in 300ml 1M Tris pH 8.0 with agitation. Gels were then transferred to 100ml of 4x Gelred solution and left for two hours in darkness with agitation. After rinsing twice with tap water gels were imaged using Genesnap software (Syngene, Cambridge, UK). Images were then used for quantification of viral DNA using Gene tools software (Syngene, Cambridge, UK). Output raw volume and background values for the intensity of each band were exported into an excel file. To calculate viral titre, background was subtracted from raw volume to obtain net volume values and a standard curve was generated by plotting ng of DNA in the Hyperladder against corresponding net volumes. The equation from the chart was used to calculate ng of DNA in each sample and these values were multiplied by 40 to derive DNA concentration in ng/ml. Viral titre was then calculated in terms of vector genome copies/ml based on the sequence of the viral genome in question.

For example:

- An amount of sample containing 6.02×10^{23} particles is a mole
- The molecular mass of a substance in grams is equal to its molar mass
- Therefore, the molecular mass of the theoretical ssDNA sequence TTAAGCGCTTAA is 3723.43 Daltons (Da) and the molar mass is 3723.43g
- Thus 1ng contains:
$$1 \times 10^{-9} \times 6.02 \times 10^{23} / 3723.43 = 1.62 \times 10^{11} \text{ copies}$$

2.2.6 Coomassie Stain of Capsid Proteins

Buffers

10X HEPES running buffer: 121g Tris, 238g HEPES, 10g SDS in 1 litre ddH₂O

Coomassie blue dye: 500ml methanol, 400ml ddH₂O, 100ml acetic acid, 2.5g Coomassie Brilliant blue R-250

Destain solution: 250ml methanol, 680ml ddH₂O, 70ml acetic acid

To quantify viral titre by relative band intensity of capsid proteins (VP1, VP2 and VP3), 20µl virus samples were heated at 95°C in an equal volume of Laemmli buffer (Sigma-Aldrich Company Ltd, Poole, UK) for 5 min to denature proteins. Samples, protein ladder and a control virus sample of known titre were then run on a pre-made polyacrylamide gel (Thermo Scientific, Loughborough, UK) in 1×HEPES running buffer at 150V for 30 min. Gels were then stained for 1hr using Coomassie blue dye. After destaining gels were imaged using Genesnap software (Syngene, Cambridge, UK).

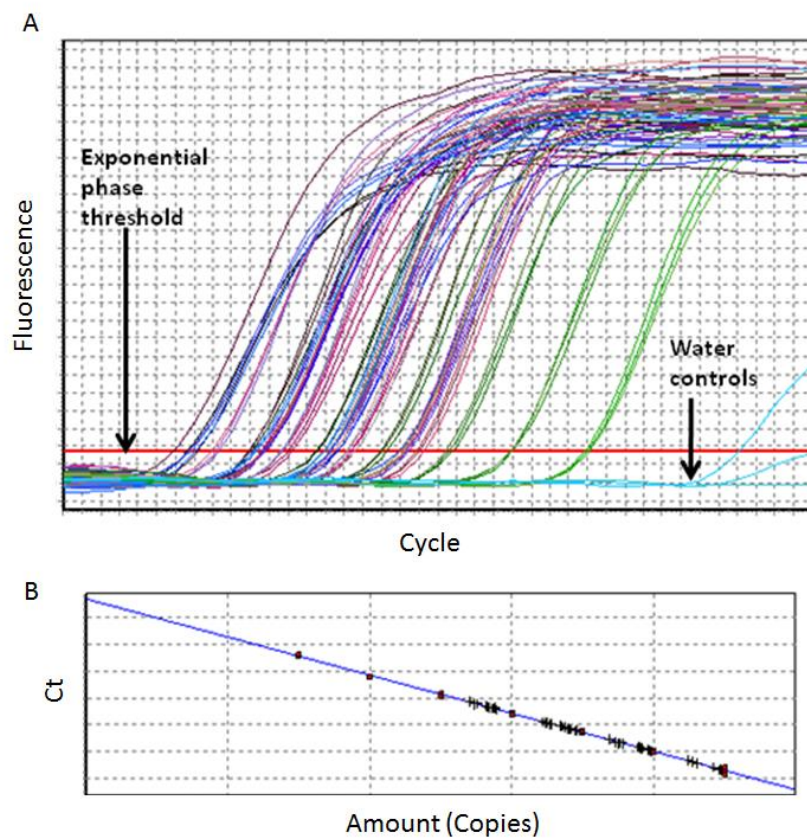


Figure 2.2: Typical QPCR traces and standard. (A) Q-PCR reactions were carried out in triplicate to quantify vector genome copies per 10 μ l of virus sample. Traces for each sample are plotted as a curve measuring the increment in product (fluorescence units) over time (cycles). Threshold cycle values (C_t) are recorded where product levels enter the exponential phase of the Q-PCR reaction (indicated as a red horizontal line). Negative control samples correspond to the three blue curves at the far right end of the trace. **(B)** Q-PCR standards used to derive viral titre are linear plots of C_t values recorded for serial dilutions of a plasmid DNA of known copy number.

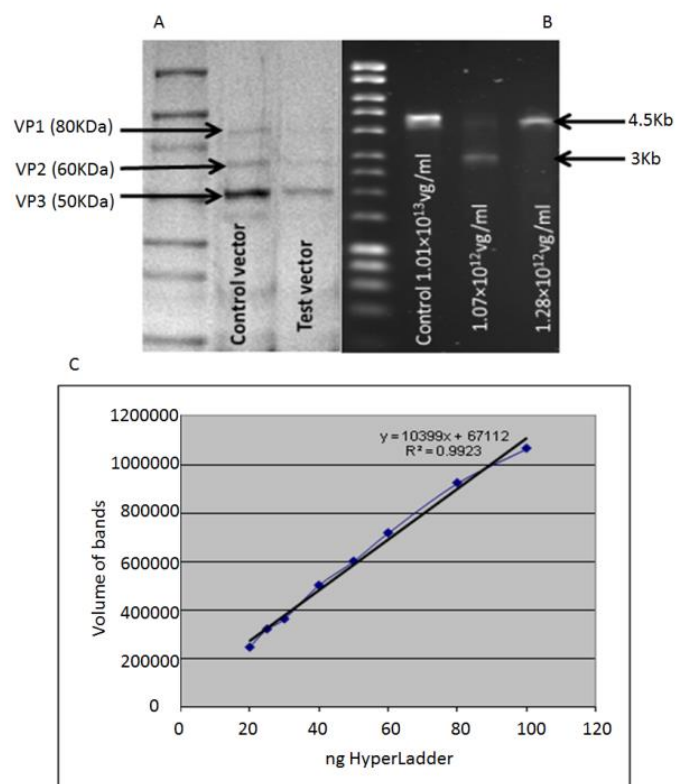


Figure 2.3: Gel based titration of AAV8. (A) A typical acrylamide gel including a protein ladder, a control sample of known concentration (left sample 5×10^{12} vg/ml), and a sample under analysis (right sample titred as 1×10^{11} vg/ml). VP1, VP2 and VP3 bands correspond to upper middle and lower bands respectively. **(B)** A typical alkaline gel with a DNA standard, 5 μ l of a control sample of known concentration (left sample 1.01×10^{13} vg/ml) and 25 μ l of two samples under analysis (centre and right samples 1.07 and 1.28×10^{12} /ml respectively). **(C)** A typical alkaline gel standard plotted as band intensity (volume of bands) against ng of DNA in the hyperladder.

2.3 Animal studies

All procedures were performed in accordance with institutional guidelines under protocols approved by the Institutional Biosafety Committee and the Institutional Animal Care and Use Committee at St Jude Children's Research Hospital and the University of Tennessee Health Science Center, Memphis. All animal work carried out in the United Kingdom was performed under the authority of the UK Home Office Project and Personal Licences regulations and was compliant with the guidelines of the University College London ethical review committee.

All mice used in the study were male C57BL/6 aged between 6 and 8 weeks (Purchased from Charles River UK Ltd, Margate, UK). AAV2/8 viruses were prepared in X-VIVO 10 (GIBCO, Paisley, UK) media and administered via tail vein injection at 1×10^9 to 1×10^{11} vector genomes (vg)/animal with 3-4 mice per group (Nathwani *et al*, 2001). Mice were bled from the tail vein with 1ml insulin syringes at regular intervals and plasma was collected by centrifugation ($4000 \times g$ for 15 min at 4°C) of blood samples in trisodium citrate buffer. 2 to 4 weeks after the injection date mice were sacrificed and livers were taken for further investigations.

Captive-bred male *Macaca mulatta* used in this study were aged 4 years and weighed between 4 and 5 kg (purchased from Charles River Laboratories, Reno, NV). Peripheral vein infusion entailed insertion of an intravenous catheter into the saphenous vein of anesthetized animals. The vector was diluted in PBS at 10 ml/kg of the total body weight of the macaque and administered through the catheter whilst monitoring the animal's vital signs and oxygen saturation (Nathwani *et al*, 2007).

2.4 Assessment of human factor IX (hFIX) antigen levels

2.4.1 Reagents

- DMEM (PAA Laboratories Ltd, Yeovil, UK)
- FBS (GIBCO, Paisley, UK)
- Trypsin EDTA (PAA Laboratories Ltd, Yeovil, UK)
- Eugene HD (Roche Diagnostics Ltd, Burgess Hill, UK)
- X-VIVO 10 (GIBCO, Paisley, UK)
- Sodium bicarbonate (NaHCO_3) (VWR International Ltd, Lutterworth, UK)

- PBS tablets (OXOID, Basingstoke, UK)
- Bovine serum albumin (BSA) (Sigma-Aldrich Company Ltd, Poole, UK)
- Tween 20 (Sigma-Aldrich Company Ltd, Poole, UK)
- 36% Hydrochloric acid (HCl) (VWR International Ltd, Lutterworth, UK)
- 1000% recombinant hFIX coagulation reference (Technoclone, Dorking, UK)
- Rhesus anti-human antisera (prepared at St Jude Children's research Hospital, Memphis, TN)
- Goat anti human FIX-HRP peroxidase labelled antibody (Affinity Biological Inc, Epsom, UK)
- SIGMA-ALDRICH FAST™ OPD peroxidase substrate (Sigma-Aldrich Company Ltd, Poole, UK)
- PBS (PAA Laboratories Ltd, Yeovil, UK)
- Recombinant hFIX protein (Sigma-Aldrich Company Ltd, Poole, UK)
- Streptavidin-Coupled dynabeads (Invitrogen Life Technologies, Paisley, UK)
- Protease inhibitor cocktail (Sigma-Aldrich Company Ltd, Poole, UK)
- NuPAGE LDS sample buffer (4X) (Invitrogen Life Technologies, Paisley, UK)
- NuPAGE sample reducing agent (10X) (Invitrogen Life Technologies, Paisley, UK)
- NuPAGE antioxidant (Invitrogen Life Technologies, Paisley, UK)
- Molecular biology water (Sigma-Aldrich Company Ltd, Poole, UK)
- NuPAGE 4-12% Bis-Tris gels (Invitrogen Life Technologies, Paisley, UK)
- NuPAGE MOPS SDS running buffer (20X) (Invitrogen Life Technologies, Paisley, UK)
- Bicine (VWR International Ltd, Lutterworth, UK)
- Bis-Tris (Sigma-Aldrich Company Ltd, Poole, UK)
- EDTA (VWR International Ltd, Lutterworth, UK)
- Methanol (VWR International Ltd, Lutterworth, UK)
- Tris base (VWR International Ltd, Lutterworth, UK)
- NaCl (VWR International Ltd, Lutterworth, UK)
- Hybond-C Extra (GE Healthcare UK Ltd, Buckinghamshire, UK)
- Milk powder (Sigma-Aldrich Company Ltd, Poole, UK)
- Enhanced chemiluminescence substrate (ECL) (Thermo Scientific, Loughborough, UK).
- Fujifilm Super RX X-ray films (Fisher Scientific, Loughborough, UK)
- DNeasy® Blood and Tissue kit (Qiagen, Crawley, UK)
- Custom primers (Integrated DNA Technologies, Leuven, Belgium)

- 2X QuantiFast SYBR Green Mastermix (Qiagen, Crawley, UK)

2.4.2 Transfection of HuH7 cells

To test for human factor IX expression from plasmid DNA, transient transfection was carried out on HuH7 cells for subsequent hFIX ELISA on supernatants. All HuH7 cells used in this study were cultured at 37°C, 5% CO₂ in DMEM (PAA Laboratories Ltd, Yeovil, UK) with 10% FBS (GIBCO, Paisley, UK) and enzymatically passaged with 1X trypsin EDTA (PAA Laboratories Ltd, Yeovil, UK) every 2-3 days. The transfection reagent used in this study was Fugene HD (Roche Diagnostics Ltd, Burgess Hill, UK). For negative control experiments, cells were left untransfected.

For a standard transfection, the day before transfecting, 5×10^5 HuH7 cells were plated per well in 6 well plates (with 3 wells used for each construct tested). On the day of transfection 2µg of the plasmid of interest and 0.2µg of pCl10.1-EF1α-GFP lentiviral vector plasmid were added to 100µl of serum free DMEM (PAA Laboratories Ltd, Yeovil, UK). In a separate tube 6µl of Fugene HD was added to 100µl DMEM. The two solutions were then mixed, incubated at room temperature for 1 hour and added to the cells. After 24 hours DMEM was replaced with 1ml X-VIVO 10 (GIBCO, Paisley, UK). After 72 hours of incubation at 37°C supernatants were harvested and stored at -80°C for subsequent use in ELISA. Transfected cells were used for flow cytometry (using a Beckman Coulter, CyAn ADP flow cytometer) in order to determine transfection efficiency in terms of percentage GFP positivity. All results from hFIX ELISA were subsequently normalised by the percentage of GFP positive cells.

2.4.3 Transduction of HuH7 cells with AAV2/8 vectors

For *in-vitro* analysis of hFIX expression levels by ELISA, supernatants were collected from AAV2/8 transduced HuH7 cells. HuH7 cells were cultured as described in 2.4.2. For negative control cells were left untransduced. As a positive control transduction was carried out with AAV2/8-CMV-GFP virus and cells were subsequently used for flow cytometry (using a Beckman Coulter, CyAn ADP flow cytometer) to approximate transduction efficiency in terms of percentage GFP positivity.

For a standard HuH7 transduction, the day before transduction, cells were plated at a density of 5×10^4 cells per well in six well plates. The following day media containing serum

was replaced with the desired amount of virus (1×10^5 - 1×10^7 vg/cell) in X-VIVO 10 (GIBCO, Paisley, UK) to a final volume of 600 μ l. Plates were incubated at 37°C and gently shaken at 1 hour intervals for the next 8 hours. X-VIVO 10 was then topped up to 1ml in each well. 48 hours later supernatants were collected and stored at -80°C for subsequent use in hFIX ELISA. Each transduction was performed in triplicate including positive and negative controls.

2.4.4 Human Factor IX enzyme-linked immunosorbent assay (ELISA)

Buffers

Coating buffer: 0.1M NaHCO₃ pH 9.2 (4.201g of NaHCO₃ in 500ml ddH₂O)

Washing buffer (PBST): 10 PBS tablets, 500 μ l Tween20 in 1 litre ddH₂O

Blocking buffer: 6g Bovine serum albumin (BSA) in 100ml washing buffer

Dilution buffer: 2g BSA in 100ml washing buffer

Stop solution (3M HCl): 25.86 ml 36% HCl in 100ml ddH₂O

Levels of hFIX in mouse and rhesus plasma or supernatants from transduced cell cultures were determined by FIX enzyme-linked immunosorbent assay (ELISA) (Nathwani *et al*, 2002). Standards for analysis on cell supernatants and mouse/rhesus plasma were prepared by serial dilutions of 1000% recombinant hFIX coagulation reference (Technoclone, Dorking, UK) in X-VIVO 10 (GIBCO, Paisley, UK) or naïve plasma respectively. HuH7 supernatants and corresponding standards were diluted 1:2 in dilution buffer. Plasma samples and corresponding standards were diluted 1:100 in dilution buffer (where required, plasma samples were initially diluted in naïve murine/rhesus plasma to ensure values fell within the range of the standard curve). All Samples and standards were prepared on ice and stored long term at -80°C where required. Negative controls consisted of X-Vivo 10 only diluted 1:2 for *in-vitro* analysis or naïve plasma diluted 1:100 for *in-vivo* analysis.

In a standard factor IX ELISA, 50 μ l Coating antibody (9 μ l rhesus anti-human antisera diluted in 5ml coating buffer) was added to each well of 96 well microtitre plates and incubated at 4°C overnight. The following day all wells were washed 5 times with 200 μ l washing buffer and then blocked in blocking buffer for 1 hour at 37°C. Plates were washed 5 times in

washing buffer (200µl/well) and 50µl of diluted standards and samples were then added to the wells in duplicate. Plates were incubated with the samples at 37°C for 2 hours. Following incubation plates were washed 5 times in washing buffer (200µl/well). Secondary antibody was prepared by adding 5µl Goat anti human FIX-HRP peroxidase labelled antibody (Affinity Biological Inc, Epsom, UK) to 10ml of dilution buffer (final concentration of 1µg/ml). 100µl of diluted secondary antibody was added to each well. Plates were incubated with secondary antibody for 1 hour at 37°C followed by 5 washes with PBST. 200µl SIGMA-ALDRICH FAST™ OPD peroxidase substrate (Sigma-Aldrich Company Ltd, Poole, UK) was then added to each well and colour was allowed to develop for 3 to 4 minutes. To stop the reaction 50ul/well of 3M HCL was added and colour change was assessed spectrophotometrically at 490 nm (Anthos 2001 spectrophotometer).

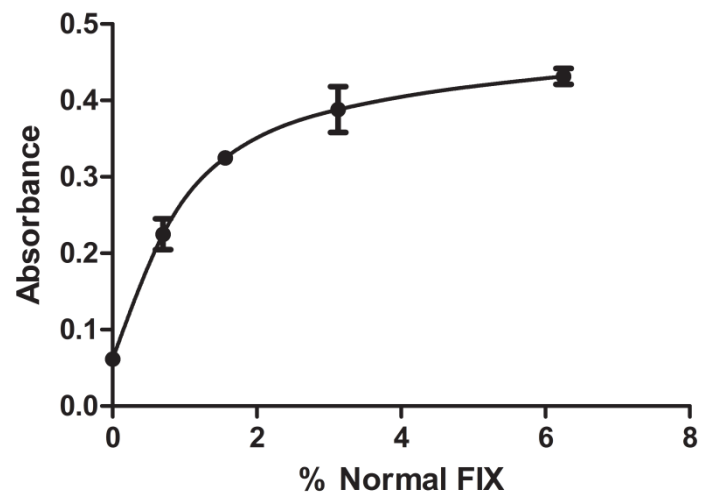


Figure 2.4: A typical hFIX ELISA standard curve. Absorbance values (Y axis) read at 490nm are plotted for samples of known %normal hFIX (X axis) prepared by serial dilutions of a coagulation reference.

2.4.5 Factor IX immunoprecipitation

Buffers

PBST: 50µl Tween20 (final concentration 0.01%) in 500ml PBS without calcium or magnesium (PAA Laboratories Ltd, Yeovil, UK)

Human Factor IX immunoprecipitation was carried out on murine plasma samples to purify the protein of interest (hFIX) prior to western blotting. For control, Immunoprecipitation was carried out on hFIX negative and positive samples (naïve plasma and recombinant hFIX standard prepared as serial dilutions of 5mg/µl hFIX concentrate in naïve plasma respectively). Streptavidin dynabeads, poly-acrylamide gels, gel loading buffer and reducing agent used in this work were all supplied by Invitrogen Life Technologies (Paisley, UK).

In a standard hFIX immunoprecipitation, 40µl of plasma sample was mixed with 4µl of biotinylated rhesus anti-hFIX antibody (350µg/ml) and 0.4µl of protease inhibitor cocktail followed by incubation at 37°C for 75 minutes. In a separate tube, magnetic streptavidin dynabeads (100µl/sample) were washed in 500µl PBST then placed on a magnet to remove the buffer. The washing step was then repeated twice with 200µl PBST. Beads were resuspended in 200µl PBST and added to the plasma sample followed by incubation at room temperature for 30 minutes on a rotator. Beads were then washed 3 times in 200µl PBST. To elute proteins bound to the streptavidin beads 10µl of reducing loading dye (2.5µl 4× loading buffer, 6.5µl water and 1µl reducing agent) was added to each sample followed by incubation at 70°C for 10 minutes. Samples were then placed on a magnet to separate the beads and eluted proteins were loaded directly onto 4-12% Bis-Tris poly-acrylamide gels for western blotting.

2.4.6 Western blotting

Buffers

1X Running buffer: 50ml 20X MOPS buffer (Life Technologies, Paisley, UK) in 1 litre ddH₂O

Transfer buffer: 10ml 20X transfer buffer (81.6g Bicine, 104.6g Bis Tris, 7.5g EDTA in 1 litre ddH₂O); 40ml Methanol; 200µl anti-oxidant (Invitrogen Life Technologies, Paisley, UK); 150ml ddH₂O

Wash buffer (TBST): 50ml 20X TBS (48.4g Tris base, 160g NaCl, approximately 24ml 36% HCL/until pH is between 7.4 and 7.8); 2ml Tween 20 in 1 litre ddH₂O

Western blotting was used as a secondary method of determining murine plasma hFIX levels in order to verify ELISA results. Standards consisted of serial dilutions of recombinant hFIX concentrate (5mg/μl) in naïve C57BL/6 mouse plasma. Negative control samples consisted of naïve plasma only. Prior to sample loading on poly-acrylamide gels, all samples and standards were subject to immunoprecipitation as described in section 2.4.5. Unless otherwise stated all equipment and reagents used in this work were supplied by Invitrogen life technologies (Paisley, UK).

For a standard western blot, pre-cast 4-12% tris glycine poly-acrylamide gels were placed in electrophoresis tanks and the reservoir between the gel and the plastic dam was filled with 1X MOPS running buffer. To maintain proteins in a reduced state, 500μl of antioxidant was added to this central reservoir and mixed well using a Pasteur pipette. The remaining 1X running buffer was used to fill the outer compartment of the tank. 10μl of samples and standards were loaded into wells of the gel and electrophoresed at 125V, 35mA, 5W for approximately 2 hours. To transfer proteins, gels were placed on top of three pieces of 1mm filter paper soaked in transfer buffer. A piece of Hybond-C Extra (GE Healthcare UK Ltd, Buckinghamshire, UK) nitrocellulose membrane soaked in transfer buffer was then placed on top of the gel followed by another 3 pieces of wet filter paper. To remove air bubbles a 5ml plastic pipette was rolled over the top of the gel stack. The stack was then placed in a transfer cassette on top of two sponges soaked in transfer buffer. The remaining space in the cassette was filled with more soaked sponges before clamping the cassette into an electrophoresis tank. Inside the tank, the cassette was filled with transfer buffer and the outer chamber was filled with tap water to cool the transfer system. The transfer was then run at 25V, 125mA, 15W for 90 minutes. After transfer membranes were blocked in 10% milk at 4°C overnight with shaking. Membranes were then washed with PBST 4 times over a period of 30 minutes at room temperature. Goat anti human FIX-HRP peroxidise labelled antibody (Affinity Biological Inc, Epsom, UK) was diluted 1 in 5000 with 10% milk (final concentration of 0.4μg/ml) and incubated with the membranes for 2 hours at room temperature. Washing of the membranes 4 times with PBST was then repeated followed by a 3 minute incubation with enhanced chemiluminescence substrate (ECL) prepared in a 1:1 ratio of solution 1 to solution 2 (Thermo Scientific, Loughborough, UK).

Protein bands were visualised on Fujifilm Super RX X-ray films (Fisher Scientific, Loughborough, UK) using a KONICA MINOLTA SRX-101A film processor.

2.4.7 Proviral copy number correction

To ensure that differences in plasma hFIX levels achieved with different vectors was not due to discrepancy in transduction efficiencies, %hFIX levels were normalised by proviral copies per hepatocyte. To determine proviral copy number, genomic DNA was extracted from transduced mouse liver samples using the DNeasy® Blood and Tissue kit (Qiagen, Crawley, UK) as per the manufacturer's instructions. Each DNA sample was diluted to a final concentration of 7.5ng/μl and subsequently subjected to a quantitative real-time PCR (Q-PCR) assay. Using primers designed against a 283bp region of the LP1 promoter (5' primer, 5'-GGA GAG GAG CAG AGG TTG TC-3'; 3' primer, 5'- TGG TGG TGC CTG AAG CTG AG -3'), copy number was determined from a standard generated by serial dilutions of LP1 containing plasmid DNA. In a separate reaction, equivalent DNA loading was established using primers against murine GAPDH (5' primer, 5'-TGGAGAGCCCGCTCAGACCC-3'; 3' primer, 5'-GGATTGGGTGTCCCTGCGCC-3') and a standard of known DNA concentration (ng) generated from serial dilutions of mouse genomic DNA.

In a standard copy number Q-PCR, 5μl of liver DNA samples; negative control samples (Water) and standards were added to a 96 well plate in duplicate. To each well the following master mix was added: 12.5μl 2× QuantiFast SYBR Green Mastermix (Qiagen, Crawley, UK), 1μl 5' primer, 1μl 3' primer (each 2.5μM) and 5.5μl molecular biology water (20μl master mix/well). Plates were then sealed, briefly spun by centrifugation and placed in a Realplex thermal cycler (Eppendorf, Stevenage, UK). After an initial heating period of 5 minutes at 95°C the following steps were carried out for 40 cycles: 95°C 10 seconds and 60°C 30 seconds. Copy number of viral genomes and the amount of DNA loaded per well was calculated by Realplex software (Eppendorf, Stevenage, UK) using Ct values recorded for LP1 and GAPDH standards respectively.

To calculate copies per cell LP1 copy number results were divided by the amount of DNA (ng) in each sample; these figures were then multiplied by 37.5 (the theoretical amount of DNA loaded in each well) and divided by 6528.5 (the approximate number of murine cells from which 37.5ng of DNA is derived). To normalise plasma hFIX levels by viral genome copy number, values of % normal hFIX were divided by copy number/cell observed for the corresponding liver DNA sample.

2.5 Assessment of S/MAR function

2.5.1 Reagents

- RNAlater® (Qiagen, Crawley, UK)
- Qias shredder® (Qiagen, Crawley, UK)
- RNeasy Plus® kit (Qiagen, Crawley, UK)
- cDNA synthesis kit (Bioline, London, UK)
- Molecular biology water (Sigma-Aldrich Company Ltd, Poole, UK)
- 2× QuantiFast SYBR Green Mastermix (Qiagen, Crawley, UK)
- Custom primers (Integrated DNA Technologies, Leuven, Belgium)
- Mm_Gapdh_3_SG QuantiTect primer assay (Qiagen, Crawley, UK)
- EZ-Magna ChIP A-Chromatin Immunoprecipitation Kit (Millipore, Feltham, UK)
- PBS (PAA Laboratories Ltd, Yeovil, UK)
- Complete protease inhibitor cocktail (Roche Diagnostics Ltd, Burgess Hill, UK)
- FBS (GIBCO, Paisley, UK)
- Formaldehyde (Sigma-Aldrich Company Ltd, Poole, UK)
- Glycine (MP Biomedicals, Cambridge, UK)
- ChIP antibodies (Supplied by Millipore, Feltham, UK or Abcam, Cambridge, UK or Active Motif, Rixensart, Belgium)
- Murine β -actin primers (Active Motif, Rixensart, Belgium)

2.5.2 Determination of hFIX mRNA levels

To determine hFIX RNA levels produced per proviral genome copy, RNAlater® (Qiagen, Crawley, UK) stabilised transduced murine liver samples were placed in liquid nitrogen and disrupted with a mortar and pestle. Samples were homogenised using Qias shredder® (Qiagen, Crawley, UK) columns and RNA was extracted using the RNeasy Plus® kit (Qiagen, Crawley, UK) as per the manufacturer's instructions. RNA was then converted to cDNA by using the cDNA synthesis kit (Bioline, London, UK) and cDNA was subsequently used in a Q-PCR assay.

In a standard cDNA synthesis reaction approximately 1 μ g of total RNA was mixed with 1 μ l random hexamers, 10mM dNTP mix and DEPC-treated water (up to 10 μ l final volume).

Reactions were then incubated at 70°C for 5 minutes followed by chilling on ice for 1 minute. To each reaction 4µl 5×RT buffer, 1µl Ribosafe RNase inhibitor, 0.25µl reverse transcriptase (omitted for –RT negative control reactions) and 4.75µl DEPC-treated water was added. Samples were incubated for 10 minutes at 25°C followed by 30 minutes at 45°C using a Dyad® thermal cycler (BioRad Laboratories Ltd, Hemel Hempstead, UK). The reaction was terminated by heating samples to 85°C for 5 minutes followed by cooling on ice.

For a standard Q-PCR, 2µl of cDNA samples; cDNA standards (LP1 containing plasmid DNA) and negative controls (-RT and water) were loaded onto a 96well Q-PCR plate in duplicate. To each well the following master mix was added: 12.5µl 2× QuantiFast SYBR Green Mastermix (Qiagen, Crawley, UK), 1µl 5' LP1 primer, 1µl 3' LP1 primer (each 2.5µM see 2.4.7 for primer sequences) and 8.5µl molecular biology water (23µl master mix/well). Q-PCR cycling conditions were carried out as previously described in section 2.4.7. LP1 cDNA copy number was calculated by Realplex software (Eppendorf, Stevenage, UK) using Ct values plotted for the LP1 standard curve.

To normalise the data by the amount of cDNA loaded for each sample, a separate Q-PCR to quantify levels of housekeeping gene cDNA was performed using murine Gapdh primers (Qiagen, Crawley, UK). To calculate RNA/copy/cell values of LP1 copies were divided by results for cDNA concentration in ng (derived from a murine liver cDNA standard of known concentration). Results were then divided by viral genome copy number per cell to give an approximation of transcription levels per copy.

2.5.3 Chromatin immunoprecipitation

Chromatin immunoprecipitation (ChIP) was used to determine protein interactions with rAAV genomes. Through crosslinking of DNA-protein complexes followed by immunoprecipitation with antibodies against a specific protein of interest, ChIP allows for the isolation and subsequent quantification (by Q-PCR) of vector genomes in association with the chosen precipitated protein. For negative controls immunoprecipitation was carried out using either no antibody or rabbit IgG. This work was carried out with the use of the EZ-Magna ChIP A-Chromatin Immunoprecipitation Kit (Millipore, Feltham, UK). Unless otherwise stated, reagents were sourced from this kit.

In a standard ChIP, 200mg of transduced murine liver was cut into small pieces; resuspended in 1ml ice cold PBS containing complete protease inhibitor cocktail (Roche Diagnostics Ltd, Burgess Hill, UK) and 2% foetal bovine serum (FBS) and pushed through a 40µm nylon cell strainer (BD Biosciences, Oxford, UK) using the end of a 5ml syringe plunger. A further 10ml of PBS solution was added and Cell suspensions were pelleted by centrifugation at 3500rpm for 10 minutes at 4°C. Cell pellets were then washed twice in 10ml PBS solution and resuspended in a further 10ml. To form DNA-protein crosslinks 270µl of 37% formaldehyde (final concentration of 1%) was added followed by incubation at room temperature for 10 minutes. 0.125M Glycine (final concentration) was added to quench formaldehyde for 5 minutes at room temperature. Cells were centrifuged as above and washed twice in ice cold PBS with protease inhibitor and 2% FBS. With the EZ-Magna ChIP A-Chromatin Immunoprecipitation Kit, cell pellets were resuspended in 500µl cell lysis buffer containing 2.5µl Protease Inhibitor Cocktail II. All samples were incubated on ice for 15 minutes whilst vortexing to mix at 5 minute intervals. Samples were then centrifuged at 800 × g at 4°C for 5 minutes, supernatants were removed and pellets were resuspended in 500µl nuclear lysis buffer containing 2.5µl Protease Inhibitor Cocktail II. To fragment DNA (~size 200 to 500 nucleotides), samples were subjected to sonication. Chromatin sonication parameters used were 15 s pulse on and 15 s pulse off for 45 min using a Bioruptor sonicator (Diagenode, Liège, Belgium). After sonication, samples were spun at 13000 × g to remove debris and supernatants were divided into 50µl aliquots. To each 50µl chromatin sample 450µl dilution buffer and 2.25µl Protease Inhibitor Cocktail II was added. From the sample designated as the no antibody negative control, 5µl (1%) of the chromatin solution was removed and reserved as 'input'. To each sample 4µg of specific antibody, 5µg rabbit IgG or no antibody was added. 20µl of magnetic protein A beads was added to each sample followed by overnight incubation at 4°C with rotation. The following day beads were pelleted using a magnet and washed once with 500µl of the following solutions for 5 minutes at 4°C with rotation: 1) Low Salt Immune Complex Wash Buffer, 2) High Salt Immune Complex Wash Buffer, 3) LiCl Immune Complex Wash Buffer, 4) TE Buffer (with each wash beads were separated using a magnet). To elute protein-DNA complexes and reverse crosslinks, after removing TE buffer, 100µl ChIP elution buffer and 1µl Proteinase K was added to each sample. This step was also carried out on the 5µl Input sample reserved before immunoprecipitation. Samples were incubated in elution buffer at 62°C with shaking for 2 hours followed by incubation at 95°C for 10 minutes. After a brief cooling period, beads were separated using a magnet and DNA was purified from each sample

using spin columns from the EZ- Magna CHIP A-Chromatin Immunoprecipitation Kit as per the manufacturer's instructions.

DNA pull down was quantified by Q-PCR using the following primer pairs designed against the AAV genome: 152 (LP1 promoter) 5' primer, 5'-GGAGTCGTGACCCCTAAAATG-3'; 3' primer, 5'-CTCTGACCTCTGCCCCAGCTC-3'. 366 (LP1 promoter) 5' primer, 5'-TTCGGTAAGTGCACTGGAAG-3'; 3' primer, 5'-GTTATCGGAGGAGCAAACAG-3'. 1988 (hFIXco cDNA) 5' primer, 5'-GCTTCCTGACTGGCATCATC-3'; 3' primer, 5'-CAGGTCAGCTTGGTCTTCTC-3'. For a standard Q-PCR, 2µl of each DNA sample (including negative controls and input) was loaded in duplicate onto a 96 well plate. To each well the following master mix was added: 7.5µl 2× QuantiFast SYBR Green Mastermix (Qiagen, Crawley, UK), 2µl 5' primer, 2µl 3' primer (each 1.5µM) and 1.5µl molecular biology water (13µl master mix/well). Plates were then sealed, briefly spun by centrifugation and placed in a Realplex thermal cycler (Eppendorf, Stevenage, UK). After an initial heating period of 5 minutes at 95°C the following steps were carried out for 40 cycles: 95°C 10 sec and 60°C 30 sec. Ct values were determined by Realplex software (Eppendorf, Stevenage, UK). In a separate reaction, the same Q-PCR was performed using primers against β-actin (Active Motif, Rixensart, Belgium); this was done to ensure that levels of background DNA pull down were similar between samples under comparison.

To calculate DNA pull down as a percentage of total input chromatin, the average Ct value of the input samples were determined and 6.644 cycles was subtracted from this value (the number of cycles subtracted to account for the 100-fold dilution of the input chromatin). The Ct value observed for each sample (CtS) was then subtracted from the input Ct value (CtI). To calculate the percentage of input this value was used in the following formula:

$$100 \times 2^{(CtI-CtS)}.$$

For example:

- If the average Ct value of input is 22.4 the adjusted CtI value is $22.4 - 6.644 = 15.8$
- If the hypothetical Ct value for viral DNA pull down (CtS) with an anti H3K92me antibody is 18.6 then % input is calculated as $100 \times 2^{(15.8-18.6)} = 14\%$
- The percentage of viral DNA out of the total input chromatin associated with H3K92me is therefore 14%.

CHAPTER 3 SCAFFOLD/MATRIX ATTACHMENT REGIONS ENHANCE THE IN-VIVO POTENCY OF AAV VECTORS

3.1 Introduction

3.1.1 AAV genomes are maintained as episomal chromatin

As previously described, after entering the cell nucleus, adeno-associated viral vector genomes undergo single stranded to double stranded DNA conversion followed by intermolecular concatemerisation (Nonnenmacher & Weber, 2012). Vector genomes are then predominantly maintained as high molecular weight concatemers in an extrachromosomal form. Indeed, the episomal persistence of AAV genomes *in-vivo* has been observed in murine skeletal muscle and in liver with extrachromosomal forms representing approximately 99.5% and 90% of vector genomes mediating stable transduction in each tissue respectively (Miao *et al*, 2000a; Nakai *et al*, 2001; Schnepf *et al*, 2003; Schnepf *et al*, 2005).

Multiple episomal viral genomes are known to be maintained in chromatin-like structures. Examples of such viruses include Epstein-Barr virus, Simian virus 40, polyoma virus and Kaposi's sarcoma-associated herpesvirus (Cremisi *et al*, 1975; Lu *et al*, 2003; Shaw *et al*, 1979). Members of the parvovirus family have also been observed in association with nucleosome structures both *in-vitro* and *in-vivo*; this includes minute virus of mice (MVM) and AAV (Ben-Asher *et al*, 1982; Marcus-Sekura & Carter, 1983). Upon digestion of the nuclei of AAV infected KB cells (human mouth epidermal carcinoma cells) with micrococcal nuclease (an enzyme that hydrolyses chromatin at nucleosome linker regions) a typical nucleosomal ladder pattern was revealed on agarose gels; this observation was reproducible in both the presence and absence of adenoviral co-infection (Marcus-Sekura & Carter, 1983). In a similar study, rAAV genomes were found to persist as chromatin-like, supercoiled episomes in the skeletal muscle of non-human primates (NHPs) (Penaud-Budloo *et al*, 2008). Thus, given that AAV genomes are known to be associated with nucleosomes, it is reasonable to assume that rAAV transgenes may be subject to epigenetic silencing through histone modification.

3.1.2 Histone deacetylase inhibitors (HDAC inhibitors) enhance AAV mediated transgene expression.

Histone deacetylase inhibitors are chemical compounds commonly used to modify the acetylation status of histones so that chromatin is arranged in an open euchromatin state that allows for gene expression. Examples of FDA (Food and Drug Administration) approved HDAC inhibitors include Romidepsin and Vorinostat (Suberoylanilide hydroxamic acid (SAHA)) which are used in patients with cutaneous T-cell lymphoma (CTCL); sodium phenylbutyrate (used to stimulate foetal haemoglobin expression in sickle cell anaemia patients) and Valproic acid (used as an anticonvulsant in the treatment of epilepsy and as a mood stabiliser) (Dover *et al*, 1994; Mann *et al*, 2007; Phiel *et al*, 2001; VanderMolen *et al*, 2011). In an attempt to understand whether the AAV provirus is subject to repressive silencing effects, previous *in-vivo* studies involving the co-administration of AAV vector and HDAC inhibitors have been carried out.

One such example includes the 2006 study carried out by Okada *et al* (Okada *et al*, 2006). In this study, U251MG cells were transduced with and AAV2 vector expressing luciferase at a dose of 1×10^4 vg/cell. 3×10^6 transduced cells were then injected subcutaneously into BALB/c mice along with intraperitoneal injection of Romidepsin at 1mg/kg. At 24 hours after injection of Romidepsin, a 37.4-fold increase in bioluminescence signal intensity was observed in subcutaneous tumours of the cohort that received Romidepsin as compared to non Romidepsin treated animals ($1.5 \pm 0.9 \times 10^6$ photons/s/cm²/sr and $4.0 \pm 2.4 \times 10^4$ photons/s/cm²/sr respectively). Similarly, after subcutaneously injecting 3×10^6 U251MG cells transduced with AAV-HSV-tk vector into athymic nude mice, a significant reduction in tumour growth was observed in mice treated with Romidepsin and Ganciclovir (GCV) as compared to animals that received HSV-tk/GCV therapy only. Impressively, in the Romidepsin treated cohort 8 out of 10 tumours were completely eliminated at 4 weeks post transduction. Crucially, the observation that a HDAC inhibitor is able to enhance AAV mediated transgene expression infers that the AAV provirus may be subject to transcriptionally repressive histone modifications.

In support of this notion, we have observed an increase in human factor IX (hFIX) levels following co-administration of SAHA with 4×10^{12} vg/kg of AAV vector expressing hFIX in non-human primates (unpublished data). However, this data is at odds with that of Penaud-Budloo *et al* whereby no increase in rAAV mediated LEA29Y expression was observed following injection of sodium phenylbutyrate into transduced NHPs (Penaud-

Budloo *et al*, 2008). Crucially, in the latter mentioned strategy, it is implied that the HDAC inhibitor was administered at a time at which transgene expression had plateaued. Yet, in our SAHA studies and in the study of Okada *et al*, the need for early administration (before expression reaches steady state) of HDAC inhibitor to observe any increase in transgene expression has been noted.

3.1.3 The use of matrix attachment regions in gene transfer

As previously described, matrix attachment regions are frequently used in the context of gene transfer vectors to enhance transgene expression and to prevent epigenetic silencing (Gluch *et al*, 2008). For instance, in 2003, Kurre *et al* demonstrated the enhancer activity of a S/MAR element (taken from the human IFN β gene) when cloned into an EGFP expressing retroviral vector (Kurre *et al*, 2003). In this study, 1×10^7 CD34-enriched cells taken from baboons (*Papio cynocephalus cynocephalus* or *Papio cynocephalus anubis*) were transduced with EGFP vector with or without the S/MAR element at an MOI (multiplicity of infection) of 0.1 to 0.3. After carrying out myeloablative irradiation on each animal, approximately 2×10^7 transduced cells/arm were re-administered to the animal from which they were derived (with one arm receiving S/MAR vector transduced cells and the other receiving control vector transduced cells). Over a period of 12 months, the mean fluorescence intensity (MFI) of EGFP in cells of all haematopoietic lineages was consistently observed to be 2- to 9- fold higher in the S/MAR-containing arm as compared to the non S/MAR-containing arm. Thus it was inferred that S/MARs improve long term proviral expression in the context of retroviral vectors.

Similarly, S/MAR elements have been shown to enhance transgene expression in plasmid vectors by preventing promoter silencing due to DNA methylation. For example, in 2008, Argyros *et al* demonstrated the stable expression of luciferase in mouse liver up to 6 months after hydrodynamic delivery of plasmid vectors containing the α 1-antitrypsin promoter, a luciferase transgene and the human IFN β S/MAR (Argyros *et al*, 2008). In comparison, luciferase expression from non-S/MAR containing plasmid vectors was shut off one week after vector delivery. By digesting the promoter regions of each vector genome with enzymes that are sensitive to cytosine methylation, it was confirmed that this shut off of transgene expression was due to DNA methylation in the absence of a S/MAR element. Thus S/MARs are able to enhance transgene expression from a variety of gene transfer vectors through the prevention of gene silencing.

The effect of cloning S/MAR elements into AAV expression cassettes, however, remains largely unexplored to date. Given that expression from AAV vectors can be enhanced by the use of HDAC inhibitors it seems reasonable to test an epigenetic modifying element in the context of AAV. As such, through the inclusion of an S/MAR element in our codon optimised human factor IX (hFIXco) AAV expression cassette, we sought to investigate whether S/MARs are able to enhance Factor IX expression levels in order to permit the use of lower vector doses. In our group, we began this analysis with the use of an 809bp S/MAR from the human Interferon β gene (IFN β) as this is the most well documented S/MAR in terms of enhancing transgene expression (Kurre *et al*, 2003; Moreno *et al*, 2011; Ramezani *et al*, 2003).

3.1.4 Preliminary results

In our initial studies, a truncated S/MAR (809bp) derived from the 5' region of the human IFN β gene was cloned immediately 3' of the hFIXco cDNA in our codon optimised human factor IX expression cassette previously described (Nathwani *et al*, 2006). The S/MAR was cloned in both forward and reverse orientation (Figure 3.1, ssAAV-LP1-hFIXco-IFN-F and ssAAV-LP1-hFIXco-IFN-R respectively) and used in the context of single stranded AAV vectors pseudotyped with serotype 8 capsid protein.

Each vector was administered to 6-8 week old male C57Bl/6 mice (N=6) via the tail vein at a dose of 4×10^{12} vector genomes (vg)/kg. Plasma hFIX levels were determined at various time points over a period of 8 weeks post vector administration. The kinetics of hFIX expression was consistent with our previous findings, with detectable hFIX levels observed by 2 weeks and steady state levels observed by 4 weeks (Figure 3.2) (Nathwani *et al*, 2001). Steady state hFIX levels were highest in the cohort transduced with ssAAV-LP1-hFIXco-IFN-R at $188 \pm 18\%$ of normal. This was an approximate 10-fold increase in transgene expression levels as compared to cohorts of mice transduced with control vector containing no S/MAR (ssAAV-LP1-hFIXco-Control, $17 \pm 1.2\%$ of normal) and ssAAV-LP1-hFIXco-IFN-F ($20 \pm 4\%$ of normal). Proviral copy numbers in liver were consistent in each cohort at approximately 0.3 copies/hepatocyte (Figure 3.3). As such, differences in transgene expression were not due to variation in transduction efficiency.

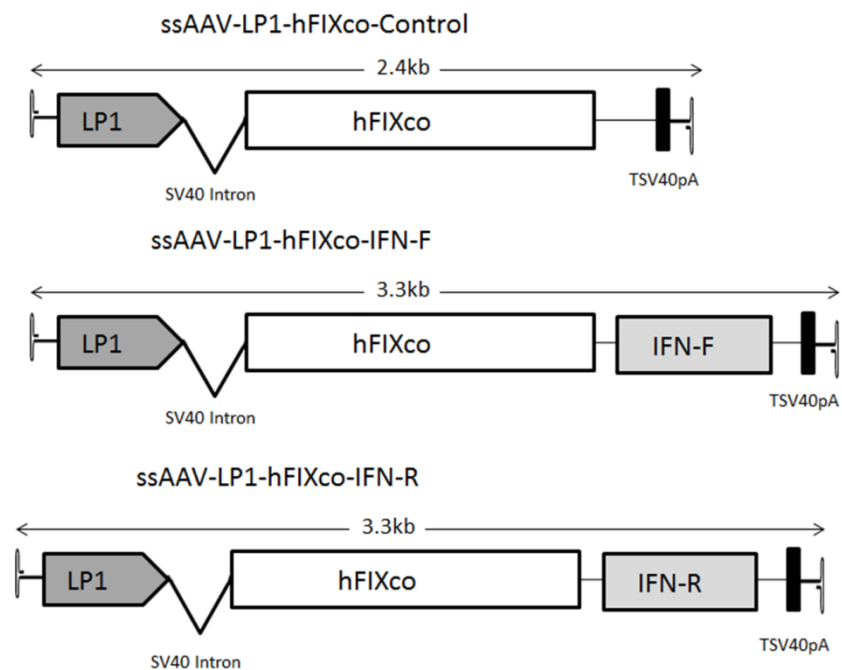


Figure 3.1: Construction of single stranded AAV-hFIXco containing IFN β S/MAR: Schematic of vectors. Each vector is represented schematically as it is packaged inside the virion. Common features include the hybrid liver specific promoter (LP1), SV40 intron, codon-optimised human FIX cDNA (hFIXco) and a truncated SV40 late polyA (tSV40pA) flanked by AAV inverted terminal repeats (ITRs represented as hairpin loops).

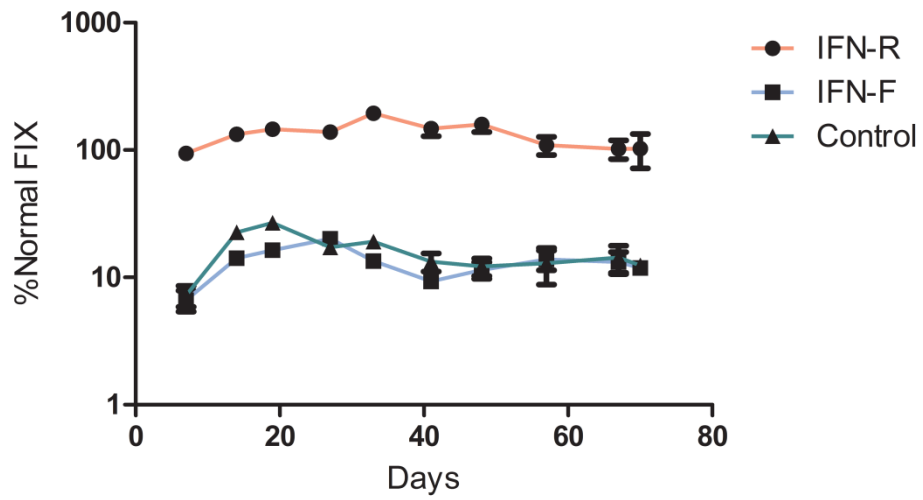


Figure 3.2 FIX expression in C57BL/6 mice. Transgene expression profiles after tail- vein administration of 4×10^{12} vg/kg (n=6) of ssAAV-hFIXco-IFN-F/R and ssAAV-hFIXco-Control vectors into 6 to 8 week old male C57BL/6 mice. All results are shown as an average together with the standard error of the mean (\pm SEM).

3.1.5 Chapter aim

The overriding goal of this study was to improve the potency of AAV vectors. This may be possible with the Interferon β S/MAR but its relatively large size compromises the packaging of an optimal expression cassette given the fact that the maximum packaging capacity of single stranded AAV is only 4.7kb. So can we enhance the potency of AAV with alternative S/MAR elements? S/MARs selected for a head to head comparison in our AAV2/8-LP1-hFIXco expression cassette included regions from the apolipoprotein B (apoB) and hypoxanthine-guanine phosphoribosyltransferase (HPRT) genes. The apoB S/MAR is well documented to have an insulatory role against positional chromatin effects (Namciu *et al*, 1998). In contrast, the HPRT S/MAR has primarily been documented to have a role in autonomous replication (Sykes *et al*, 1988). Additionally, a region of the Kaposi sarcoma herpes virus (KSHV) genome known to promote autonomous replication was utilised as a non-S/MAR control element (Stedman *et al*, 2008).

Through this analysis, at a dose of 4×10^{12} vg/kg, AAV8 vectors containing HPRT and ApoB S/MAR elements were found to enhance hFIX expression levels in mice by 28-fold as compared to control vectors containing no S/MAR or KSHV elements. This advantage in transgene expression was maintained when using the HPRT vector at a dose two orders of magnitude lower (4×10^{10} vg/kg). The HPRT vector also mediated 4-fold higher levels of hFIX expression in NHPs as compared to animals receiving the control vector containing no S/MAR. These results collectively suggest the ability to enhance AAV mediated transgene expression with S/MAR elements; this may permit the use of lower vector doses.

3.2 Materials and methods

3.2.1 AAV-hFIX vector production and purification

The ssAAV vector encoding hFIX has previously been described (Nathwani *et al*, 2001). Elements of this expression cassette include a hybrid liver-specific promoter (LP1) that consists of core domains from the human apolipoprotein hepatic control region and the human alpha-1-antitrypsin promoter followed by a codon optimized hFIX cDNA. For the subsequent insertion of S/MAR elements, 10 μ g of this vector plasmid was digested for 3 hours at 37°C in a standard 100 μ l reaction using BbsI and HpaI restriction enzymes and 10% NEBuffer 4 (standard conditions described in 2.1.3). An oligonucleotide (flanked by BbsI

and HpaI restriction sites) encoding a multiple cloning site (MCS) followed by a truncated SV40 polyadenylation (tSV40pA) sequence was then inserted into the hFIX vector backbone using a standard 20µl ligation reaction as described in section 2.1.7 (AAV-LP1-hFIX-Control). HPRT, ApoB and KSHV DNA elements were synthesised and sequenced by Genescript (Piscataway, USA) and were packaged in pUC57 plasmids flanked by NotI sites. To insert these elements into the AAV-LP1-hFIX-Control plasmid, 10µg of pUC57 and AAV-LP1-hFIX-Control plasmid (containing a NotI site in the MCS) was digested at 37°C for 3 hours using the NotI restriction enzyme and 10% NEBuffer 3 in standard 100µl reactions. Following gel purification (see sections 2.1.3 and 2.1.4) the S/MAR fragments were cloned into the NotI digested multiple cloning site (3' of hFIXco CDNA) using a standard 20µl ligation reaction. The IFNβ S/MAR was taken from the retroviral vector plasmid named MP4253.SFGmSR-preMSV.eGFP (a gift from Dr Martin Pule, UCL Cancer Institute, UK) and ligated as a blunt fragment into the EcoRV site of the MCS in LP1-hFIXco-Control plasmid. Subsequent transformations were carried out as per standard protocol (section 2.1.8). Colonies were expanded and screened as described in 2.1.8 and enzymes used for standard 10µl screening digests (carried out at 37°C for 1 hour) included: SacI and NdeI (IFNβ S/MAR plasmids), DdeI and NotI (ApoB S/MAR plasmids), HindIII (HPRT S/MAR plasmids) and PstI (KSHV control plasmids). All plasmids were also screened for the presence of intact ITRs using standard 10µl AhdI and BglI restriction digests (digested for 1 hour at 37°C).

All vectors were made by the adenovirus-free transient transfection method described in section 2.2.2, using a chimeric AAV2 Rep-8Cap packaging plasmid (pAAV8-2) and an adenoviral helper plasmid. Vectors were purified as detailed in 2.2.3. All vector titres were determined by standard quantitative real-time PCR (Q-PCR) and coomassie gel methods (sections 2.2.4 and 2.2.6 respectively).

3.2.2 Animal studies

All procedures were performed in accordance with institutional guidelines as previously described (section 2.3). Tail-vein administration of rAAV vector particles was performed in 6 to 8 week old immunocompetent male C57BL/6 mice as single bolus injections (maximum volume of 200µl) using 1ml syringes. Prior to injection or bleeding, mice were briefly warmed at 39°C to dilate the tail vein. Mice were injected with 4×10^{12} vg/kg and killed 4 to 8 weeks after vector administration. For the low dose analysis HPRT and control vectors were injected at a dose of 4×10^{10} vg/kg and mice were killed 4 weeks after administration. Blood samples were taken from the tail vein at one week intervals over the course of the

experiment. To separate plasma, blood samples were spun at 4000× g in tri-sodium citrate buffer for 15 minutes at 4°C. In all cases livers were harvested for subsequent molecular analysis. Vectors were infused into rhesus macaques at a dose of 4×10¹²vg/kg via the peripheral vein as described in section 2.3. Blood samples were taken from NHPs at variable time points over the course of 37 weeks after vector administration. Liver samples were harvested from NHPs at 37 weeks for molecular analysis.

3.2.3 HuH7 cell culture and transduction

HuH7 cells were cultured as described in section 2.4.2. Transduction of HuH7 was carried out as per standard protocol (section 2.4.3) using 1×10⁵vg of each vector per cell.

3.2.4 Determination of FIX levels

Human FIX antigen levels in cell supernatants, rhesus plasma and murine plasma samples were determined by enzyme-linked immunosorbent assay (ELISA) as previously described (section 2.4.4). Briefly, microtiter plates were coated with 50 µL of polyclonal rhesus antihuman serum and incubated overnight at 4°C followed by immunocapture of the hFIX antigen in standards, test samples and negative controls. Standards were prepared as dilutions of hFIX coagulation reference in naïve murine/rhesus plasma or serum free DMEM and all samples and standards were diluted 1:100 or 1:2 in PBST containing 2% BSA (plasma and cell supernatant samples respectively). After a 2 hour incubation at 37°C, plates were washed and incubated for 1 hour with 100 µL/well goat anti-hFIX horseradish peroxidase (HRP)–conjugated polyclonal secondary antibody at a final concentration of 1 µg/mL. Plates were developed with o-phenylenediamine dihydrochloride peroxidase substrate and colour change was assessed spectrophotometrically at 490 nm. Statistical difference between experimental groups was determined by 1-way analysis of variance (ANOVA) using GraphPad Prizm version 4.0 software (GraphPad, San Diego, CA).

Western blotting to determine hFIX protein levels was carried out as previously described in section 2.4.6 with prior antigen immunoprecipitation carried out to minimize non-specific background (section 2.4.5).

3.2.5 Molecular studies

Proviral copy number was determined by standard protocol as described in section 2.4.7. Briefly, genomic DNA extracted from ssAAV8-LP1-hFIXco transduced murine/rhesus liver

was subjected to a quantitative real-time PCR (Q-PCR) assay using primers designed to amplify a 283bp region of the LP1 promoter (see 2.4.7 for sequences). The Q-PCR reaction was performed in a total volume of 25 μ L containing 2 \times QuantiFast SYBR Green Mastermix and 37.5ng genomic DNA. Primers against murine GAPDH were used to establish equivalent DNA loading. Proviral copy number was calculated as previously described

To determine transgene expression levels, hFIX mRNA levels were detected by standard protocol as described in section 2.5.2. Briefly, approximately 1 μ g total murine liver RNA from each sample was subjected to reverse transcription. 5 μ L cDNA was then used in a Q-PCR reaction as described previously with primers designed to amplify a 127bp region of the hFIXco cDNA (see 2.5.2 for sequences). GAPDH primers were used to establish equivalent cDNA loading.

3.3 Results

3.3.1 *In-vitro* transduction analysis

To determine the ability of alternative S/MARs to enhance AAV mediated transgene expression, the 587bp S/MAR from the first intron of the human Hypoxanthine-guanine phosphoribosyltransferase (HPRT) gene (Sykes *et al*, 1988) and the 486bp S/MAR from the 3' region of the Apolipoprotein B (ApoB) gene (Namciu *et al*, 1998) were cloned into the ssAAV-LP1-hFIXco vector plasmid immediately 3' of the hFIXco cDNA in forward and reverse orientation (ssAAV8-LP1-hFIXco-HPRT-F, ssAAV8-LP1-hFIXco-HPRT-R, ssAAV8-LP1-hFIXco-ApoB-F and ssAAV8-LP1-hFIXco-ApoB-R respectively). To account for any possible artefacts of expression enhancement, a 520bp non-SMAR control element (with some S/MAR like properties) derived from the the Kaposi sarcoma herpes virus (KSHV) genome (Stedman *et al*, 2008) was also cloned downstream of the hFIXco cDNA in forward and reverse orientation (ssAAV8-LP1-hFIXco-KSHV-F and ssAAV8-LP1-hFIXco-KSHV-R respectively) (Figure 3.3).

Each vector used in this study was pseudotyped with serotype 8 capsid protein and initially tested *in-vitro* by transducing 50000 HuH7 cells at a dose of 1×10^5 vg/cell (Figure 3.4). At 72hrs after transduction hFIX levels in cell supernatants taken from ssAAV-LP1-hFIXco-HPRT-F, ssAAV-LP1-hFIXco-HPRT-R and ssAAV-LP1-hFIXco-ApoB-R transduced cells were comparable at $2.494 \pm 0.37\%$, $2.361 \pm 0.61\%$ and $2.739 \pm 0.30\%$ of normal respectively. This

was a respective 2-fold, 4-fold and 23-fold increase in transgene expression as compared to ssAAV-LP1-hFIXco-IFN-R ($1.161 \pm 0.12\%$) (Not significant), ssAAV-LP1-hFIXco-Control ($0.614 \pm 0.09\%$) ($P < 0.05$, One-way ANOVA) and ssAAV-LP1-hFIXco-ApoB-F ($0.1065 \pm 0.95\%$) transduced cells ($P < 0.05$, One-way ANOVA). hFIX levels in supernatants taken from ssAAV-LP1-hFIXco-KSHV-F/R and untransduced cells were not detectable.

3.3.2 Incorporation of HPRT and ApoB S/MARs in AAV expression cassettes enhances transgene expression *in-vivo*

As *in-vitro* hFIX levels were particularly low (because AAV8 is inefficient at transducing cells in culture for reasons that are unknown) (Martino *et al*, 2013), it was necessary to verify these trends *in-vivo*. Each AAV8 vector was administered as a single bolus injection into the tail vein of 6-8 week old immunocompetent male C57/BL76 mice at dose of 4×10^{12} vg/kg (N=3). Plasma hFIX levels were detected by ELISA over a time period of 4 weeks after vector administration. Similar to *in-vitro* observations, highest hFIX levels were observed in cohorts of mice transduced with ssAAV8-LP1-hFIXco-HPRT-F and ssAAV8-LP1-hFIXco-ApoB-R ($1401 \pm 87\%$ and $1540 \pm 149\%$ of normal respectively) (Figure 3.5). This was an approximate 3.5 and 4-fold increase in hFIX levels as compared to ssAAV8-LP1-hFIXco-IFN-R ($398 \pm 79\%$) and ssAAV8-LP1-hFIXco-HPRT-R ($403 \pm 75\%$) cohorts respectively and an approximate 28-fold increase as compared to ssAAV8-LP1-hFIXco-Control transduced mice ($52 \pm 3\%$) ($P < 0.0001$, One-way ANOVA).

Cohorts that received ssAAV8-LP1-hFIXco-ApoB-F, ssAAV8-LP1-hFIXco-KSHV-F and ssAAV8-LP1-hFIXco-KSHV-R vector showed similar hFIX expression levels as compared to those observed in the ssAAV8-LP1-hFIXco-Control transduced animals at $47 \pm 7\%$, $22 \pm 6\%$ and $62 \pm 6\%$ respectively.

After correcting transgene expression levels by proviral copies/cell, ssAAV8-LP1-hFIXco-HPRT-F was observed to be the most potent vector with hFIX levels in these transduced animals 4-fold higher than those observed in the ssAAV8-LP1-hFIXco-ApoB-R cohort ($P < 0.0001$, one way ANOVA) (Figure 3.6). Thus, the increase in transgene expression levels in the HPRT cohorts was not due to improved transduction efficiency as copy numbers were lowest in ssAAV8-LP1-hFIXco-HPRT-F and ssAAV8-LP1-hFIXco-HPRT-R transduced animals at 4.7 ± 1.3 and 2.9 ± 0.7 copies/cell respectively. The high levels of plasma hFIX observed in the HPRT-F cohort were confirmed by western blotting (Figure 3.6).

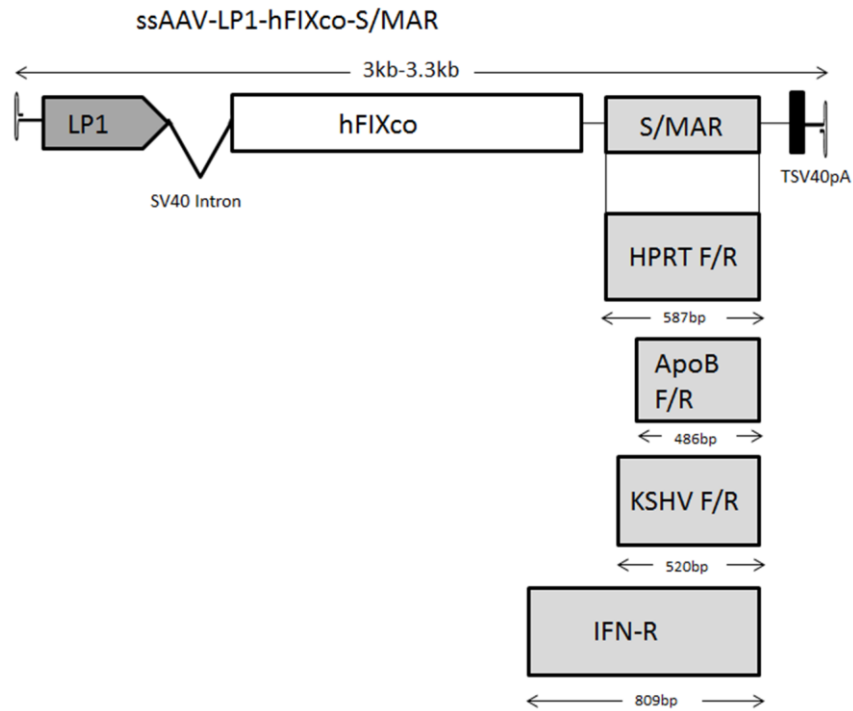


Figure 3.3: Construction of single stranded AAV-hFIXco vectors containing S/MAR elements. Vectors are represented schematically as they are packaged inside the virion. Common features of all vectors are described in figure 3.1. All S/MAR elements were cloned into the multiple cloning site of the control vector plasmid (3' of the codon optimised hFIX cDNA).

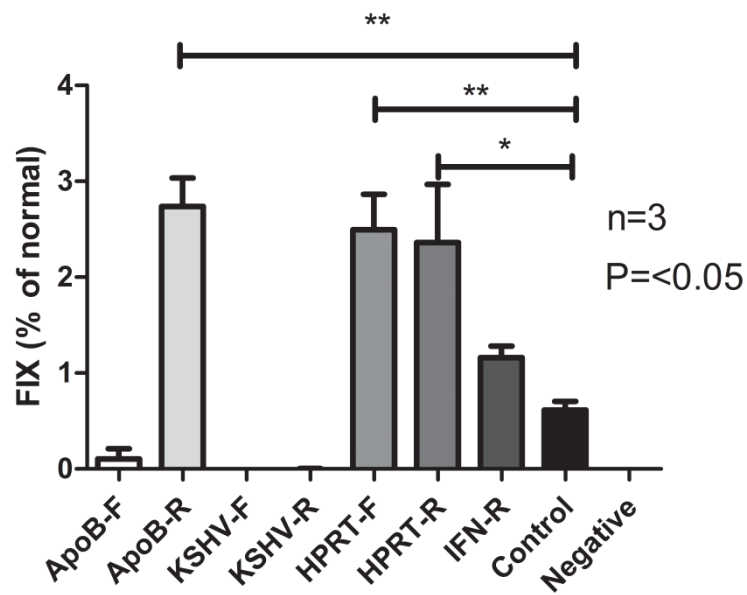


Figure 3.4: Transgene expression in HuH7 cells. FIX levels in supernatants at 72 hours after transduction of HuH7 cells with 1×10^5 vg/cell (n=3) are represented graphically as averages \pm SEM. Negative = supernatants from untransduced cells.

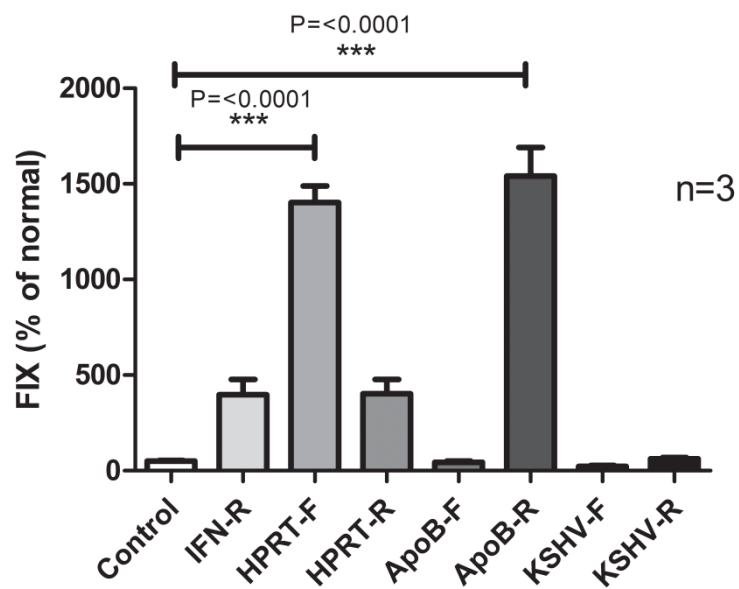


Figure 3.5: Transgene expression in C57BL/6 mice. % FIX levels at 4 weeks post tail-vein administration of 4×10^{12} vg/kg (n=4) of all vectors depicted are represented graphically as averages \pm SEM.

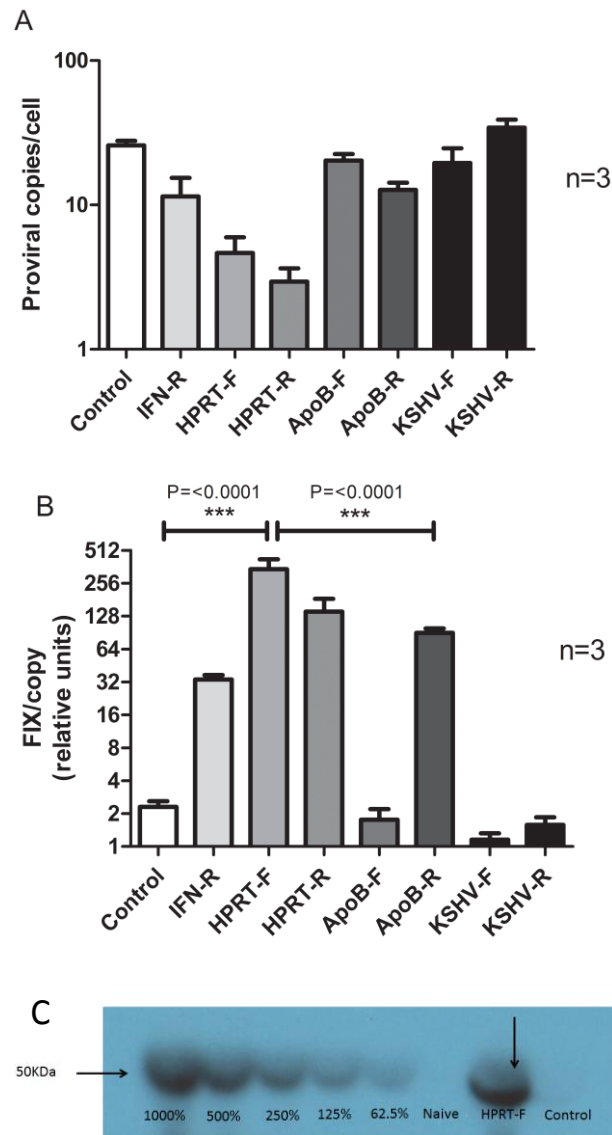


Figure 3.6: Proviral copy number correction. A) Proviral Copies/cell in liver. Proviral copy number was determined by a Q-PCR assay on liver samples collected 4 weeks after transduction and depicted as mean proviral copies/cell \pm SEM. **B) Correction of %FIX levels.** Results are presented as mean %FIX levels \pm SEM corrected for proviral copy number to account for any variation in transduction efficiency. **C) FIX western blot.** FIX antigen levels in murine plasma 4 weeks post tail-vein administration of 4×10^{12} vg/kg of ssAAV-hFIXco-Control and ssAAV-hFIXco-HPRT-F are represented by western blot. Lanes labelled with percentage values refer to serial dilutions of recombinant FIX protein (% of normal). Naive refers to a plasma sample from an untransduced animal. The strongest protein band representing plasma hFIX from a ssAAV8-LP1-hFIXco-HPRT-F transduced animal is highlighted with an arrow.

3.3.3 hFIX mRNA analysis

As the LP1 promoter restricts transgene expression to hepatocytes (Nathwani *et al*, 2006), at 4 weeks after gene transfer, we assessed hFIX mRNA levels in murine liver samples taken from a selected number of cohorts (Figure 3.7). After normalizing hFIX mRNA levels by housekeeping gene transcript levels (GAPDH) and proviral copy number, mRNA levels/copy were greatest in ssAAV8-LP1-hFIXco-HPRT-F animals at 433 ± 132 relative units (RU). This was an approximate 2-fold increase as compared to ssAAV8-LP1-hFIXco-HPRT-R (264 ± 57 RU) and ssAAV8-LP1-hFIXco-IFN-R (176 ± 81 RU) cohorts but a greater than 20-fold increase in transcript levels as compared to ssAAV8-LP1-hFIXco-Control transduced mice (18 ± 6 RU) ($P=0.0451$, one way ANOVA). This trend in mRNA levels is consistent with plasma antigen levels observed in respective cohorts. As such, it is inferred that increased hFIX protein levels observed following transduction with S/MAR containing vectors was, at least in part, due to elevated transcription levels or improved mRNA stability.

3.3.4 HPRT S/MAR element enhances transgene expression at lower vector doses

The ssAAV8-LP1-hFIXco-HPRT-F vector maintained its increased potency in terms of *in-vivo* transgene expression (when compared to ssAAV8-LP1-hFIXco-Control) following administration of a lower dose (4×10^{10} vg/kg) (Figure 3.8). At 4 weeks after vector administration, hFIX levels in the ssAAV8-LP1-hFIXco-HPRT-F cohort were approximately 85-fold higher than that observed in the ssAAV8-LP1-hFIXco-Control cohort ($508\pm 83\%$ and $6\pm 1\%$ of normal respectively) ($P=0.0038$, T test).

Proviral copy numbers in the liver of all animals were comparable at approximately 0.005-0.008 copies/hepatocyte (Figure 3.9). Therefore, the increase in hFIX levels observed following transduction with the ssAAV8-LP1-hFIXco-HPRT-F vector was not due to variation in transduction efficiency. As such this vector may allow for rAAV doses to be minimised without compromising therapeutic effect.

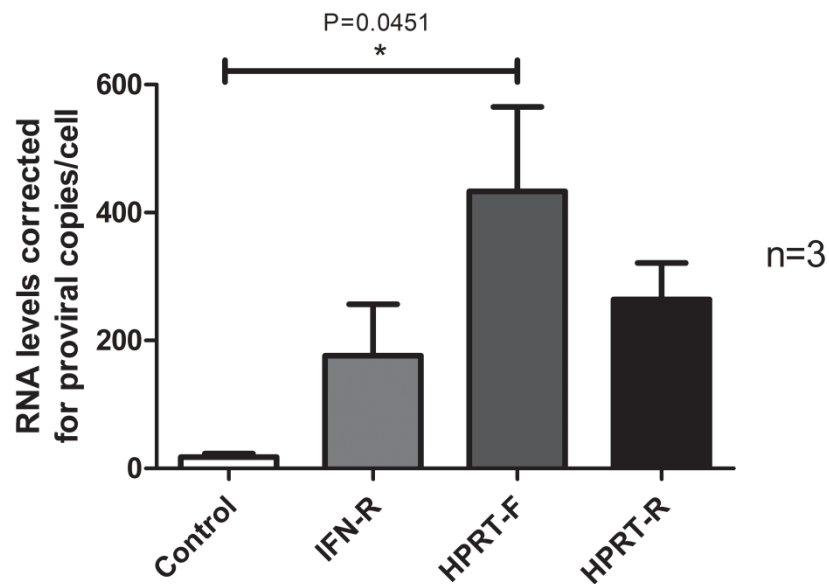


Figure 3.7: FIX mRNA levels in liver. mRNA levels were determined by a Q-PCR assay on cDNA derived from total liver RNA collected 4 weeks after tail-vein administration of 4×10^{12} vg/kg of ssAAV-hFIXco-IFN-R, ssAAV-hFIXco-HPRTF/R and ssAAV-hFIXco-Control into C57BL/6 mice. Results are presented as mean mRNA levels corrected for levels of GAPDH cDNA present in each sample \pm SEM and then corrected for proviral copy number to account for variation in transduction efficiency.

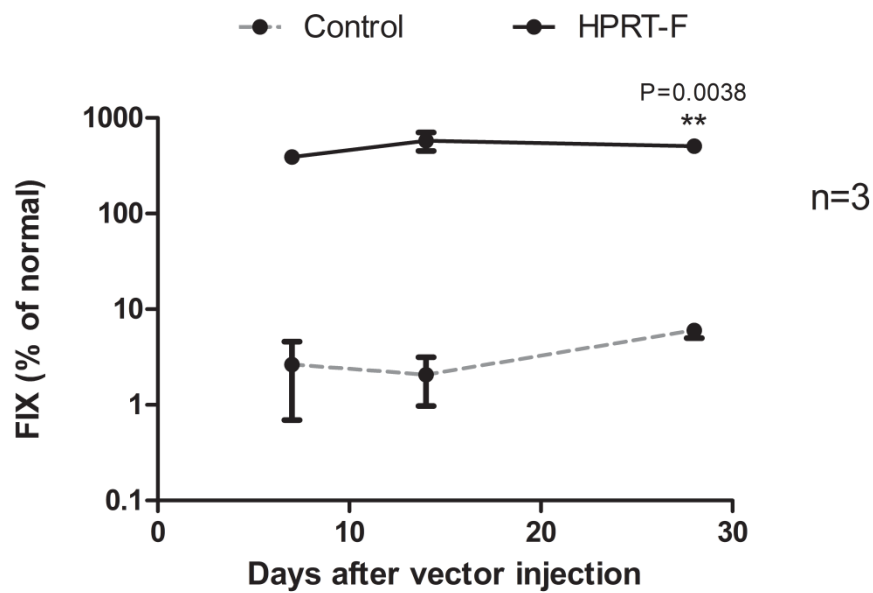


Figure 3.8: FIX expression in male C57BL/6 mice: low dose analysis. Transgene expression profiles over a period of 4 weeks after tail- vein administration of 4×10^{10} vg/kg (n=3) of ssAAV-hFIXco-Control and ssAAV-hFIXco-HPRT-F vectors into 6 to 8 week old immunocompetent male C57BL/6 mice. Results are presented as averages \pm SEM. Mean FIX values at the final time point are significantly different (P=0.0038, T test).

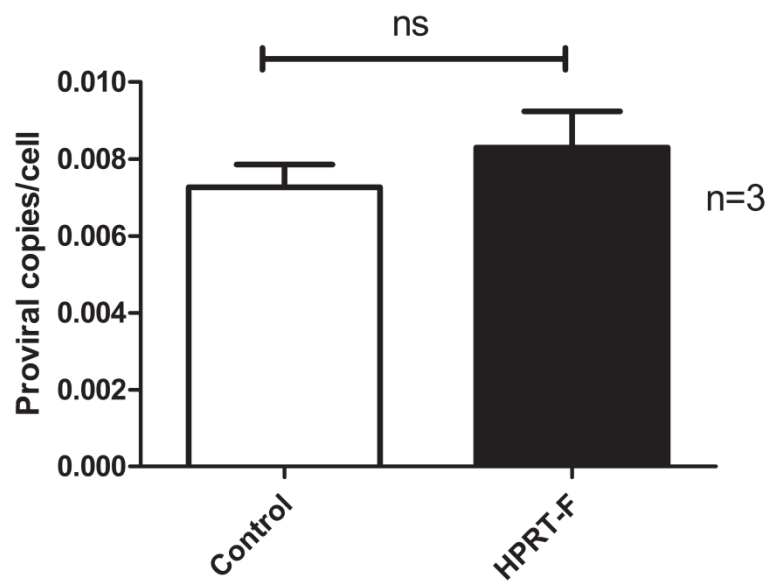


Figure 3.9: Proviral copy number correction. Proviral copy number was determined by a Q-PCR assay on C57BL/6 murine liver samples collected 4 weeks after transduction with ssAAV-LP1-hFIXco-Control and ssAAV-LP1-hFIXco-HPRT-F vectors at a dose of 4×10^{10} vg/kg. Results are depicted as mean proviral copies/cell \pm SEM.

3.3.5 Higher transgene expression with ssAAV8-LP1-hFIXco-HPRT-F and ssAAV8-LP1-hFIXco-IFN-R in nonhuman primates

All work with rhesus macaques was done in collaboration with Andrew Davidoff (St. Jude Children's research hospital Memphis, TN). 4×10^{12} vg/kg of ssAAV8-LP1-hFIXco-Control, ssAAV8-LP1-hFIXco-IFN-R or ssAAV8-LP1-hFIXco-HPRT-F vector was administered to the peripheral vein of male adolescent rhesus macaques as previously described (Nathwani *et al*, 2007). Vector administration was well tolerated with no perturbation of vital signs or liver transaminases (alanine aminotransferase < 45U/L) over a period of 37 weeks after transduction.

Plasma hFIX was detectable within 72 hours of vector administration, reaching peak levels of $53.9 \pm 10\%$ at 5 days in the ssAAV8-LP1-hFIXco-HPRT-F transduced monkey (Figure 3.10). In contrast the animals transduced with ssAAV8-LP1-hFIXco-IFN-R and ssAAV8-LP1-hFIXco-Control had respective peak hFIX levels of 7% and 5% (Figure 4). Similarly, steady state hFIX levels were 4-fold and 3-fold higher in the monkey transduced with ssAAV8-LP1-hFIXco-HPRT-F ($17 \pm 4\%$ of normal) when compared to the animals that received ssAAV8-LP1-hFIXco-Control ($4 \pm 2\%$ of normal) and ssAAV8-LP1-hFIXco-IFN-R ($6 \pm 0.1\%$) respectively. The mean transgene copy number in the liver by Q-PCR was 32 ± 9 , 12 ± 5 and 13 ± 7 proviral copies/cells respectively for the monkeys transduced with ssAAV8-LP1-hFIXco-Control, ssAAV8-LP1-hFIXco-IFN-R and ssAAV8-LP1-hFIXco-HPRT-F. Thus, single stranded AAV vectors containing HPRT and IFN-S/MAR mediated higher FIX expression/copy of proviral DNA when compared to control vector in NHPs (10-fold and 4-fold increase respectively).

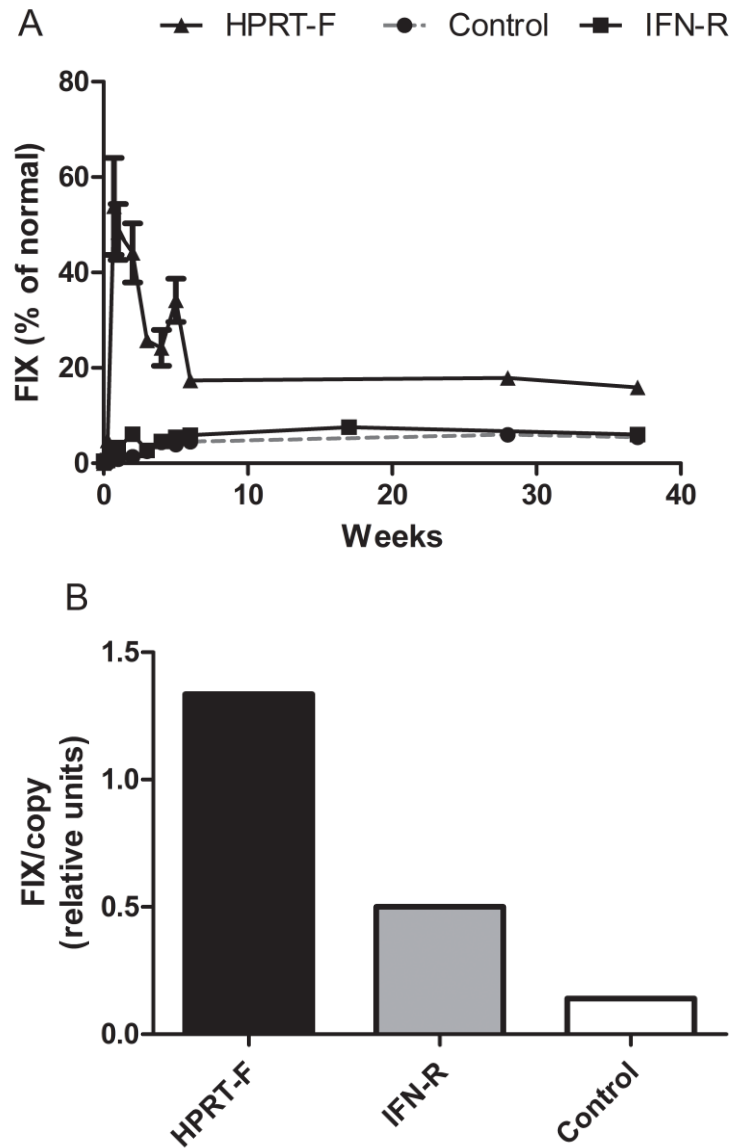


Figure 3.10: Higher potency of S/MAR containing vector in nonhuman primates. A) Transgene expression profiles. FIX levels in rhesus plasma were determined over a period of 37 weeks after peripheral vein administration of 4×10^{12} vg/kg of ssAAV-LP1-hFIXco-HPRT-F, ssAAV-LP1-hFIXco-IFN-R and ssAAV-LP1-hFIXco-Control vectors. Results are depicted as averages of repeat ELISA results \pm SEM ($n=1$). **B) Proviral copy number correction.** To account for variation in transduction efficiency, proviral copy number was determined by a Q-PCR assay on liver samples collected 37 weeks after transduction. Results are depicted as % normal FIX levels corrected for proviral copies per cell.

3.4 Discussion

The need for high vector doses to achieve a therapeutic effect has been observed in multiple rAAV gene therapy clinical studies including trials for lipoprotein lipase deficiency, Leber's congenital amaurosis, α 1-antitrypsin deficiency and haemophilia B (Bainbridge *et al*, 2008; Flotte *et al*, 2004; Flotte *et al*, 2011; Nathwani *et al*, 2011; Stroes *et al*, 2008). In many cases the administration of higher doses appears to coincide with an increased risk of toxicity mediated by T cell responses against capsid antigens (Manno *et al*, 2006; Mingozzi *et al*, 2009; Nathwani *et al*, 2011). To address this matter, this study has systematically evaluated the expression enhancement effect of multiple S/MAR elements in the context of our AAV8-LP1-hFIXco system with the overall aim of improving vector potency in order to minimise dose requirements.

Tail vein administration of 4×10^{12} vg/kg resulted in a 10 to 28-fold increase in plasma hFIX levels in mice transduced with vector containing S/MAR elements as compared to levels achieved with control vectors containing no S/MAR or S/MAR-like KSHV elements. These results are fully consistent with previous studies that document the enhancer effect of S/MARs in other gene transfer systems including retroviral constructs and plasmid DNA (Argyros *et al*, 2008; Kurre *et al*, 2003).

Although these results were found to be statistically significant, it is important to mention that sample size/power calculations should, in future, be used to determine and justify animal numbers used per group. To calculate the sample size (number of animals) required to compare means of 2 normally distributed groups of equal size, the following formula can be used:

$$n = (\sigma_1^2 + \sigma_2^2) (Z_{1-\alpha/2} + Z_{1-\beta})^2 / \Delta^2$$

In this formula n =sample size, σ is the expected standard deviation of the mean, $Z_{1-\alpha/2}$ is constant and dependent on chosen significance level, $Z_{1-\beta}$ is constant and dependent on the chosen probability/power and Δ^2 is the difference between the two expected means (Kadam & Bhalerao, 2010).

In the context of this study, these calculations would be based on the increase in gene expression that one might anticipate based on previous S/MAR related literature. For instance, from previous work, a 2 fold increase in gene expression would be a conservative estimate of expression enhancement when using the IFN β S/MAR vector (Kurre *et al*,

2003). As such, if based on our preliminary studies we assume FIX expression levels of 17% in the control group, we can assume FIX levels of 34% in the group receiving the S/MAR containing vector. As deviation from the mean can be moderately variable in these experiments, a reasonable expected standard deviation of 10% can be implemented. Using the above formula and a significance level (α) of 5% (meaning we accept a 5% possibility of results occurring through chance) and a power ($1-\beta$) of 80% (meaning we accept a 20% chance of generating false negative results) the following can be calculated for this example:

$$n=(10^2 + 10^2) (1.96+0.84)^2/(34-17)^2=5.426$$

= 6 animals per group

(Where $Z_{1-\alpha/2}$ is constant at 1.96 when using a significance level of 5% and $Z_{1-\beta}$ is constant at 0.84 when using a power of 80%.)

In this example, the requirement for 6 animals per group is calculated which was the initial number of mice used in this study per group (see page 77). In future experiments it will also be important to determine the reproducibility of these results by testing S/MAR containing vectors in further groups of animals and with new preparations of AAV vectors. This will allow us to conclusively establish that these observations were not influenced by experimental artefacts such as contamination of vector stocks, degradation of vector or injection/human error.

Following correction for proviral copy number in liver, highest hFIX levels (approximately 150-fold greater than control) were observed with ssAAV8-LP1-hFIXco-HPRT-F vector containing a S/MAR element from the HPRT gene in forward orientation. Interestingly, the orientation of the S/MAR sequences in AAV vectors appears to be important for all three elements used in this study: a feature that has also been observed in the context of retroviral and lentiviral vectors (Auten *et al*, 1999; Dang *et al*, 2000; Kurre *et al*, 2003; Ramezani *et al*, 2003). As the structure of S/MARs in relation to the transgene appears to be the primary determinant of S/MAR activity (as opposed to DNA base composition) the reason why we and others have observed an orientation dependent effect in the context of gene transfer vectors may be purely related to structure.

The 809bp human IFN β S/MAR has previously been shown to prevent repressive epigenetic modifications in the context of episomally maintained plasmid vectors and retroviral vectors (Argyros *et al*, 2011; Argyros *et al*, 2008; Dang *et al*, 2000; Moreno *et al*, 2011;

Ramezani *et al*, 2003). Similarly, the ApoB S/MAR has been shown to have a role in insulating associated transgenes from silencing effects (Namciu *et al*, 1998). However, results from ssAAV8-LP1-hFIXco-HPRT-F transduced animals were somewhat unanticipated as, in contrast, the HPRT S/MAR is primarily documented to support autonomous replication (Sykes *et al*, 1988). As such, one might expect an observation of sustained expression through episome retention as opposed to expression enhancement.

The expression enhancement effect observed with ssAAV8-LP1-hFIXco-HPRTF was reproducible in rhesus macaques with 4-fold increased levels of hFIX observed in animals transduced with 4×10^{12} vg/kg of ssAAV8-LP1-hFIXco-HPRTF as compared to control. However, plasma FIX levels observed in the macaque transduced with ssAAV-LP1-hFIXco-Control were lower than that reported previously for ssAAV-FIX vectors containing the HCR-hAAT regulatory element (peaking at 5% and 14% of normal physiological hFIX levels respectively): suggesting our synthetic small LP1 promoter may not be as strong (Davidoff *et al*, 2005). As such it will be important to test S/MAR elements in AAV vectors with alternative promoters. Nonetheless, consistent with data in mice, the addition of HPRT S/MAR to the LP1-hFIXco expression cassette appears to improve hFIX expression in NHPs. However, larger numbers of monkeys are needed to establish this observation conclusively as this result is currently limited by the use of one animal per group. As such, it is possible that heterogeneity between animals may have influenced these results. For instance, if animals treated with S/MAR containing vectors had lower serum anti-AAV8 antibody titres, it is possible that hFIX expression may be observed as increased due to reduced immune neutralisation of the vector as opposed to the incorporation of S/MAR elements. To rule out this possibility, it will be important to reproduce these results in larger numbers of animals to enable the subsequent generation of statistical conclusions.

In common with episomal plasmids and onco-retroviral vector systems, through a Q-PCR assay, we have found S/MARs to mediate expression augmentation in mice and nonhuman primates through increased levels of transcription or improved RNA stability. At the high dose of 4×10^{12} vg/kg, after correcting for proviral copy numbers, 10-fold and 24-fold higher levels of liver hFIX mRNA were observed in ssAAV8-LP1-hFIXco-IFN-R and ssAAV8-LP1-hFIXco-HPRT-F cohorts compared to ssAAV8-LP1-hFIXco-Control animals respectively. This was fully consistent with results obtained for plasma hFIX antigen levels.

AAV mediated gene transfer can be enhanced with the use of several agents. In addition to HDAC inhibitors this includes androgens (5 alpha dihydrotestosterone) and proteasome

inhibitors (e.g. carbobenzyl-L-leucyl-L-leucyl-L-leucinal and bortezomib) (Jennings *et al*, 2005; Monahan *et al*, 2010). However, the need to administer these drugs before or at the same time as gene transfer adds complexity to the scheduling of vector administration. Furthermore, these drugs give rise to significant side effects that could negatively impact the toxicity profile of the rAAV vector in use. Thus, through the incorporation of S/MAR elements in our LP1- hFIXco expression cassette we have come up with a novel, inbuilt solution to overcome some of the limitations of rAAV gene transfer. As such, this data represents a necessary step towards improving the potency and safety of rAAV vectors for broader clinical use.

However, as this analysis has only involved the use of S/MAR elements in the context of our LP1-hFIXco AAV expression cassette, we cannot rule out the possibility that S/MARs may not have the same effect when incorporated into alternative AAV transcription units. As such it will be important to test S/MARs in conjunction with different transgenes. Nevertheless, this study has clearly demonstrated the beneficial use of matrix attachment regions in the context of a vector that has been shown to work effectively in humans. Thus we have improved the potency of a vector that is applicable to a clinical setting.

To summarise, we have critically evaluated three S/MAR elements in the context of single stranded AAV vectors encoding human FIX in cell lines, mice and rhesus macaques. In all cases S/MAR elements were found to enhance transgene expression. The basic mechanism behind the up regulation of hFIX when using S/MARs was evaluated by analysing hFIX mRNA levels following gene transfer; our results are indicative of enhanced transcription levels or improved mRNA stability with S/MARs. Taken as a whole, S/MARs may help to achieve the overall goal of improved AAV vector potency.

CHAPTER 4 MATRIX ATTACHMENT REGION DELETION ANALYSIS

4.1 Introduction

4.1.1 Recombinant AAV packaging capacity

The packaging capacity of recombinant adeno-associated virus is widely accepted to be limited to the size of wild type genomes (approximately 4.7kb). The use of rAAV in gene transfer is therefore largely restricted to the treatment of disorders whereby the coding sequence of the therapeutic gene is equivalent to or shorter than 4.7Kb (Grieger & Samulski, 2005). Consequently, research into rAAV-mediated gene therapy for many disorders (including some forms of Leber congenital amaurosis, cystic fibrosis, Haemophilia A and Duchenne muscular dystrophy) has been somewhat impeded; as a result multiple groups have further investigated the upper limits of AAV packaging. In the context of single stranded rAAV vectors pseudotyped with serotype 5 capsid protein, one group has previously demonstrated the ability to package expression cassettes containing murine *Abca4*, human *MYO7A*, and human *CEP290* genes for the potential treatment of common sensorineural blinding diseases known as recessive Sargardt disease (rSTG), Usher syndrome (USH) and Leber congenital amaurosis (LCA) respectively (respective final cassette sizes of 8.9, 8.1 and 8.9kb)(Allikmets, 1997; Allocca *et al*, 2008; den Hollander *et al*, 2006; Keats & Corey, 1999). However, in a similar study, this observation was not reproduced and by southern blot analysis of vector DNA run on alkaline agarose gels, AAV vectors pseudotyped with serotype 2, 5 and 8 capsids were deemed unable to tolerate the packaging of genomes exceeding 5.2kb (demonstrated by the presence of heterogeneous; fragmentary genome populations) (Wu *et al*, 2010).

It has previously been shown that the limitation of packaging capacity can be overcome by splitting expression cassettes between two separate vectors (Duan *et al*, 2000; Nakai *et al*, 2000; Senapathy & Carter, 1984; Sun *et al*, 2000; Yan *et al*, 2000). After co-transduction, the two separate halves of the vector genome become reconstituted through ITR mediated intermolecular concatamerization: thus providing a complete platform for transgene expression. Two examples of dual vector strategies include the use of trans-splicing or homologous recombination between single stranded AAV genomes (described in figure 4.1). However, in a study carried out by Duan *et al* using the β -galactosidase gene as a template, the efficiency of both dual vector strategies was observed to be significantly

lower in comparison to the administration of a single vector only. In this study, trans-splicing and homologous recombination vectors provided respective β -galactosidase activity of 4.28% and 0.37% of that observed following transduction with a single vector only 7 weeks after injection of 5×10^{10} vg into the anterior tibialis muscle of C57BL/6 mice (Duan *et al*, 2001). As such, for efficient transgene expression to be achieved, rAAV gene transfer is limited to the capacity of a single vector.

The issue of packaging capacity becomes even more pertinent in the context of self-complementary vectors. As previously mentioned, self-complementary vectors are designed to overcome the rate limiting step of single stranded to double stranded conversion of rAAV genomes. To achieve this effect, both plus and minus strands must be packaged within the same virion (Figure 4.2); as such, the packaging capacity of self-complementary vectors is reduced by approximately 50% (2.3kb)(McCarty *et al*, 2003; McCarty *et al*, 2001).

As a result of this limitation, the first aim of this chapter was to reduce the space occupied by S/MAR elements within our LP1-hFIXco expression cassette. This was achieved by carrying out a deletion analysis on the IFN β and HPRT S/MAR sequences in order to determine the minimal sequences required for factor IX expression enhancement.

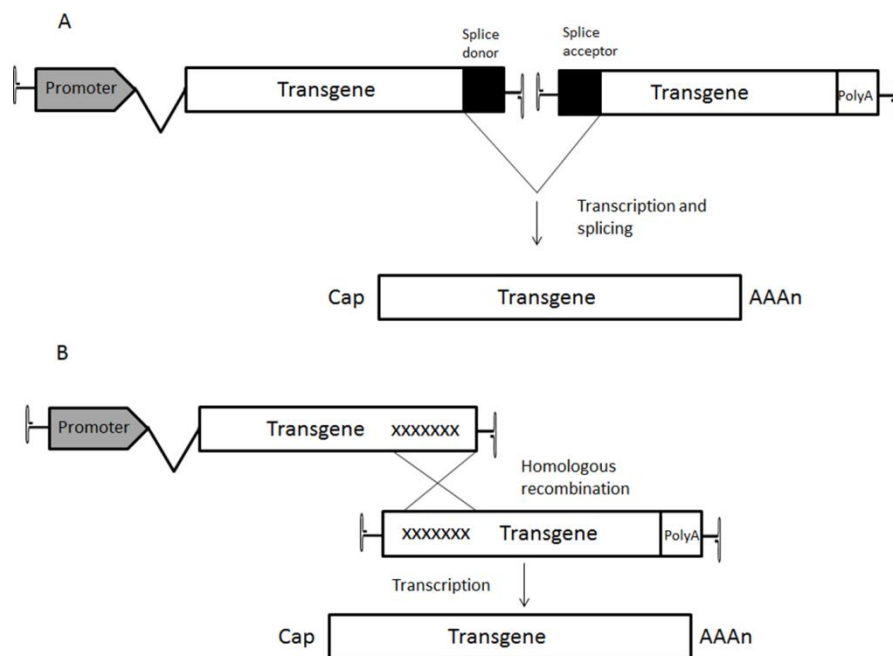


Figure 4.1: Split AAV Vector Strategies. Split vector strategies are represented schematically. **A) Trans splicing vectors.** Each vector contains either the splice donor or splice acceptor site of a common intron. Following concatemerisation the two halves of the vector are reconstituted by cellular splicing machinery. **B) Overlapping vectors.** Overlapping vectors contain a large region of identical sequence (xxxxxxx). This enables homologous recombination and subsequent reconstitution of the expression cassette.

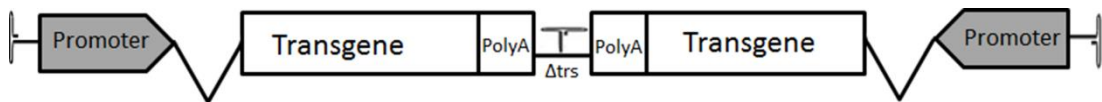


Figure 4.2: Schematic of a self-complementary AAV vector. A self-complementary AAV vector is represented schematically as it would be packaged inside a virion. Sense and antisense DNA strands are contained in the same vector (each having a maximum size of approximately 2.3Kb). The vector folds at the mutated central ITR (Δ trs) for the joining of complementary DNA strands.

4.1.2 Identifying regulatory sequences in S/MARs

The second aim of the S/MAR deletion analysis was to identify sequence motifs that may contribute to the enhancer activity of S/MARs. Through studies such as protein binding microarray (PBM) and chromatin immunoprecipitation followed by deep sequencing (ChIP-Seq) it has become possible to identify key regulatory sequences involved in transcription factor (TF) binding (Barski & Zhao, 2009; Berger & Bulyk, 2009). With this information, it is possible to generate computational models of transcription factor binding affinity (representations of biological sequence motifs) referred to as position weight matrix (PWM) models (Stormo, 2000). Databases containing information on PWMs can therefore be used for the *in-silico* elicitation of motif sequences from a user provided input sequence (Bailey *et al*, 2006). As each motif is linked to a particular group of transcription factors, the user is able to assign potential biological roles to the motifs elicited (Buske *et al*, 2010). Using the gene ontology for motifs (GOMO) algorithm, descriptive terms of possible biological function (gene ontology (GO) terms) are provided; as such there is potential to identify regions of an input sequence that are involved in processes such as gene expression, chromatin assembly or mRNA processing (to name but a few GO terms) (Ashburner *et al*, 2000; Buske *et al*, 2010). Thus, through such analysis, we aimed to identify potential motifs that contribute to the enhancer effect of potent S/MAR fragments.

As primary DNA sequence is a lesser determinant of S/MAR activity, in our deletion analysis, truncated S/MARs were either generated arbitrarily or by identifying the strongest regions of base unpairing through computational analysis (SID profiles). S/MAR fragments were cloned into the 3' region of our AAV-LP1-hFIXco expression cassette to systematically assess their impact on transgene expression in cell lines and in animal models. In this study we identified two S/MAR fragments capable of enhancing hFIX transgene expression in HuH7 cells and C57BL/6 mice (IFN β S/MAR fragment 2 and HPRT S/MAR fragment 2b). HPRT fragment 2b also demonstrated potent enhancer activity in the context of a self-complementary vector both *in-vitro* and *in-vivo*.

4.2 Materials and methods

4.2.1 AAV-hFIX vector production and purification

The ssAAV vector encoding hFIX is described in section 3.2.1. Fragments of the IFN β S/MAR were generated using the standard HotStar Taq PCR method described in section 2.1.2 with pAV-LP1-hFIXco-IFN-R plasmid DNA used as a template. HPRT S/MAR fragments were generated using the standard Phusion High-Fidelity DNA Polymerase PCR method described in section 2.1.2 with pAV-LP1-hFIXco-HPRT-F plasmid used as template DNA. All 5' primers used to generate IFN β and HPRT S/MAR fragments contained the KpnI restriction site (GGTACC) and all 3' primers contained the NotI restriction site (GCGGCCGC) for subsequent digestion of PCR products and ligation into the multiple cloning site of KpnI-NotI digested pAV-LP1-hFIXco-MCS-TSV40pA plasmid DNA. The following primer pairs were used for PCR amplification of S/MAR fragments:

IFN β FR1 5': 5'-ATCGGGTACCCAAGTTGTCAT-3'

IFN β FR1 3': 5'-ATCGGCCGCGCCTTATTTTTT-3'

IFN β FR2 5': 5'-ATCGGGTACCATTTTACAATG-3'

IFN β FR2 3': 5'-ATCGGCCGCGCCTTTTAAATT-3'

IFN β FR3 5': 5'-ACTGGGTACCCAAGTCCTAA-3'

IFN β FR3 3': 5'-ATCGGCCGCGCACTGTTCTC-3'

HPRT FR1 5': 5'-CGCGGGTACCCAAGTTATAT-3'

HPRT FR1 3': 5'-AATTGCGGCCGCGATAATTTG-3'

HPRT FR2 5': 5'-CGCGGGTACCCAAGGAGAT-3'

HPRT FR2 3': 5'-ATATGCGGCCGCTGACAGAGC-3'

HPRT FR2a 5': 5'-CGCGGGTACCAGGTGTTTTT-3'

HPRT FR2a 3': 5'-ATATGCGGCCGCCAACTTCT-3'

HPRT FR2b 5': 5'-GCGCGGGTACCGGAAATATTA-3'

HPRT FR2b 3': 5'-ATATGCGGCCGCTGACAGAGC-3'

Annealing temperatures used to generate IFN β FR1, IFN β FR2, IFN β FR3, HPRT FR1, HPRT FR2, HPRT FR2a and HPRT FR2b were 56.8, 53.9, 61.8, 57.3, 64.7, 61.3 and 60.3°C respectively. Following the PCR reactions S/MAR fragments were electrophoresed on 1% agarose gels and purified by gel extraction methods as detailed in sections 2.1.3 and 2.1.4. NotI and KpnI Restriction digests were carried out for 3 hours at 37°C on total extracted S/MAR fragment DNA in 50 μ l reactions containing 10% NEBuffer 2 and 1% BSA (standard conditions described in 2.1.3). To prepare the vector backbone 10 μ g of pAV-LP1-hFIXco-MCS-TSV40pA plasmid DNA was NotI and KpnI digested 3 hours at 37°C in a 100 μ l reaction with the same conditions as described above. Vector backbone DNA was purified by gel extraction and ligated with S/MAR fragment DNA as detailed in 2.1.7. Subsequent transformation was carried out as per standard protocol (section 2.1.8). Colonies were expanded and screened as described in 2.1.8 and enzymes used for standard 10 μ l screening digests (carried out at 37°C for 1 hour) were SspI (IFN β fragments 1 and 3) NdeI (IFN β fragment 2) and PstI together with NotI (HPRT fragments 1-2b). Competent E.coli containing correct plasmid constructs were expanded as described in section 2.1.8.

To generate self-complementary vector plasmids, a DNA fragment containing the MCS and TSV40pA was first generated using the standard Phusion High-Fidelity DNA Polymerase PCR method described in section 2.1.2 with pAV-LP1-hFIXco-MCS-TSV40pA plasmid DNA as a template. The 5' primer was designed with the addition of a BbsI restriction site (GAAGAC) for subsequent BbsI digestion of the PCR product and ligation of the sticky-blunt fragment into vector backbone DNA (Sc-LP1-hFIXco-SV40pA) with a 5' BbsI digested end and 3' blunt end. Primer sequences used for this PCR were 5': 5'-ATGAGAAGACCAAGCTGACCTG-3' and 3': 5'-TGTAGTTAATGATTACAAATAAAGC-3'. The annealing temperature used was 50.9°C. To generate the vector backbone 10 μ g of Sc-LP1-hFIXco-SV40pA plasmid DNA was digested with SpeI-HF (high fidelity) for 3 hours at 37°C with 10% NEBuffer 4 in a standard 100 μ l reaction. Total backbone DNA was then gel extracted and blunt ends were generated as described in 2.1.5. Total backbone DNA was then digested with BbsI for 2 hours at 37°C with 10% NEBuffer 2 in a standard 50 μ l reaction. The MCS-TSV40pA PCR product was gel purified and digested with BbsI for 2hrs as described above. Ligation, transformation and plasmid propagation were carried out as previously described. Screening digests for the

detection of correct Sc-LP1-hFIXco-MCS-TSV40pA construct were carried out as standard 1 hour 10µl reactions using EcoRI and NotI restriction enzymes (double digest).

To insert HPRT fragment 2b into the multiple cloning site of Sc-LP1-hFIXco-MCS-TSV40pA, standard Phusion High-Fidelity DNA Polymerase PCR was carried out to amplify fragment 2b using the pAV-LP1-hFIXco-FR2b-tSV40pA plasmid as a template. Primers were designed with KpnI restriction sites for subsequent cloning of fragment 2b into KpnI digested Sc-LP1-hFIXco-MCS-TSV40pA DNA. Primer sequences used for this PCR were 5': 5'-GGCGTGGTACCGGAAATATTA-3' and 3': 5'-TGAGGTACCGCTGACAGAGCA-3'. The annealing temperature used was 60.3°C. Total fragment 2b and 10µg Sc-LP1-hFIXco-MCS-TSV40pA DNA was digested with KpnI for 3 hours at 37°C with 10% NEBuffer 1 and 1% BSA in standard 50µl and 100µl reactions respectively. Vector backbone DNA was then alkaline phosphatase treated as described in 2.1.6. Subsequent cloning steps were carried out as previously described with SspI and PstI double digests used for 10µl screening reactions.

All plasmids generated were sequenced to ensure the presence of correct DNA inserts (data not included). All plasmids were also screened for the presence of intact ITRs using standard 10µl AhdI and BglII restriction digests (digested for 1 hour at 37°C).

All vectors were made by the adenovirus-free transient transfection method described in section 2.2.2, using a chimeric AAV2 Rep-8Cap packaging plasmid (pAAV8-2) and an adenoviral helper plasmid. Vectors were purified as detailed in 2.2.3. All vector titres were determined by standard quantitative real-time PCR (Q-PCR) and coomassie gel methods (sections 2.2.4 and 2.2.6 respectively). HPRT short fragment vectors were additionally titred by alkaline agarose gel electrophoresis as described in section 2.2.5.

4.2.2 Animal studies

All procedures were performed in accordance with institutional guidelines as previously described. Tail-vein administration of rAAV vector particles was performed in 6 to 8 week old immunocompetent male C57BL/6 mice as single bolus injections (maximum volume of 200µl) using 1ml syringes. Prior to injection or bleeding, mice were briefly warmed at 39°C to dilate the tail vein. For the IFNβ S/MAR vectors, mice were injected with 4×10^{12} vg/kg and killed 4 weeks after vector administration. HPRT vectors were injected at a dose of 4×10^{10} vg/kg and mice were killed 2 weeks after administration. Blood samples were taken from the tail vein at one week intervals over the course of the experiment. To separate

plasma, blood samples were spun at 4000× g in tri-sodium citrate buffer for 15 minutes at 4°C. In all cases livers were harvested for subsequent molecular analysis.

4.2.3 HuH7 cell culture and transduction

HuH7 cells were cultured as described in section 2.4.2. Transduction of HuH7 was carried out as per standard protocol (section 2.4.3) using 1×10^7 vg of each vector.

4.2.4 Determination of FIX levels

Human FIX antigen levels in cell supernatants and murine plasma samples were determined by enzyme-linked immunosorbent assay (ELISA) as previously described (section 2.4.4 and 3.2.4).

Western blotting to determine hFIX protein levels was carried out as previously described in section 2.4.6 with prior antigen immunoprecipitation carried out to minimize non-specific background (section 2.4.5).

4.2.5 Molecular studies

Proviral copy number was determined by standard Q-PCR protocol as described in section 2.4.7 and 3.2.5.

4.3 Results

4.3.1 Deletion analysis of IFN- β S/MAR identifies a smaller region with potent enhancer activity

As S/MARs do not contain obvious consensus sequences, in order to identify the smallest region required for enhancement of hFIX expression in the context of rAAV vectors, the 809bp IFN- β S/MAR was arbitrarily divided into three fragments of approximately 300bp. Each fragment was then cloned into the ssAAV-LP1-hFIXco vector plasmid downstream of the hFIXco cDNA in reverse orientation (Figure 4.3). ssAAV8-LP1-hFIXco-FR1, ssAAV8-LP1-hFIXco-FR2 and ssAAV8-LP1-hFIXco-FR3 vectors contained the proximal 290bp, central 297bp or distal 375bp of the IFN β S/MAR respectively. Each ssAAV expression cassette containing a truncated IFN- β S/MAR fragment was pseudotyped with serotype 8 capsid protein and initially tested by *in-vitro* transduction of HuH7 cells at a dose of 1×10^7 vg/cell. For comparison a group of cells was transduced with the same dose of ssAAV8-LP1-hFIXco-IFN-R containing the full 809bp IFN- β S/MAR.

By this analysis, the highest levels of hFIX were observed in cells transduced with ssAAV-LP1-hFIXco-FR2 vector at $0.575 \pm 0.03\%$ of normal (Figure 4.4). This was significantly higher than hFIX levels observed with all other vectors tested ($P < 0.0001$, one way ANOVA) with an approximate increase of 2-fold as compared to ssAAV-LP1-hFIXco-IFN R ($0.312 \pm 0.045\%$) and ssAAV-LP1-hFIXco-FR1 ($0.245 \pm 0.030\%$) transduced cells and a respective 4-fold and 5-fold increase as compared to ssAAV-LP1-hFIXco-Control ($0.160 \pm 0.014\%$) and ssAAV-LP1-hFIXco-FR3 ($0.114 \pm 0.005\%$) transduced cells.

As hFIX expression levels observed *in-vitro* were particularly low, it was necessary to verify trends in transgene expression *in-vivo*. As such, each vector was administered as a single bolus injection into the tail vein of 6-8 week old male C57BL/6 mice ($n=4$) at a dose of 4×10^{12} vg/kg. Transduction efficiency was assessed at 4 weeks after gene transfer by assessing plasma hFIX levels and transgene copy number in the liver. At 4 weeks post injection mice transduced with ssAAV8-LP1-hFIXco-IFN-R expressed hFIX at $398 \pm 79\%$ of normal levels (Figure 4.5). Human FIX expression in the cohorts transduced with ssAAV8-LP1-hFIXco-FR1 or ssAAV8-LP1-hFIXco-FR3 was comparable at $467 \pm 19\%$ and $406 \pm 42\%$ of normal respectively. In contrast, transduction with ssAAV8-LP1-hFIXco-FR2 resulted in a significant threefold increase in hFIX expression to $1202 \pm 205\%$ of normal ($P < 0.0001$, one way ANOVA). Observed trends in transgene expression were verified by western blot to

detect hFIX protein in murine plasma samples taken at 4 weeks post vector administration (Figure 4.5). Collectively, these results suggest the possible presence of repressive motifs in fragments 1 and 3.

To confirm that these observations were not due to increased transduction efficiency with S/MAR containing vectors, all results were normalised by genome copies per hepatocyte as determined by a Q-PCR assay on transduced liver DNA samples. Although average values of copies per cell varied between individual cohorts (7.7 ± 0.9 to 27.6 ± 1.9), overall trends of transgene expression levels remained unchanged after correcting hFIX levels (Figure 4.6). Indeed by this analysis the ssAAV-LP1-hFIXco-FR2 vector maintained the approximate 3-fold advantage over ssAAV-LP1-hFIXco-IFN-R with normalised hFIX levels of 86.9 ± 12 RU (relative units) and 33.6 ± 3.4 RU respectively.

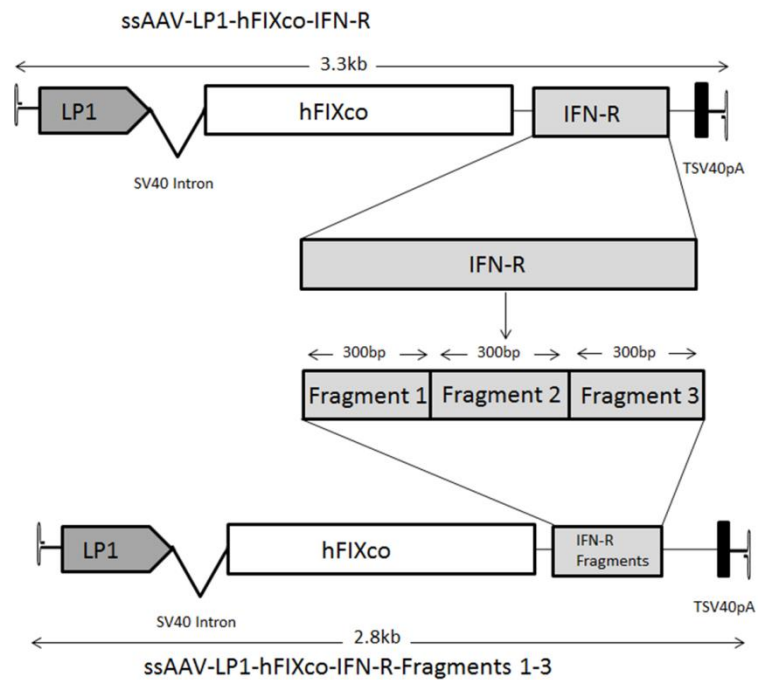


Figure 4.3: Construction of single stranded AAV-hFIXco vectors containing truncated IFN β S/MAR fragments. Vectors are represented schematically as they are packaged inside the virion. Common features of all vectors are described in figure 3.1. IFN β S/MAR fragments were generated by a standard PCR method and cloned immediately downstream of the hFIXco cDNA in reverse orientation. ssAAV-LP1-hFIXco-IFN-R and vector genomes containing IFN β S/MAR fragments are approximately 3.3Kb and 2.8Kb in size respectively.

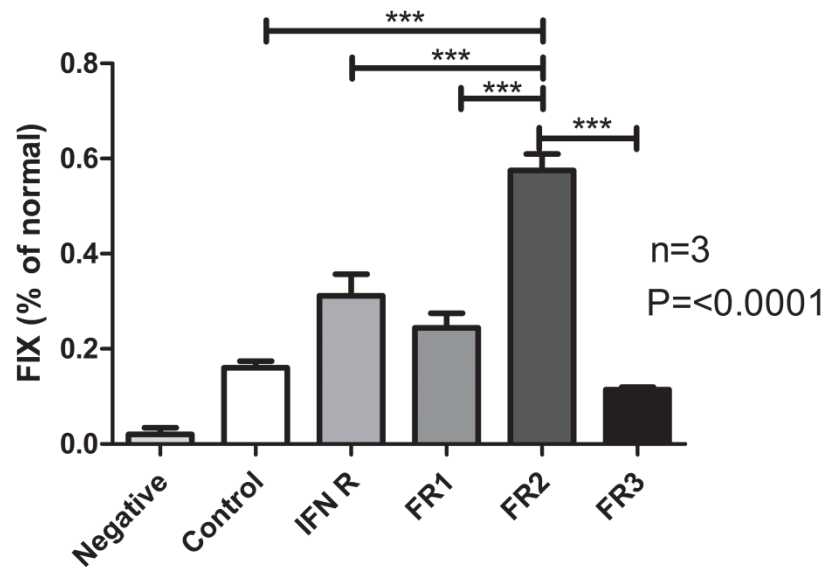


Figure 4.4: Transgene expression in HuH7 cells. FIX levels in supernatants at 72 hours after transduction of HuH7 cells with 1×10^7 vg/cell (n=3) are represented graphically as averages \pm SEM. Negative = untransduced cell supernatants. Control, IFN-R, FR1, FR2 and FR3 refers to ssAAV-LP1-hFIXco-control, ssAAV-LP1-hFIXco-IFN-R, ssAAV-LP1-hFIXco-FR1, ssAAV-LP1-hFIXco-FR2 and ssAAV-LP1-hFIXco-FR3 vectors respectively.

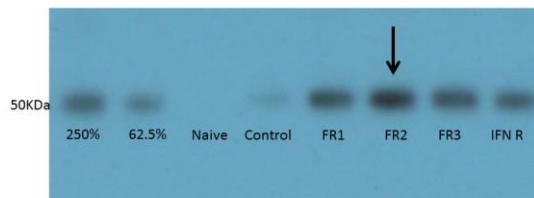
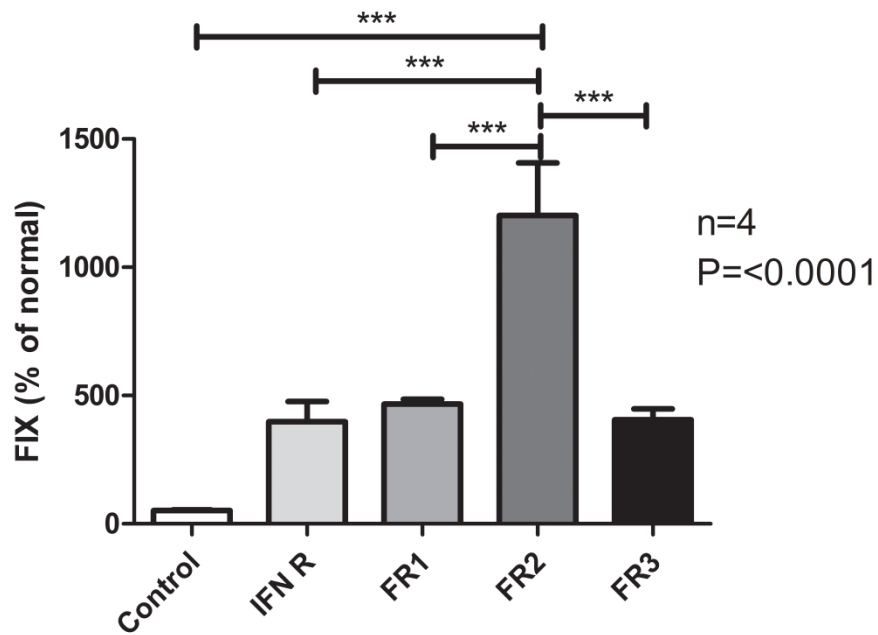


Figure 4.5: Transgene expression in C57BL/6 mice. Top) % FIX levels at 4 weeks post tail-vein administration of 4×10^{12} vg/kg ($n=4$) of all vectors depicted are represented graphically as averages \pm SEM. Bottom) FIX antigen levels in murine plasma 4 weeks after administration of 4×10^{12} vg/kg of all vectors depicted are represented by western blot. 250% and 62.5% refers to the amount of recombinant hFIX protein (% of normal) loaded into each respective well. Naïve refers to a plasma sample from an untransduced animal. The strongest protein band (representing plasma hFIX from a ssAAV8-LP1-hFIXco-FR2 transduced animal) is highlighted with an arrow.

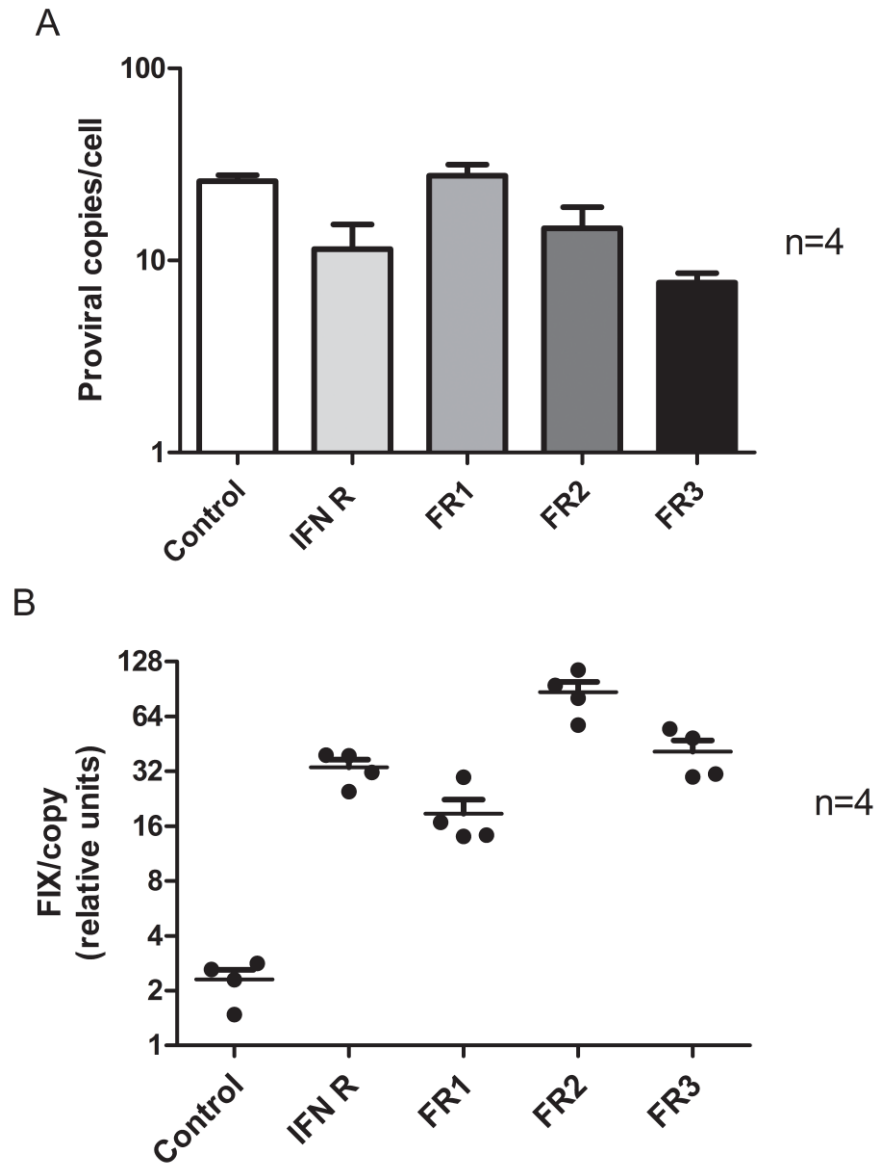


Figure 4.6: Proviral copy number correction. A) Proviral Copies/cell in liver. Proviral copy number was determined by a Q-PCR assay on murine liver samples collected 4 weeks after transduction and depicted as mean proviral copies/cell \pm SEM. **B) Correction of %FIX levels.** Results are presented as mean %FIX levels \pm SEM corrected for proviral copy number to take account variation in transduction.

4.3.2 Deletion analysis of HPRT S/MAR identifies a smaller region containing core enhancer activity

In a separate study the HPRT S/MAR was divided into four fragments. S/MAR fragments in this analysis were chosen using the *in-silico* SIDD profiling technique that serves to map regions of DNA helix unwinding (an S/MAR property) within a given sequence (Benham *et al*, 1997). By this method two regions requiring low theoretical energy levels to undergo DNA strand separation were identified in the HPRT S/MAR sequence (analysed in the context of the full ssAAV expression cassette). Fragment 1 of the HPRT S/MAR corresponds to the proximal 150bp region of helix destabilization whilst fragment 2 corresponds to a central 250bp region. Fragment 2 was then further subdivided into fragments of 90bp and 130bp (fragments 2a and 2b respectively) (Figure 4.7).

Each ssAAV expression cassette containing a truncated HPRT S/MAR fragment was pseudotyped with serotype 8 capsid protein and assessed *in-vitro* by transducing HuH7 cells at a dose of 1×10^7 vg/cell. For comparison a group of cells was transduced with the ssAAV8-LP1-hFIXco-HPRT F vector containing the full 587bp HPRT S/MAR at the same dose. Highest levels of hFIX expression were observed in ssAAV-LP1-hFIXco-HPRT-F and ssAAV-LP1-hFIXco-FR2b transduced cells at $4.313 \pm 0.009\%$ and $4.079 \pm 0.830\%$ respectively (Figure 4.8). This was a respective 3-fold, 7-fold and 12-fold increase as compared to ssAAV-LP1-hFIXco-FR2 ($1.463 \pm 0.330\%$), ssAAV-LP1-hFIXco-FR2a (0.586 ± 0.045) and ssAAV-LP1-hFIXco-FR1 ($0.344 \pm 0.081\%$) transduced cells ($P < 0.05$, one way ANOVA).

To verify trends of transgene expression *in-vivo* all vectors were administered as a single bolus injection into the tail vein of 6-8 week old male C57Bl/6 mice ($n=3$) at a dose of 4×10^{10} vg/kg (determined by alkaline gel titration). hFIX levels were assessed 2 weeks after vector administration and variations in transduction efficiency were determined by proviral copy number analysis in the liver. Highest hFIX expression levels were observed in the ssAAV8-LP1-hFIXco-HPRT-F transduced cohort at $46 \pm 9\%$ of normal (Figure 4.9). This was an approximate 11.5 and 15-fold increase in transgene expression as compared to ssAAV8-ssAAV8-LP1-hFIXco-FR1 ($4 \pm 1\%$) and ssAAV8-LP1-hFIXco-FR2a ($3 \pm 2\%$) transduced animals respectively. However, hFIX levels observed in the LP1-hFIXco-FR2 and ssAAV8-LP1-hFIXco-FR2b cohorts were not found to be significantly different to those observed in ssAAV8-LP1-hFIXco-HPRT-F transduced mice ($P > 0.05$, one way ANOVA) with hFIX levels in these cohorts reaching $24 \pm 5\%$ and $35 \pm 7\%$ of normal respectively.

Changes in transgene expression were not accounted for by discrepancy in transduction efficiency as average proviral copy number in the liver of mice transduced with each of the 5 different vectors was comparable at approximately 0.5 ± 0.1 to 2.6 ± 2.3 copies/hepatocyte (Figure 4.10A). Mean %hFIX/copy levels were not found to be significantly different between ssAAV8-LP1-hFIXco-FR2, ssAAV8-LP1-hFIXco-FR2b and ssAAV8-LP1-hFIXco-HPRT-F ($P > 0.05$, one way ANOVA) at 52.4 ± 26.6 RU, 68.5 ± 7.7 RU and 97.1 ± 29.5 RU respectively (Figure 4.10B). In agreement with *in-vitro* data, these results collectively suggest that the 130bp HPRT fragment 2b present in ssAAV8-LP1-hFIXco-FR2, ssAAV8-LP1-hFIXco-FR2b and ssAAV8-LP1-hFIXco-HPRT-F vectors may contain the core elements required for enhancing the AAV transgene expression *in-vivo*.

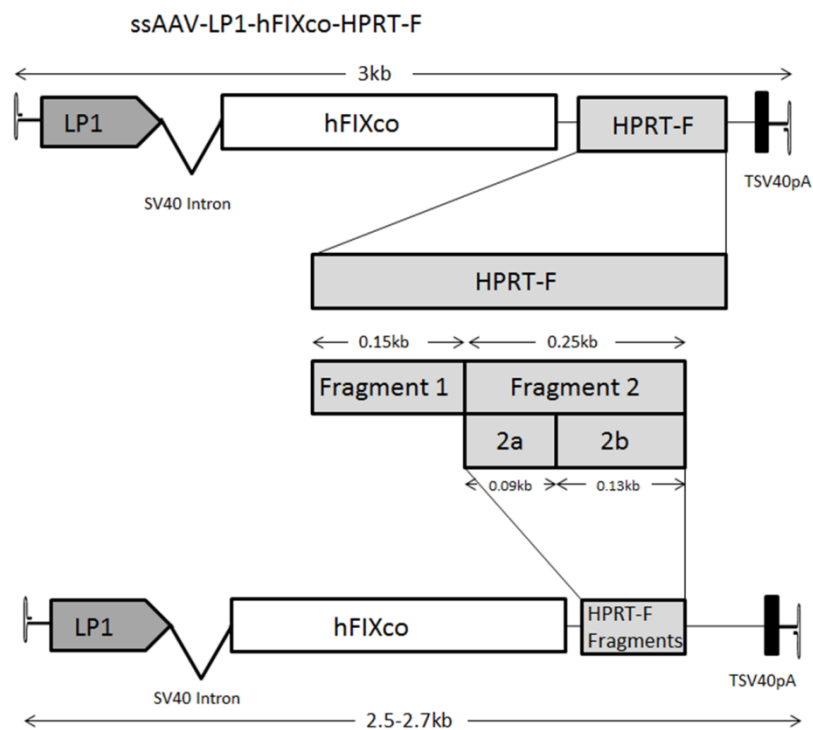


Figure 4.7: Construction of single stranded AAV-hFIXco vectors containing truncated HPRT S/MAR fragments. Vectors are represented schematically as they are packaged inside the virion. HPRT S/MAR fragments were generated by a standard PCR method and cloned immediately downstream of the hFIXco cDNA in forward orientation (FR1, FR2, FR2a and FR2b).

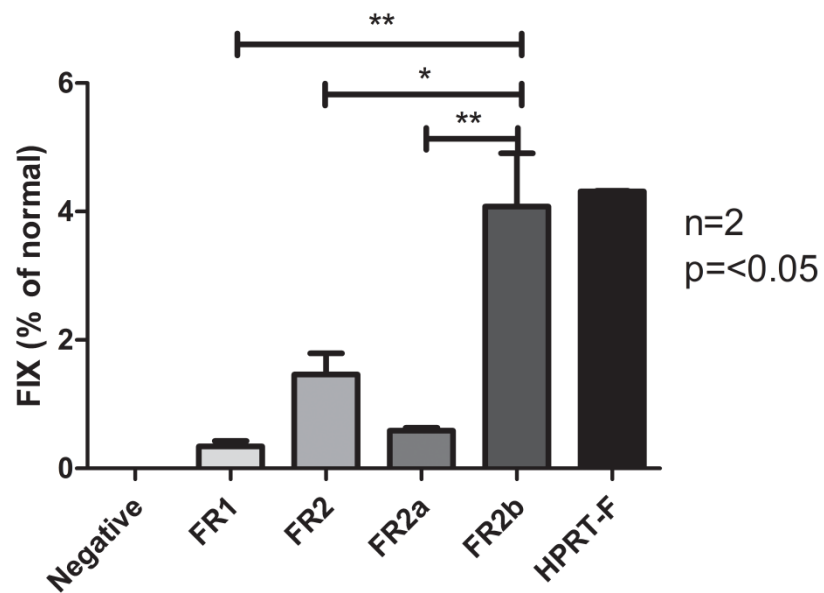


Figure 4.8: Transgene expression in HuH7 cells. FIX levels in supernatants at 72 hours after transduction of HuH7 cells with 1×10^7 vg/cell (n=3) are represented graphically as averages \pm SEM. Negative = untransduced cell supernatants. Control, HPRT-F, FR1, FR2 FR2a and FR2b refers to ssAAV-LP1-hFIXco-control, ssAAV-LP1-hFIXco-HPRT-F, ssAAV-LP1-hFIXco-FR1, ssAAV-LP1-hFIXco-FR2, ssAAV-LP1-hFIXco-FR2a and ssAAV-LP1-hFIXco-FR2b transduced cells respectively.

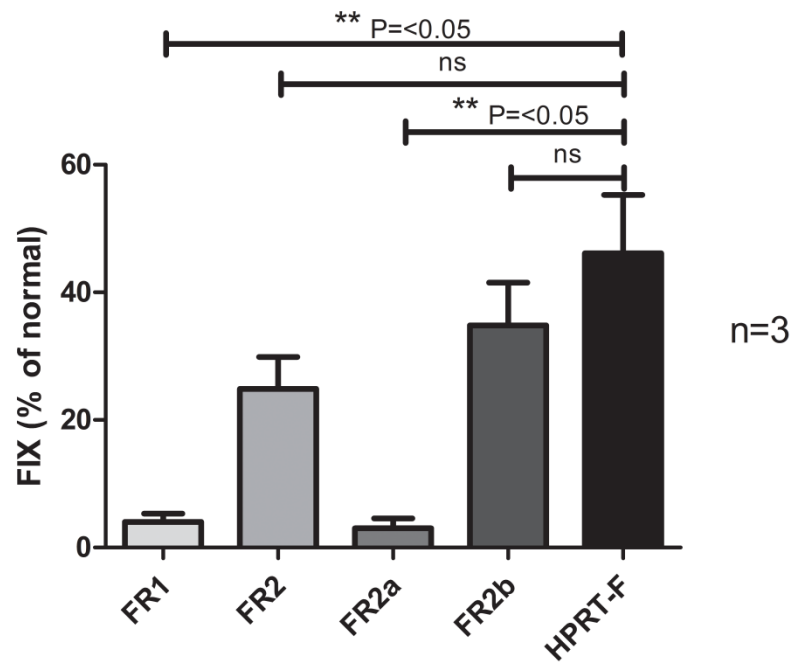


Figure 4.9: Transgene expression in C57BL/6 mice. % FIX levels at 2 weeks after tail-vein administration of 4×10^{10} vg/kg (n=3) of all vectors depicted are represented graphically as averages \pm SEM.

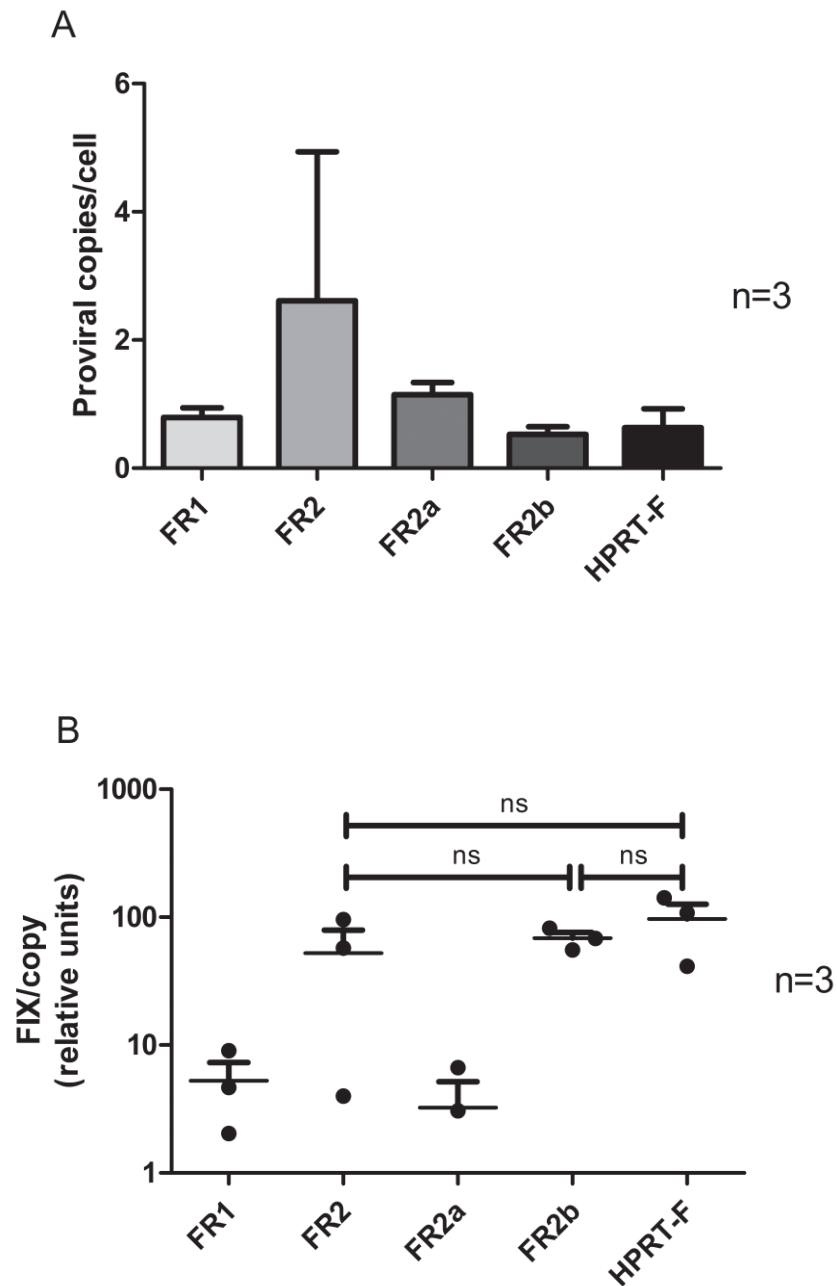


Figure 4.10: Proviral copy number correction. A) Proviral Copies/cell in liver. Proviral copy number was determined by a Q-PCR assay on murine liver samples collected 2 weeks after transduction with 4×10^{10} vg/kg of each vector depicted. Results are presented as mean proviral copies/cell \pm SEM. **B) Correction of %hFIX levels.** Results are presented as mean %FIX levels \pm SEM corrected for proviral copy number to account for variation in transduction.

4.3.3 HPRT Fragment 2b enhances transgene expression in self-complementary vectors

Due to its reduced size, we were able to assess the HPRT fragment 2b S/MAR in the context of a self-complementary vector with the S/MAR sequence again cloned immediately 3' of the hFIXco transgene. Each scAAV cassette (containing no S/MAR or fragment 2b) was pseudotyped with serotype 8 capsid protein and used to transduce HuH7 cells at a dose of 1×10^7 vg/cell. As detailed in figure 4.11, 20-fold higher hFIX antigen levels were observed in sc-LP1-hFIXco-FR2b transduced cells ($1.283 \pm 0.269\%$) as compared to sc-LP1-hFIXco-Control transduced cells ($0.064 \pm 0.026\%$) ($P=0.0093$, student T-test).

For *in-vivo* analysis both vectors were administered as a single bolus injection into the tail vein of 6 to 8 week old male C57BL/6 mice at a dose of 4×10^{10} vg/kg ($n=3$). hFIX levels were assessed over a period of 4 weeks after gene transfer followed by proviral copy number analysis in the liver.

At 4 weeks hFIX levels in the scAAV8-LP1-hFIXco-HPRT-FR2b transduced cohort were approximately $105 \pm 6\%$ (Figure 4.12). This was a 35-fold increase ($P=0.0038$, student T-test) in transgene expression as compared to scAAV8-LP1-hFIXco-Control transduced animals ($3 \pm 1\%$). Differences in transgene expression levels were not accounted for by variance in proviral copy number as copies in the liver of transduced animals were comparable at approximately 2.1-3.1 copies/hepatocyte (Figure 4.13). These data suggest that S/MAR elements are also effective in a self-complementary format.

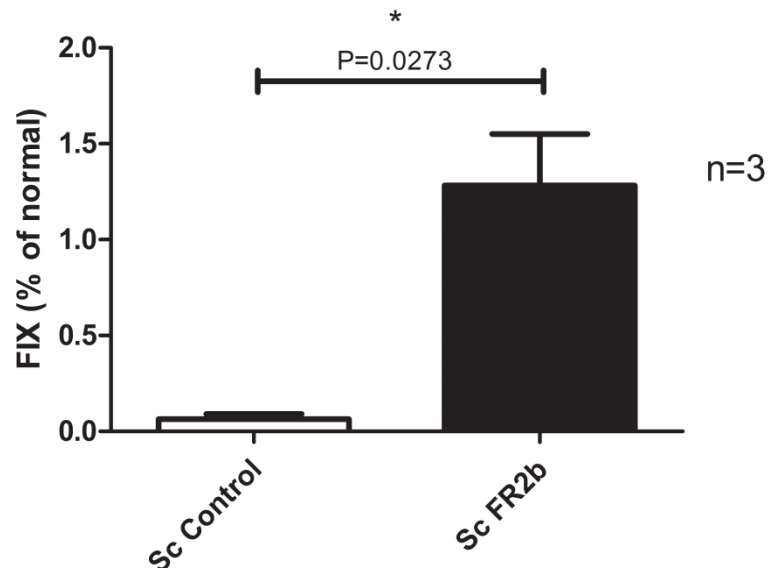


Figure 4.11: Transgene expression in HuH7 cells. FIX levels in supernatants at 72 hours after transduction of HuH7 cells with 1×10^7 vg/cell (n=3) are represented graphically as averages \pm SEM.

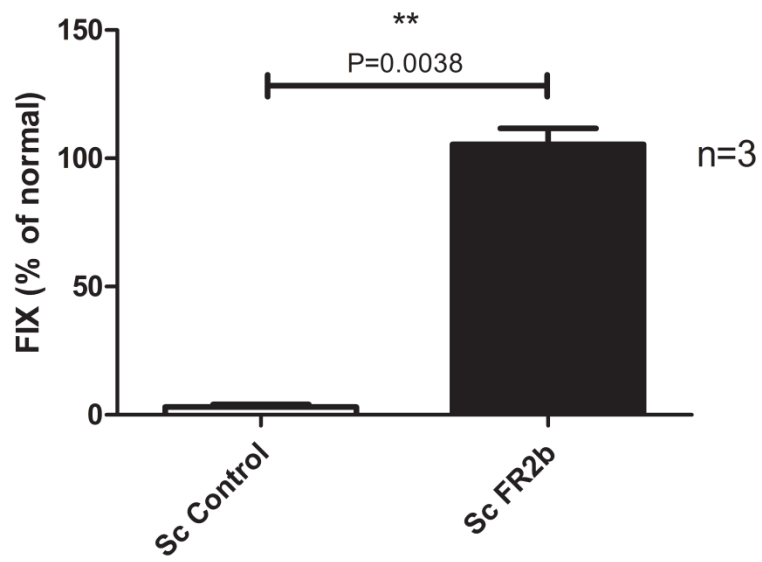


Figure 4.12: HFIX levels in C57BL/6 mice. % FIX levels at 4 weeks after tail-vein administration of 4×10^{10} vg/kg (n=3) of scAAV-LP1-hFIXco-control and scAAV-LP1-hFIXco-FR2b are represented graphically as averages \pm SEM.

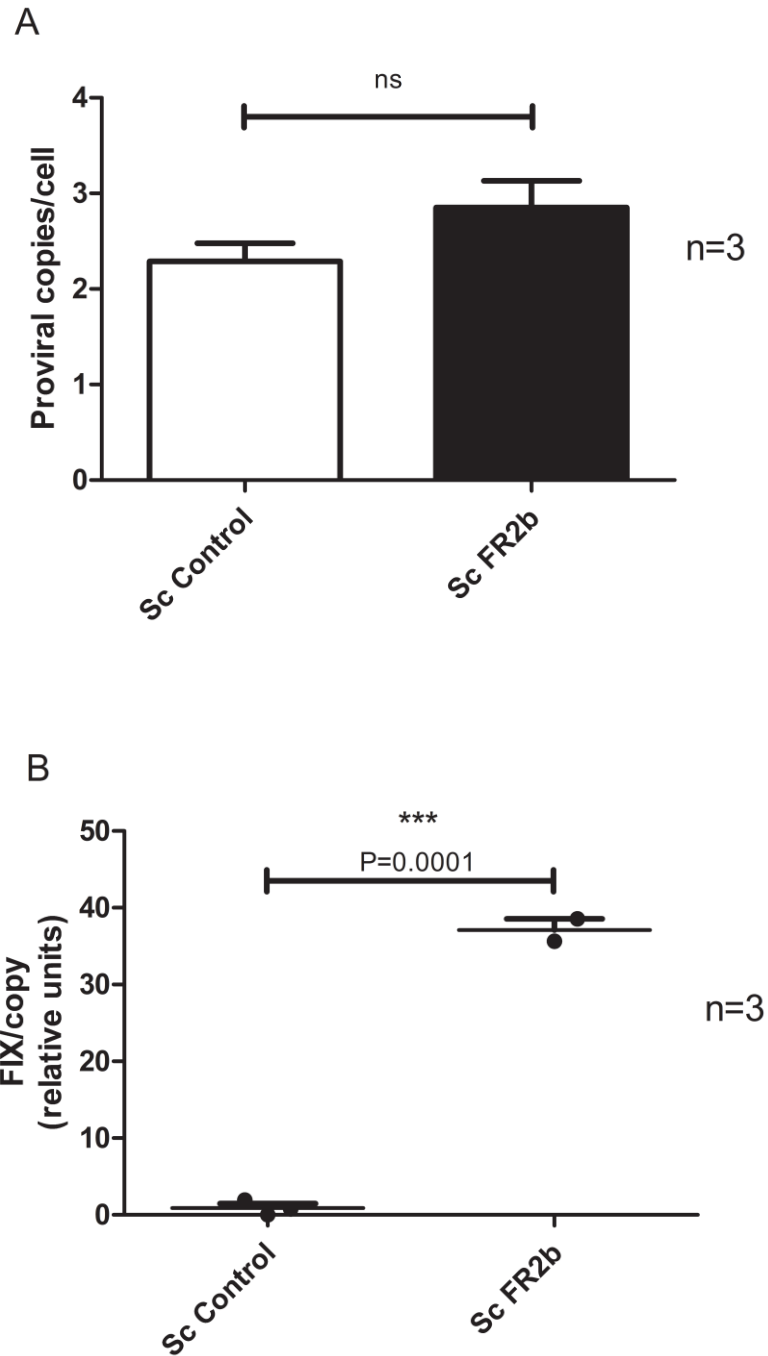


Figure 4.13: Proviral copy number correction. A) Proviral Copies/cell in liver. Proviral copy number was determined by a Q-PCR assay on murine liver samples collected 4 weeks after transduction with 4×10^{10} vg/kg of each vector depicted. Results are presented as mean proviral copies/cell \pm SEM. **B) Correction of %FIX levels.** Results are presented as mean %FIX levels \pm SEM corrected for proviral copy number to take account of variation in transduction.

4.4 Discussion

The relatively small packaging capacity of rAAV vectors imposes a degree of limitation on rAAV mediated gene therapy (Grieger & Samulski, 2005). Indeed, AAV research for the treatment of multiple disorders has been somewhat constrained by vector packaging capacity. Consequently, the ability to improve gene expression from AAV cassettes whilst minimising increases in cassette size is of great interest. As such, in order to minimise the space occupied by S/MARs within AAV expression cassettes and to discover minimal sequences required to enhance transgene expression, we carried out a deletion analysis on IFN β and HPRT S/MARs.

Through this analysis we identified one region of each S/MAR that was able to mediate potent enhancer activity. In the case of the IFN β S/MAR, transduction with a fragment 2 containing vector demonstrated a 2-fold increase in hFIX antigen levels as compared to ssAAV-LP1-hFIXco-IFN-R vector *in-vitro*. As this assay was limited by poor *in-vitro* transduction with serotype 8 vectors, this trend was verified by *in-vivo* analysis. Following tail vein administration of 4×10^{12} vg/kg of each IFN β S/MAR vector to C57BL/6 mice, a 3-fold increase in transgene expression was maintained in the ssAAV-LP1-hFIXco-FR2 cohort as compared to ssAAV-LP1-hFIXco-IFN-R transduced animals. In the HPRT S/MAR analysis, respective hFIX levels were comparable both *in-vitro* ($4.313 \pm 0.009\%$ and $4.079 \pm 0.830\%$) and *in-vivo* ($46 \pm 9\%$ and $35 \pm 7\%$) following transduction with ssAAV-LP1-hFIXco-HPRT-F and ssAAV-LP1-hFIXco-FR2b vectors. In the context of a self-complementary vector, the HPRT fragment 2b was also found to enhance hFIX levels by 35-fold as compared to control vector in mice. These observations suggest that truncated S/MAR elements are able to mediate enhanced transgene expression; as such, S/MAR elements have potential use in conjunction with larger transgenes or in the context of self-complementary expression cassettes. However, it is again worth mentioning that these experiments should, in future, be repeated with further groups of animals and fresh batches of vector in order to ensure that these observations are reproducible and not the result of experimental artefacts. Animal numbers must also be justified through the use of sample size calculations as described in section 3.4.

In an attempt to identify key regulatory motifs in our truncated S/MARs, the IFN β fragment 2 sequence was entered into a motif elicitation programme (MEME). Discovered motifs were then entered into the Gene Ontology for Motifs (GOMO) algorithm in order to deduce

potential biological roles of the sequences (Boden & Bailey, 2008; Buske *et al*, 2010). By this analysis, the only gene ontology (GO) term unique to fragment 2 was 'nucleosome assembly' which was associated with the sequence AAAAGM (where M is the IUPAC degenerate base symbol for C or A) that is present twice in the fragment 2 sequence. As such we speculate that IFN β S/MAR fragment 2 may contain a nucleation site for helix unwinding otherwise known as the core unwinding element (CUE). In previously published literature all S/MARs are documented to have multiple base unwinding regions (BURs) with one region typically containing a CUE (Bode *et al*, 2000). Indeed the loose CUE consensus sequence (AAATATATT) that is found in a few but not all S/MARs is present in our fragment 2 sequence. However, through motif elicitation we were unable to identify sequences to suggest the presence of repressive motifs in IFN β S/MAR fragments 1 and 3. As such, it is possible that one of these fragments may demonstrate structural as opposed to sequence based hindrance on transgene expression.

The only unique nucleotide motif found in HPRT fragment 2b was TYRTTT (where Y=pyrimidine and R=purine). This motif occurs twice in the 2b sequence and was associated with the GO term 'gene expression'. As such, this motif may represent a core enhancer sequence, although this matter requires further validation. Future investigation into this matter could include a mutational analysis on motif sequences to observe potential inhibitory effects on transgene expression. Alternatively, the potency of fragment 2b may be purely structural due to the large quantity of poly-pyrimidine and poly-purine tracts present in the sequence. As suggested in previous literature reports, these sequences may enable the formation of non-B DNA structures: which in turn catalyze transcription (Boulikas, 1993).

One limitation of this study was the inability to test multiple variants of truncated S/MAR elements. For instance, it is possible that through high-throughput elicitation of every possible sequence permutation available, we may have identified a more potent S/MAR fragment. However, due to the burden on vector production and subsequent analysis that this would cause, such an approach falls beyond the scope of this project.

To summarise, through deletion analysis, we have successfully identified two truncated S/MAR regions that enhance transgene expression levels both *in-vitro* and *in-vivo*. Overall, this makes the use of S/MAR elements more applicable to AAV research by minimizing the amount of space occupied by S/MAR sequences within a given expression cassette. The

exact explanation for the potency of these sequences remains to be defined and may be due to specific sequence motifs or secondary structure.

CHAPTER 5 THE FUNCTION OF MATRIX ATTACHMENT REGIONS IN AAV EXPRESSION CASSETTES

5.1 Introduction

5.1.1 The role of S/MARs in preventing transcriptional gene silencing

As previously described, the theory of repeat induced gene silencing (RIGS) suggests that transgenes arranged in multicopy concatemeric arrays are subject to silencing through an 'aberrant' RNA based mechanism (Garrick *et al*, 1998; Selker, 1999). These silencing events can take the form of post transcriptional mRNA degradation or transcriptional gene silencing (TGS) by histone modification (Moazed, 2009). In the context of our LP1-hFIXco expression cassette, S/MAR elements are observed to enhance levels of hFIX mRNA. As such, it is plausible that RIGS is active following rAAV mediated gene transfer and that, in the absence of a S/MAR, exogenous mRNAs are degraded and/or transcription is halted by repressive chromatin configurations. This would infer that S/MARs function to maintain an open euchromatin state and to stabilise exogenous transcripts in the context of rAAV.

In proviral DNA extracted from the liver of rhesus macaques transduced with ssAAV-LP1-hFIXco-Control, no CpG methylation of the LP1 promoter was observed by bisulphate sequencing at up to one year (full duration of the study) after gene transfer (Figure 5.1). Thus, differences in FIX expression between the control vector (ssAAV-LP1-hFIXco-Control) and S/MAR containing vectors (ssAAV-LP1-hFIXco-IFN-R and ssAAV-LP1-hFIXco-HPRT-F) were not due to methylation of the LP1 promoter. Any TGS events occurring in conjunction with rAAV gene transfer must therefore result from repressive histone modification.

Therefore, to determine whether S/MARs prevent transcriptional gene silencing, the first aim of this study was to compare histone modification profiles of ssAAV-LP1-hFIXco-Control, ssAAV-LP1-hFIXco-IFN-R and ssAAV-LP1-hFIXco-HPRT-F proviral genomes. This was assessed by chromatin immunoprecipitation (ChIP) using antibodies against histone proteins H3K9me2 (histone 3 dimethylated on lysine 9), H3K4me2 (histone 3 dimethylated on lysine 4) and H3Ac (acetylated histone 3).

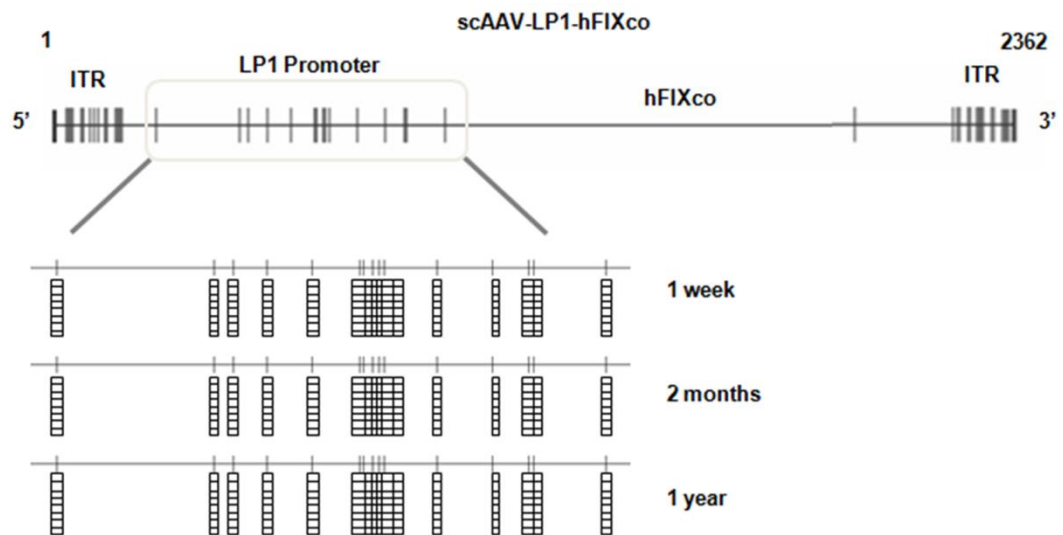


Figure 5.1: Cytosine methylation profiles of the AAV LP1 promoter revealed by bisulphite sequencing. Bisulphite sequencing was carried out on DNA extracted from rhesus liver samples 1 week, 2 months and 1 year after peripheral vein administration of scAAV8-LP1-hFIXco vector at a dose of 2×10^{12} vg/kg. The vector genome is represented schematically (top). Boxes represent CpG regions of the LP1 promoter (bottom). Unfilled boxes depict non-methylated CpG regions.

5.1.2 Polycomb group (PcG) complexes are recruited during RNAi based silencing

In order to investigate whether S/MARs reduce the binding of proteins involved in RIGS, ChIP experiments using an antibody against a Polycomb group (PcG) protein were carried out on chromatin extracted from ssAAV-LP1-hFIXco-Control and ssAAV-LP1-hFIXco-IFN-R transduced mouse livers.

Polycomb group (PcG) proteins were first discovered in *Drosophila Melanogaster* and are well known for their ability to maintain genes in a silenced state (Okulski *et al*, 2011). The most commonly known example of PcG function involves the silencing of homeotic (Hox) genes in the early embryo when Hox expression is no longer required for axis formation and gastrulation (Czermin *et al*, 2002). In the fruit fly, the recruitment of PcG complexes is also observed in conjunction with repeat induced gene silencing (Pal-Bhadra *et al*, 1997). For example, the introduction of two to six copies of the Alcohol dehydrogenase (Adh) gene in flies resulted in the progressive decrease in Adh expression as opposed to the enhanced expression effects anticipated after increasing gene dosage (Pal-Bhadra *et al*, 2002). This effect was analogous to the events of cosuppression/RIGS as transcriptional silencing of the Adh gene occurred simultaneously with the production of RNAi. Through immunostaining of the chromosomes of transduced flies, sites of Adh gene insertion were found in association with PcG proteins; thus it is inferred that polycomb proteins are involved in the maintenance of TGS that is brought about by repeat induced gene silencing (Pal-Bhadra *et al*, 1997). This study provided the context for our aim to compare levels of polycomb protein associated with control and S/MAR containing AAV genomes.

In the fly, the Enhancer of Zeste (E(Z)) protein is continually required to maintain gene silencing even after embryogenesis (Czermin *et al*, 2002). Therefore, enhancer of Zeste homolog 2 (EZH2) was our chosen mammalian PcG protein target. This homolog forms the catalytic subunit of Polycomb repressive complex 2 (PRC2) and is known for its methyltransferase activity which results in the repressive histone mark of lysine 27 trimethylation on histone 3 (H3K27me3) (Cavalli, 2012). EZH2 is also known for its ability to transfer methyl groups to lysine 9 on histone 3; therefore levels of this marker (H3K9me2) were also assessed in this study.

5.1.3 S/MAR binding proteins are involved in chromatin remodelling

By using S/MAR affinity columns, multiple S/MAR binding proteins have been isolated from cell extracts via chromatography techniques (Kohwi-Shigematsu *et al*, 1998). Examples of such proteins include Scaffold attachment factor A (SAF-A), high mobility group (HMG) proteins, special AT-rich sequence binding 1 (SATB1) protein and nucleolin. All of these proteins can be broadly categorised as components of chromatin remodelling complexes. For instance SATB1 acts as a 'docking site' for the recruitment of chromatin remodelling proteins that serve to regulate gene expression through the modification of histones or through the mobilization of nucleosomes (Yasui *et al*, 2002). Similarly SAF-A and HMG proteins also play a fundamental role in nucleosome dynamics and are known to interact with the SWItch Sucrose NonFermentable (SWI/SNF) complex which redistributes nucleosomes along DNA sequences (Bianchi & Agresti, 2005; Vizlin-Hodzic *et al*, 2011). HMG proteins are also involved in the recruitment of transcription factors and DNA bending activities which facilitate transcription (Bianchi & Agresti, 2005). Nucleolin is a further example of a known histone chaperone that possesses a HMG-like domain and binds to S/MAR affinity columns with high stringency. The nucleolin protein is able to destabilise histone octamers and consequently activates the dissociation of histone 2A-histone 2B (H2A-H2B) dimers by SWI/SNF. Furthermore, nucleolin has been shown to facilitate the elongation of RNA Polymerase II through nucleosomes during transcription (Angelov *et al*, 2006; Dickinson & Kohwi-Shigematsu, 1995).

As known S/MAR binding proteins are heavily involved in nucleosome assembly and histone eviction during transcription, the final aim of this study was to determine whether proteins involved in nucleosome dynamics are associated with S/MAR containing AAV expression cassettes. To assess this matter, ChIP experiments using an antibody against nucleolin were carried out on chromatin extracted from ssAAV-LP1-hFIXco-Control and ssAAV-LP1-hFIXco-IFN-R transduced murine livers.

In this study we consistently observed a 2 to 4-fold enrichment of the repressive H3K9me2 marker in association with ssAAV-LP1-hFIXco-Control genomes as compared to ssAAV-LP1-hFIXco-IFN-R and ssAAV-LP1-hFIXco-HPRT-F. This was accompanied by a decrease in association of active H3K4me2 and H3Ac markers on ssAAV-LP1-hFIXco-Control DNA. In comparison to control genomes a significant increase in the binding of nucleolin and a 2.4-fold decrease of EZH2 binding was observed in association with ssAAV-LP1-hFIXco-IFN-R

genomes, although these observations require further validation. Collectively, these data suggest that S/MARs prevent transcriptional gene silencing of rAAV expression cassettes through the recruitment of proteins that maintain DNA in an open euchromatin state.

5.2 Materials and methods

5.2.1 Chromatin immunoprecipitation

Chromatin immunoprecipitation (ChIP) was carried out on murine liver samples as described in section 2.5.3. Briefly 200mg of transduced or naïve liver was pushed through a nylon cell strainer in 2ml of PBS solution containing 2% foetal bovine serum (FBS) and protease inhibitor cocktail. Cells were then centrifuged at 3500rpm for 10 minutes and cell pellets were washed twice in 10ml of the aforementioned PBS solution. Formaldehyde was added to final concentration of 1% followed by incubation at room temperature for 10 minutes to form DNA-protein crosslinks. To quench formaldehyde, glycine was added to a final concentration of 0.125M and solutions were incubated for 5 minutes at room temperature. Cells were then pelleted and washed twice in ice cold PBS solution as above. To shear DNA, a Bioruptor sonicator was used with the sonication parameters set to 15 seconds pulse on and 15 seconds pulse off for 45 minutes. Chromatin immunoprecipitation was carried out using the EZ-Magna ChIP A-Chromatin Immunoprecipitation Kit (Millipore, Feltham, UK) as per the manufacturer's instructions. All immunoprecipitations were carried out at 4°C overnight with either 4µg of specific antibody or with no antibody as control. Pull down of LP1 promoter DNA was quantified by Q-PCR using primers described in section 2.5.3.

5.3 Results

5.3.1 S/MARs confer higher transgene expression through epigenetic modification of the ssAAV-LP1-hFIXco genome

To evaluate the *in-vivo* chromatin status of ssAAV-LP1-hFIXco-Control vector genomes in comparison to ssAAV-LP1-hFIXco-IFN-R or ssAAV-LP1-hFIXco-HPRT-F genomes, we carried out ChIP experiments on chromatin extracted from murine liver collected 4-8 weeks after tail vein administration of 4×10^{12} vg/kg of ssAAV-LP1-hFIXco-Control, ssAAV-LP1-hFIXco-IFN-R or ssAAV-LP1-hFIXco-HPRT-F.

In comparison to ssAAV-LP1-hFIXco-IFN-R transduced animals, vector genomes from the ssAAV-LP1-hFIXco-Control cohort consistently showed 2 to 4-fold enrichment of repressive heterochromatin markers (dimethylation of lysine 9 on histone 3 [H3K9me2] (not significant) and heterochromatic adaptor proteins [HP1 α]) (P=0.0003 to 0.0012, T test) in the LP1 promoter region (Figure 5.2). Both H3K9me2 and HP1 α marks correlate with inactive gene promoters (Lienert *et al*, 2011). An increase in association of histone 3 with dimethylation on lysine 4 (H3K42me) as well as acetylation of histone 3 lysine residues (H3Ac) was also observed within the distal region of the LP1 promoter of ssAAV-LP1-hFIXco-IFN-R genomes when compared to the promoter of ssAAV-LP1-hFIXco-Control (not significant, P=0.396 and 0.367 respectively, student T tests). As previously described, both H3K4me2 and H3Ac represent markers of transcriptionally active genes (Yan & Boyd, 2006).

When compared to the ssAAV-LP1-hFIXco-HPRT-F cohort, ssAAV-LP1-hFIXco-Control genomes again showed a significant 2 to 3-fold enrichment of the H3K9me2 heterochromatin marker (Figure 5.3) (P=0.002 to 0.023, student T tests). Additionally, a significant 2 to 4-fold enrichment of H3K4me2 and 2 to 6-fold enrichment of H3Ac was observed in association with LP1 promoter regions of ssAAV-LP1-hFIXco-HPRT-F genomes (P=0.034 to 0.013 and 0.003 to 0.001 respectively, student T tests).

Collectively, these results suggest that the higher levels of hFIX expression observed in ssAAV-LP1-hFIXco-IFN-R and ssAAV-LP1-hFIXco-HPRT-F cohorts was due to the maintenance of S/MAR containing expression cassettes in a chromatin configuration that is permissive to transcription.

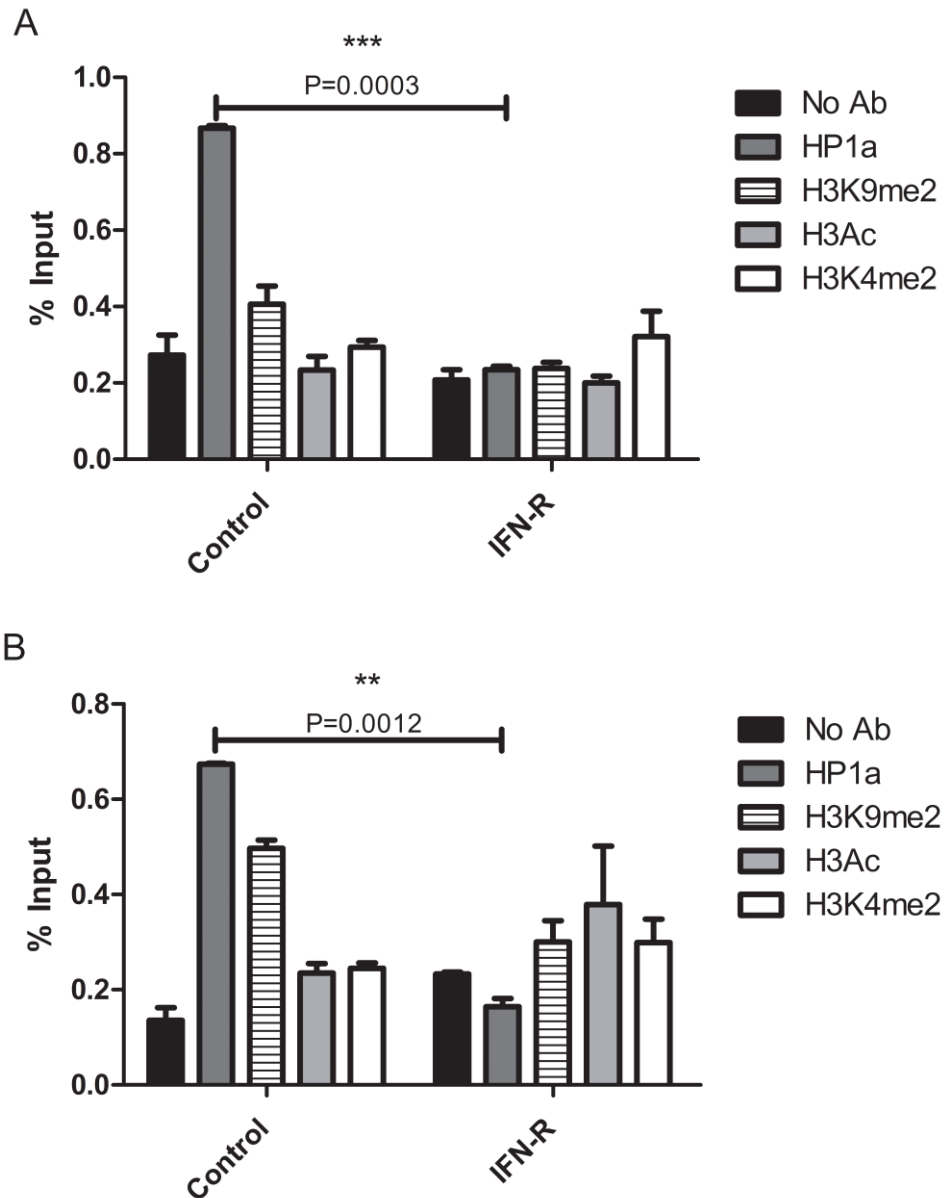


Figure 5.2: Epigenetic modification of ssAAV-LP1-hFIXco proviral DNA. ChIP was carried out on chromatin extracted from liver samples collected 6 weeks after tail-vein administration of 4×10^{12} vg/kg of ssAAV-LP1-hFIXco-IFN-R and ssAAV-LP1-hFIXco-Control vectors into 4 to 6 week old male C57BL/6 mice. All results are presented as a percentage of total input chromatin (calculated as an average from 2 Ct values) \pm SEM. Data are from one animal and representative of results that were reproduced in a minimum of three animals. **(A) ChIP analysis on proximal LP1 chromatin.** The vector genome region amplified by Q-PCR corresponds to the proximal region of the promoter (position152). **(B) ChIP analysis on distal LP1 chromatin.** The vector genome region amplified by Q-PCR was the distal region of the promoter (position366). Antibodies used for ChIP included anti H3K9me2, anti HP1 α , anti H3K4me2 and anti H3Ac.

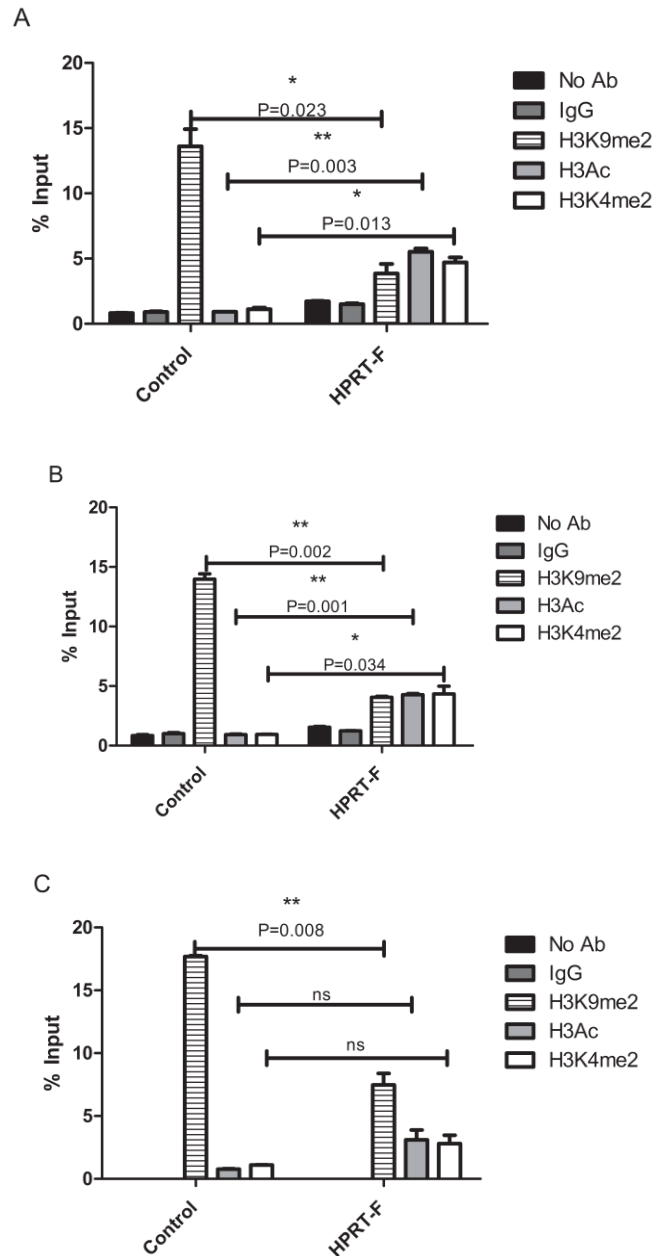


Figure 5.3: ChIP analysis on ssAAV-LP1-hFIXco-Control and ssAAV-LP1-hFIXco-HPRT-F chromatin. ChIP was carried out on chromatin extracted from liver samples collected 4 weeks after tail-vein administration of 4×10^{12} vg/kg of ssAAV-LP1-hFIXco-HPRT-F and ssAAV-LP1-hFIXco-Control vectors into 4 to 6 week old male C57BL/6 mice. All results are presented as a percentage of total input chromatin (calculated as an average from 2 Ct values) \pm SEM. Data are from one animal and representative of results that were reproduced in three animals. **A**, **B** and **C** refers to ChIP analysis on proximal promoter (152), distal promoter (366) and transgene (1988) chromatin regions respectively. Antibodies used for ChIP included anti H3K9me2, anti H3K4me2 and anti H3Ac.

5.3.2 Preliminary mechanistic data

To assess potential mechanisms behind the maintenance of S/MAR containing genomes in a transcriptionally active state, we carried out further ChIP studies on ssAAV-LP1-hFIXco-Control and ssAAV-LP1-hFIXco-IFN-R genomes extracted from murine livers taken 4 weeks after tail vein administration of 4×10^{12} vg/kg of ssAAV-LP1-hFIXco-Control and ssAAV-LP1-hFIXco-IFN-R vectors. Antibodies used for this analysis included anti nucleolin (a known S/MAR binding protein and histone chaperone) and anti EZH2 (a PcG protein involved in the methylation of histone 3).

In comparison to ssAAV-LP1-hFIXco-Control genomes, preliminary results show a significant 69-fold and 94-fold increase in nucleolin association with promoter and hFIX transgene regions of ssAAV-LP1-hFIXco-IFN-R genomes respectively ($P=0.003$ and 0.005 respectively, T tests) (Figure 5.4). Additionally, an approximate 2.4-fold enrichment of EZH2 was observed in association with the promoter of ssAAV-LP1-hFIXco-IFN-R genomes as compared to the promoter of ssAAV-LP1-hFIXco-Control genomes although this was not found to be significant ($P=0.241$) (Figure 5.5).

Taken as a whole these results suggest that, in the context of our LP1-hFIXco rAAV vector, S/MARs enhance transgene expression through the recruitment of known S/MAR binding proteins involved in the movement of histones. Furthermore, S/MARs may also have a role in preventing the binding of PcG group proteins that are involved in the formation of heterochromatin by methylation of histone 3 at lysine residues 9 and 27.

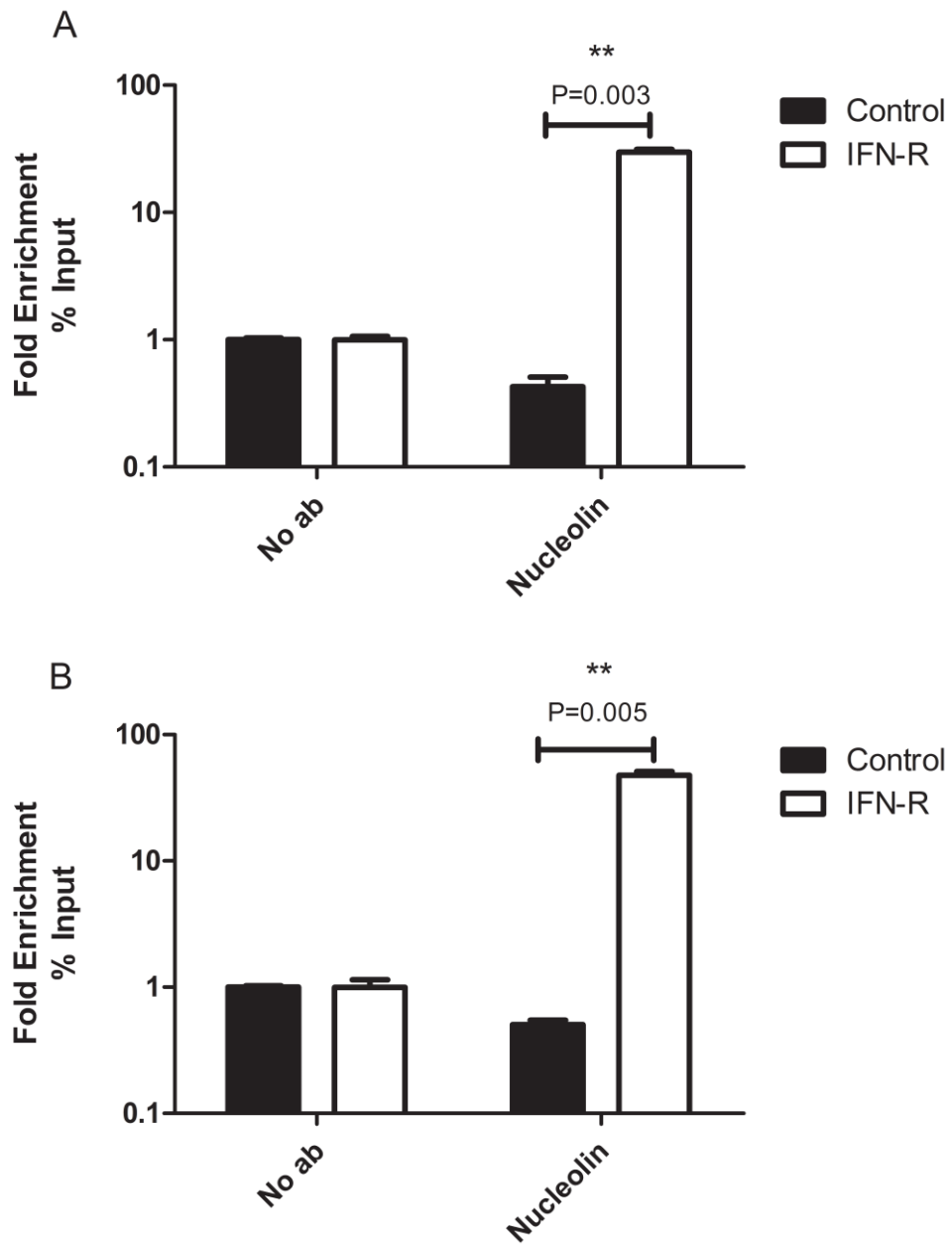


Figure 5.4 Preliminary nucleolin ChIP analyses. ChIP was carried out on chromatin extracted from the liver of 4-6 week old male C57BL/6mice transduced with 4×10^{12} vg/kg of ssAAV-LP1-hFIXco-control or ssAAV-LP1-hFIXco-IFN-R. All results are presented as a fold enrichment of % input against % input values from no antibody experiments (calculated as an average from 2 Ct values divided by average %Input values from experiments using no antibody \pm SEM). Data are from one animal only. **A** and **B** correspond to experiments using Q-PCR primers against proximal promoter (366) and transgene regions (1988) respectively.

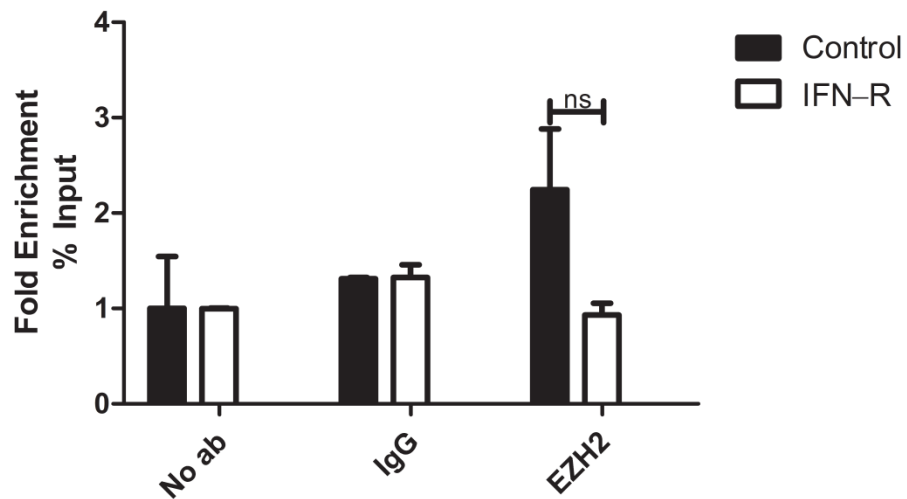


Figure 5.5: Preliminary EZH2 ChIP analyses. ChIP was carried out on chromatin extracted from the liver of 4-6 week old male C57BL/6 mice transduced with 4×10^{12} vg/kg of ssAAV-LP1-hFIXco-control or ssAAV-LP1-hFIXco-IFN-R. Results are calculated as an average from 2 Ct values divided by average %Input values from experiments using no antibody \pm SEM. Data are from one animal only. Q-PCR was carried out using primers against vector genome region 366 (distal LP1 promoter).

5.4 Discussion

Repeat induced gene silencing is a phenomenon known to occur simultaneously with gene transfer as a host defence mechanism against viral infection (Moazed, 2009). These gene silencing events halt transcription of exogenous sequences through the recruitment of proteins that enable the formation of repressive chromatin configurations. In this study we assessed whether rAAV genomes are subject to such silencing events and whether this is prevented through the incorporation of S/MAR elements into rAAV expression cassettes.

Consistent with the work of other groups, we did not detect any methylation of our LP1 promoter sequence by bisulphate sequencing (Leger *et al*, 2011). This infers that any silencing events occurring after gene transfer must be due to histone modifications. As such, we analysed the association of histones H3K9me2, H3K4me2 and H3Ac with control and S/MAR containing genomes by ChIP. Through this analysis we consistently found the IFN β and HPRT S/MAR elements to decrease the association of repressive histone modifications (H3K9me2) and increase the association of euchromatin marks (H3K4me2 and H3Ac) with our AAV expression cassettes (Lienert *et al*, 2011; Yan & Boyd, 2006). We also observed a significant decrease in association of the repressive HP1 α mark with ssAAV-LP1-hFIXco-IFN-R genomes (Wreggett *et al*, 1994). Collectively, these results suggest that silencing events may indeed occur following rAAV gene transfer. These observations are in agreement with previous gene transfer studies, involving the use of HDAC inhibitors to enhance gene expression, which suggest that AAV genomes are subject to epigenetic silencing (Okada *et al*, 2006). Thus, the increase in mRNA levels observed with S/MAR vectors may be mediated through the prevention of such silencing events. In future experiments to determine S/MAR function, it may be interesting to see whether the co-administration of a S/MAR vector with a HDAC inhibitor results in a synergistic or additive effect on gene expression.

To understand how S/MARs mediate the prevention of gene silencing, we carried out ChIP experiments against the nucleolin protein. Nucleolin is a S/MAR binding protein involved in the movement of histones and facilitating transcription (Angelov *et al*, 2006; Dickinson & Kohwi-Shigematsu, 1995). Although this work requires repetition, in this study we observed a significant increase in the association of nucleolin with ssAAV-LP1-hFIXco-IFN-R genomes as compared to ssAAV-LP1-hFIXco-Control. As such, it is inferred that S/MARs mediate their enhancer properties through the recruitment of proteins involved in nucleosome assembly

and histone eviction. This is consistent with data from previous chromatography studies designed to detect S/MAR binding proteins (Kohwi-Shigematsu *et al*, 1998). However, in addition to chromatin remodelling function, S/MARs have other biological properties that could potentially influence AAV transgene expression. For instance, S/MARs have the ability to bring the AAV proviral DNA into close proximity to key nuclear regulatory elements within the nucleus by forming “anchor points” with nuclear matrix (Bode *et al*, 2000). This may, in turn, enhance promoter activity by bringing promoter sequences into close proximity with key transcription factors required for the initiation of gene expression. Therefore, there would be value in investigating whether there is an increased binding of proteins that attach DNA to the nuclear matrix (such as SATB1) in S/MAR containing AAV genomes (Dickinson *et al*, 1997). Furthermore, it is also possible that the increased levels of mRNA observed when using S/MAR elements may be due to improved RNA stability as opposed to increased transcription levels through the prevention of silencing. To assess this matter, the integrity of mRNA samples could be determined more scrupulously by carrying out a quantitative PCR analysis using primers designed against 5’ and 3’ ends of the transcript (Fajardy *et al*, 2009). This would allow us to determine whether hFIX mRNA is more readily degraded in the absence of S/MAR elements.

As described above, polycomb proteins have previously been detected at silenced genes in association with RIGS events (Pal-Bhadra *et al*, 1997). To determine whether AAV silencing is analogous to RIGS, we carried out CHIP experiments against the EZH2 polycomb protein. By this analysis we observed a 2.4-fold enrichment of EZH2 at the promoter regions of ssAAV-LP1-hFIXco-Control genomes compared to ssAAV-LP1-hFIXco-IFN-R. However, this observation was not statistically significant and will therefore need further validation through repeat experiments. In future work it would also be valuable to assess levels of alternative polycomb proteins in association with control and S/MAR containing vector genomes. From this experiment we can say that S/MAR elements may prevent the binding of polycomb proteins that is mediated by RIGS. However, to conclusively establish whether repeat induced genome silencing occurs after AAV gene transfer, it will be important to detect RNAi complementary to transgene sequences through strategies such as northern blotting.

In summary, detailed epigenetic analysis showed that the AAV-LP1-hFIXco provirus does not undergo DNA methylation in the liver of macaques following systemic administration. However, LP1 promoter sequences within the proviral genome become associated with

histones containing repressive marks. The inclusion of S/MARs appears to decrease the level of proviral DNA heterchromatinization and facilitate the maintenance of AAV concatemers in an open chromatin, and therefore transcriptionally active configuration. This may be achieved through the recruitment of proteins that reassemble nucleosomes and/or through preventing the binding of repressive chromatin remodelling complexes such as polycomb group proteins. Although the exact mechanism through which S/MARs exert their chromatin remodelling function remains to be elucidated, these data are fully consistent with previous reports of S/MAR function, of nucleosome association with AAV genomes, and of repeat induced gene silencing following viral infection (Garrick *et al*, 1998; Gluch *et al*, 2008; Penaud-Budloo *et al*, 2008). Therefore, S/MARs may help to achieve the overall goal of improved AAV vector potency by preventing silencing of the provirus.

CHAPTER 6 CONCLUSIONS AND FUTURE DIRECTIONS

The need for large numbers of vector particles to achieve a therapeutic effect has been observed in multiple clinical trials for rAAV mediated gene transfer. In the absence of immune suppression, such a large vector load appears to provoke T cell responses against capsid antigens resulting, in some cases, in the abrogation of transgene expression and the potential risk of toxicity due to immune mediated clearance of transduced cells (Manno *et al*, 2006; Nathwani *et al*, 2011). To address this matter, this study aimed to enhance the potency of rAAV vectors allowing lower doses, shown to be safe in humans, to be utilised.

The transduction of target cells by AAV can be influenced by multiple factors including inefficient cell surface binding, endosomal degradation, conversion of single stranded genomes to transcriptionally active double stranded forms and recipient gender (Davidoff *et al*, 2003; Fisher *et al*, 1996; Mackus *et al*, 2003; Yan *et al*, 2002). These insights into the biology of AAV transduction have enabled the generation of various enhanced vectors ranging from constructs with mutated capsid proteins to vectors with altered DNA configurations or expression cassettes (Loiler *et al*, 2003; McCarty *et al*, 2003; Miao *et al*, 2000b; Nathwani *et al*, 2009; Pang *et al*, 2011; Petrs-Silva *et al*, 2009; Rabinowitz *et al*, 2004; Wu *et al*, 2008). However, the possibility to prevent epigenetic silencing of rAAV genomes remains relatively unexplored. As vector genomes of the parvovirus family, including MVM and AAV, have been shown to adopt a chromatin-like configuration *in-vitro* and *in-vivo*, it is rational to anticipate epigenetic silencing of the rAAV provirus (Ben-Asher *et al*, 1982; Marcus-Sekura & Carter, 1983; Penaud-Budloo *et al*, 2008). Furthermore, studies that demonstrate enhanced AAV mediated transgene expression in mice, following administration of HDAC inhibitors, suggest that AAV genomes may be subject to repressive histone modifications (Okada *et al*, 2006). As such, we aimed to enhance the potency of our ss-AAV8-LP1-hFIXco-TSV40pA vector through the incorporation of S/MAR elements into the AAV8-LP1-hFIXco expression cassette previously used in the clinic.

Following tail vein administration of 4×10^{12} vg/kg to 6 to 8 week old male C57BL/6 mice, S/MAR containing vectors were found to mediate a 10 to 28-fold increase in plasma hFIX levels as compared to vectors containing no S/MAR or control KSHV elements. These data are fully supported by previous reports of S/MAR function in other gene transfer vectors (Argyros *et al*, 2008; Auten *et al*, 1999; Dang *et al*, 2000; Moreno *et al*, 2011; Ramezani *et al*, 2003). After correcting for proviral copy numbers in the mouse liver, the ssAAV-LP1-

hFIXco-HPRT-F vector was found to mediate the highest levels of transgene expression. As such, this vector was selected for a low dose analysis (4×10^{10} vg/kg) in mice. At 4 weeks after transduction with the lower vector dose, the ssAAV-LP1-hFIXco-HPRT-F cohort expressed hFIX at levels approximately 85-fold higher than those observed in ssAAV-LP1-hFIXco-control transduced animals. Thus, it is inferred that S/MARs are indeed able to enhance the potency of AAV and consequently allow for the use of lower vector doses. Although enhanced transgene expression was the desired effect of incorporating S/MAR elements into our expression cassette, it is important to mention that overexpression of hFIX could potentially have adverse effects. For instance, in mice, elevated circulatory levels of hFIX have been shown to cause thrombosis, myocardial fibrosis and reduced survival age (Ameri *et al*, 2003). As such, it is possible that after a longer follow up period we may have observed these effects in animals injected with S/MAR containing vectors. Furthermore, over-production of transgenic proteins may potentially result in the activation of cellular stress responses, cell growth arrest and cytotoxicity (Narayanan *et al*, 2011). As a result, the appropriate dose of these vectors must be considered carefully for future applications. In future studies it may also be possible to assess cell toxicity *in-vitro* after transduction with S/MAR containing vectors at a range of doses followed by enumeration of dead and live cells.

Studies in nonhuman primates provided the opportunity to validate our observations in an animal model that is more relevant to translational research. After peripheral vein injection of 4×10^{12} vg/kg, steady state hFIX levels corrected for proviral copy number were approximately 4-fold and 10-fold higher in ssAAV-LP1-hFIXco-IFN-R and ssAAV-LP1-hFIXco-HPRT-F transduced animals respectively as compared to the macaque receiving ssAAV-LP1-hFIXco-control. This is a crucial observation as the potential for a reduction of vector doses by an order of magnitude would have an important impact on the safety of AAV gene transfer to the human population. In future studies it will be important to assess the biological activity of the hFIX protein produced from S/MAR containing vectors. However, in our unpublished data using lentiviral constructs we have not found the HPRT S/MAR to interfere with the activity of human coagulation factor VIII by chromogenic assay. We are therefore confident that hFIX activity will not be affected in the context of rAAV. Although the need to repeat this analysis in a greater number of animals and with new batches of vector is acknowledged, as a proof of principle study these results have strong implications for the use of S/MAR elements in AAV vectors.

However, as previously mentioned, we cannot conclusively say that S/MARs enhance the potency of all AAV vectors. Thus, in future experiments it would be valuable to test S/MARs in the context of different expression cassettes. Furthermore, as the effect of S/MARs depends heavily on DNA structural influences, it may also be interesting to test S/MAR elements at alternative positions within the AAV genome (Schubeler *et al*, 1996). Nonetheless, the strength of this study lies with the fact that we have assessed S/MARs in an expression cassette that has been used clinically. As such, this study will be of interest to those working on translational strategies for the treatment of haemophilia B.

Through hFIX mRNA quantification and ChIP analysis, our data suggests that S/MARs improve AAV transgene expression by maintaining AAV concatamers in an open chromatin configuration that is permissive to transcription. This was inferred by the decrease in repressive histone modifications (H3K9me2 and HP1 α) and increase in active histone modifications (H3K4me2 and H3Ac) associated with S/MAR containing proviral chromatin compared to control vector chromatin extracted from transduced murine liver. Furthermore, we observed a respective 69 and 94-fold enrichment of the histone chaperone protein nucleolin at the distal promoter and transgene regions of the ssAAV-LP1-hFIXco-IFN-R genome in comparison to the same regions of the ssAAV-LP1-hFIXco-control genome. Therefore, we speculate that AAV proviral DNA may be subject to repeat induced gene silencing events that are prevented in the presence of a S/MAR through the recruitment of chromatin remodelling complexes.

In the fruit fly Polycomb proteins are known to be involved in the maintenance of transcriptional gene silencing brought about by RIGS (Pal-Bhadra *et al*, 1997; Pal-Bhadra *et al*, 2002). In our ChIP studies using an antibody against EZH2 (PcG protein) we observed a 2.4-fold enrichment of EZH2 binding in association with control vector genomes as compared to ssAAV-LP1-hFIXco-IFN-R. This analysis supports the notion that AAV silencing may be analogous to RIGS and that S/MARs may prevent such silencing events. However, as this was a preliminary study only, this observation will require repetition. In follow up studies it may also be valuable to carry out ChIP experiments against alternative PcG proteins or histone modifications that PcG proteins give rise to, such as methylation of lysine 27 on histone 3 (H3K27me) (Cheutin & Cavalli, 2012). Alternatively, for high throughput elicitation of proteins bound to control and S/MAR containing genomes, it may be possible to carry out analyses such as Global ExoNuclease-based Enrichment of Chromatin-Associated Proteins for Proteomics (GENECAPP) (explained in figure 6.1) (Smith *et al*, 2011;

Wu *et al*, 2011). However, to conclusively establish that AAV proviral genomes are subject to RIGS, future studies could include northern blotting on RNA extracted from transduced livers to detect siRNA that is complementary to exogenous DNA sequences. As murine models exist for the conditional knockout of the Dicer gene (a ribonuclease involved in siRNA production) it may also be possible to analyse whether AAV mediated transgene expression is enhanced in the absence of RNAi *in-vivo* (Figure 6.2) (Martins *et al*, 2008).

As previously discussed in section 5.4, it will also be of interest to assess other potential mechanisms of S/MAR activity. For example, the attachment of vector DNA to the nuclear matrix may enable enhanced expression levels through putting promoter regions into close proximity with key nuclear factors required for transcription. As such, the enhanced transgene expression that we have observed may be due to increased promoter activity as opposed to prevention of gene silencing. As the nuclear matrix is also a location for proteins involved in RNA transport and processing, it is also possible that the mechanism behind our observations may be due to RNA stability and not increased levels of gene expression. As previously discussed, this matter could be assessed through further chromatin immunoprecipitation experiments using antibodies against matrix attachment factors or matrix associated proteins.

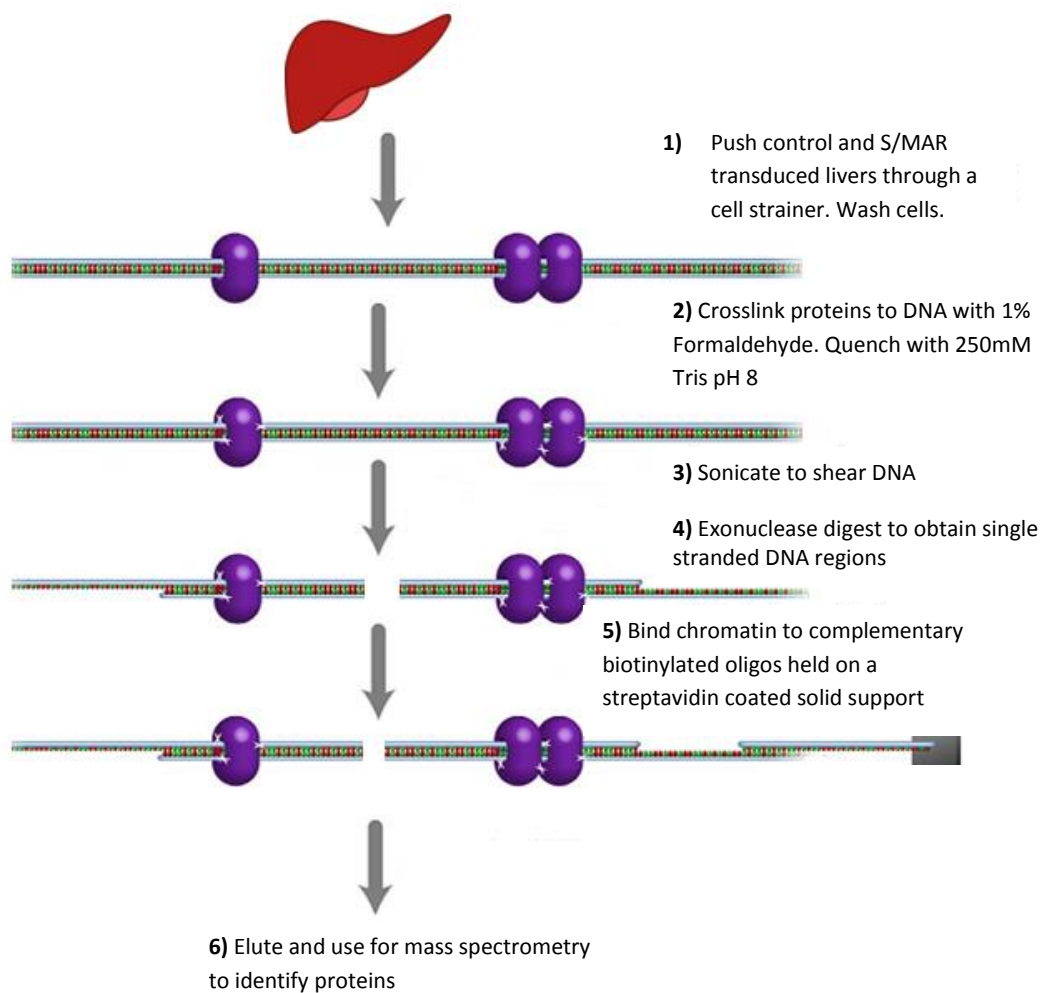


Figure 6.1: Schematic of the GENECAPP protocol. In the GENECAPP process, chromatin is prepared from mouse liver cells by crosslinking proteins to DNA using formaldehyde. Chromatin is then sheared by sonication and enzymes such as E.coli Exonuclease III are used to generate regions of single stranded DNA. Single stranded regions are then able to bind to complementary biotinylated oligos that are held on a streptavidin coated solid support. Proteins are eluted using high salt or urea buffers or through the use of competitive biotin. Eluted proteins can then be used for protein identification by mass spectrometry. Adapted from: (Wu *et al*, 2011).

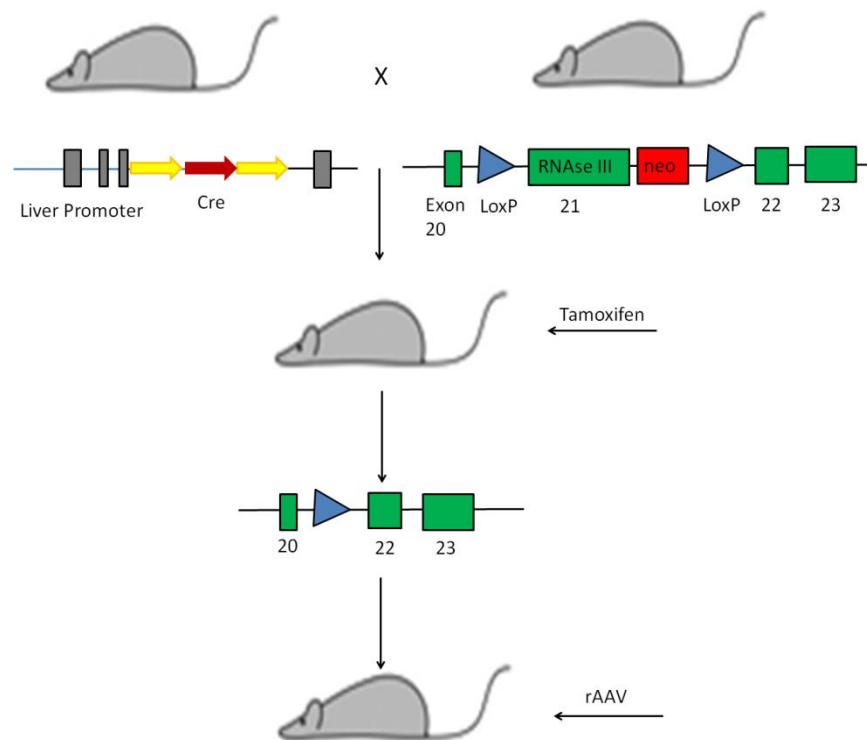


Figure 6.2: Schematic of conditional Dicer knockouts. Mice expressing Cre recombinase (flanked by estrogen-receptor ligand-binding domains) under the control of a liver specific promoter are crossed with mice carrying loxP sites either side of exon 21 of the Dicer (RNase III) gene. In the offspring of these animals injection of Tamoxifen stimulates the activity of Cre and Dicer is knocked out in the liver through recombination of loxP sites. rAAV vectors can then be injected to assess transgene expression in the absence of RNAi. Adapted from: (Martins *et al*, 2008).

Through deletion analysis we have identified a 297bp region of the IFN β S/MAR with potent enhancer activity (fragment 2). At the equivalent dose (4×10^{12} vg/kg) we observed an approximate 3-fold increase in murine plasma hFIX levels when using the ssAVV8-LP1-hFIXco-FR2 vector as compared to ssAVV8-LP1-hFIXco-IFN-R, ssAVV8-LP1-hFIXco-FR1 and ssAVV8-LP1-hFIXco-FR3 vectors. To identify key regulatory motifs in our truncated S/MAR, the fragment 2 sequence was entered into a motif elicitation programme (MEME) (Bailey *et al*, 2006). Discovered motifs were then entered into the Gene Ontology for Motifs (GOMO) algorithm in order to deduce potential biological roles (Buske *et al*, 2010). By this analysis relevant gene ontology (GO) terms elicited for motifs in fragment 2 included: positive regulation of transcription from RNA polymerase II promoter, mRNA processing, positive regulation of gene-specific transcription, and nucleosome assembly. These GO terms are consistent with our findings from ChIP and RNA analyses. However, through the same *in-silico* approach we were unable to discover any motifs in fragments 1 and 3 which would allow us to label these sequences as categorically repressive. The only GO term that was unique to fragment 2 was nucleosome assembly. As such we speculate that the fragment 2 sequence may contain a nucleation site for helix unwinding otherwise known as the core unwinding element (CUE) (Bode *et al*, 2000). In support of this notion, the loose CUE consensus sequence (AAATATATT) that is found in some but not all S/MARs is present in our fragment 2 sequence.

In the HPRT S/MAR deletion analysis we identified a 130bp region (Fragment 2b) that was able to enhance hFIX expression to levels comparable to those achieved with the ssAAV8-LP1-hFIXco-HPRT-F vector following administration of 4×10^{10} vg/kg to the tail vein of C57BL/6 mice ($35 \pm 7\%$ and $46 \pm 9\%$ respectively). At the same dose, this S/MAR fragment also mediated a 35-fold increase in transgene expression as compared to control transduced mice in the context of self-complementary vectors. Through *in-silico* motif analysis key GO terms associated with motifs of HPRT fragment 2b included: chromatin assembly, mRNA processing, gene expression and regulation of production of small RNA involved in gene silencing by RNA. Again, this is fully consistent with our RNA and chromatin immunoprecipitation results and supports the idea that S/MARs may prevent RNA based gene silencing. As previously described, to identify whether these motifs are in fact critical for S/MAR function, future work could include a mutational analysis of motif sequences. If the enhancer effect of the S/MAR fragment is ablated after site directed mutagenesis of the motif, it would infer that the sequence is required for S/MAR activity. Alternatively, to determine the importance of primary DNA sequence, random scrambled

sequences of the S/MAR fragment could be generated using the EMBOSS Shuffleseq programme.

Taken as a whole our deletion analyses suggest that truncated S/MAR elements are able to mediate enhanced levels of transgene expression when incorporated into AAV expression cassettes. Therefore, our short S/MAR fragments may prove to be useful in self-complementary vectors as well as in single stranded vectors where the vector genome is close to the packaging capacity of AAV. The exact sequence composition of S/MAR fragments that is necessary for this effect remains to be conclusively determined. Therefore, in addition to mutation of motifs previously elicited *in-silico*, methods for discovering protein binding motifs (such as protein binding microarray described in figure 6.3) may be valuable to identify sequences that are required to enhance the potency of AAV vectors (Berger & Bulyk, 2009). However, it should be noted that the enhancer effect of S/MARs could be mediated through DNA structure alone as opposed to primary sequence (Boulikas, 1993). Finally, from this study, we are unable to say whether we have discovered the optimum S/MAR fragment. Generating a greater number of fragments to assess every possible sequence permutation would be required to optimise these elements. This can be achieved through protocols such as incremental truncation (described in figure 6.4) that utilise enzymes such as exonuclease III to progressively shorten a DNA sequence over a given time course (Ostermeier *et al*, 1999). However, due to the time required to embark on this endeavour and the heavy burden in terms of vector production and subsequent experimentation, this approach was not employed in the current study.

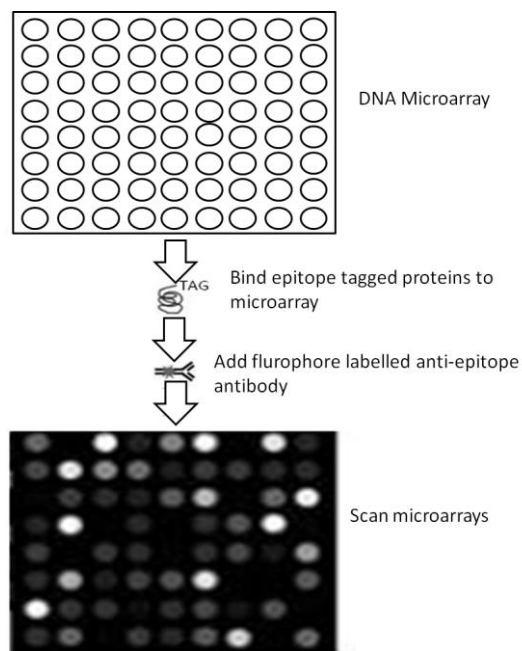


Figure 6.3: Schematic of protein binding microarrays (PBMs). To carry out a PBM, array plates are coated with double stranded DNA regions of interest. Candidate binding proteins are labelled with an epitope and added to the array to bind to DNA with the required recognition sequence. A flurophore labelled antibody against the protein is then used to detect DNA-protein binding through fluorescence imaging. Adapted from: (Bulyk, 2007).

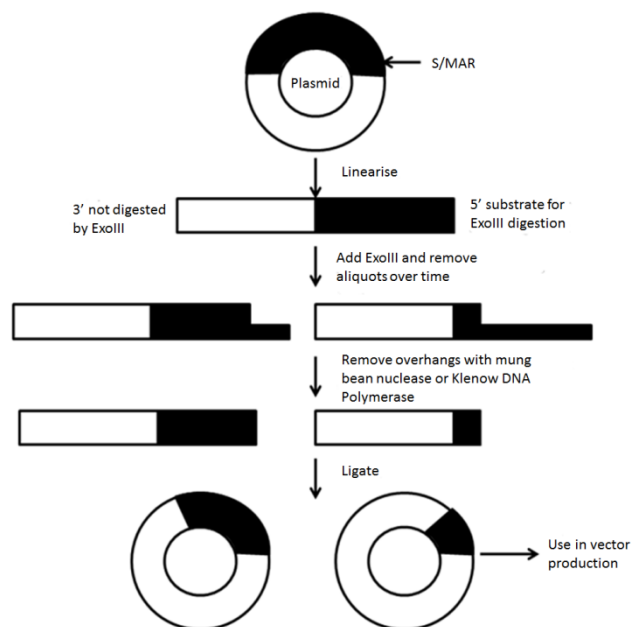


Figure 6.4: Generation of incremental truncation libraries. To generate multiple truncations of a DNA sequence, plasmid DNA containing the sequence of interest is linearised by restriction digest and then subject to digestion with Exonuclease enzymes that remove nucleotides in a unidirectional manner. Several aliquots are removed over the digestion period to obtain truncated sequences of variable lengths. DNA overhangs are removed enzymatically for subsequent ligation of vector DNA. Plasmids with truncated sequences can then be used in virus production.

To conclude, we have critically evaluated S/MAR elements in the context of single stranded rAAV vectors encoding human FIX in murine models and rhesus macaques. In all cases S/MAR elements were found to enhance transgene expression. The basic mechanism behind the up regulation of hFIX when using S/MARs was evaluated by analysing hFIX mRNA levels following gene transfer. Our results are indicative of enhanced transcription levels or improved mRNA stability with S/MARs. Chromatin immunoprecipitation results suggest that S/MARs mediate this effect through the prevention of repressive histone modifications. However, the exact mechanism through which expression augmentation occurs remains to be defined. Through deletion analysis we were able to identify short regions of the IFN β and HPRT S/MAR that enhance transgene expression in single stranded and self-complementary vectors. This reduced the space occupied by S/MARs in our AAV vector and also allowed us to identify sequence motifs that may have a role in S/MAR function. Taken as a whole, S/MARs have demonstrated a significant enhancer effect in the context of rAAV vectors. As such, S/MARs may help to achieve the overall goal of improved vector potency leading to reduced vector doses. This will have an important impact on the safety of rAAV gene transfer in humans.

Bibliography

Ahlenstiel CL, Lim HG, Cooper DA, Ishida T, Kelleher AD, Suzuki K (2012) Direct evidence of nuclear Argonaute distribution during transcriptional silencing links the actin cytoskeleton to nuclear RNAi machinery in human cells. *Nucleic acids research* **40**(4): 1579-95

Aiuti A, Biasco L, Scaramuzza S, Ferrua F, Cicalese MP, Baricordi C, Dionisio F, Calabria A, Giannelli S, Castiello MC, Bosticardo M, Evangelio C, Assanelli A, Casiraghi M, Di Nunzio S, Callegaro L, Benati C, Rizzardi P, Pellin D, Di Serio C, Schmidt M, Von Kalle C, Gardner J, Mehta N, Neduva V, Dow DJ, Galy A, Miniero R, Finocchi A, Metin A, Banerjee PP, Orange JS, Galimberti S, Valsecchi MG, Biffi A, Montini E, Villa A, Ciceri F, Roncarolo MG, Naldini L (2013) Lentiviral hematopoietic stem cell gene therapy in patients with Wiskott-Aldrich syndrome. *Science* **341**(6148): 1233-151

Aiuti A, Cattaneo F, Galimberti S, Benninghoff U, Cassani B, Callegaro L, Scaramuzza S, Andolfi G, Mirolo M, Brigida I, Tabucchi A, Carlucci F, Eibl M, Aker M, Slavin S, Al-Mousa H, Al Ghoniaim A, Ferster A, Duppenthaler A, Notarangelo L, Wintergerst U, Buckley RH, Bregni M, Marktel S, Valsecchi MG, Rossi P, Ciceri F, Miniero R, Bordignon C, Roncarolo MG (2009) Gene therapy for immunodeficiency due to adenosine deaminase deficiency. *The New England journal of medicine* **360**(5): 447-58

Akache B, Grimm D, Pandey K, Yant SR, Xu H, Kay MA (2006) The 37/67-kilodalton laminin receptor is a receptor for adeno-associated virus serotypes 8, 2, 3, and 9. *Journal of virology* **80**(19): 9831-6

Alexander IE, Russell DW, Spence AM, Miller AD (1996) Effects of gamma irradiation on the transduction of dividing and nondividing cells in brain and muscle of rats by adeno-associated virus vectors. *Human gene therapy* **7**(7): 841-50

Allikmets R (1997) A photoreceptor cell-specific ATP-binding transporter gene (ABCR) is mutated in recessive Stargardt macular dystrophy. *Nature genetics* **17**(1): 122

Allocca M, Doria M, Petrillo M, Colella P, Garcia-Hoyos M, Gibbs D, Kim SR, Maguire A, Rex TS, Di Vicino U, Cuttillo L, Sparrow JR, Williams DS, Bennett J, Auricchio A (2008) Serotype-dependent packaging of large genes in adeno-associated viral vectors results in effective gene delivery in mice. *The Journal of clinical investigation* **118**(5): 1955-64

Allocca M, Mussolino C, Garcia-Hoyos M, Sanges D, Iodice C, Petrillo M, Vandenberghe LH, Wilson JM, Marigo V, Surace EM, Auricchio A (2007) Novel adeno-associated virus serotypes efficiently transduce murine photoreceptors. *Journal of virology* **81**(20): 11372-80

Ameri A, Kurachi S, Sueishi K, Kuwahara M, Kurachi K (2003) Myocardial fibrosis in mice with overexpression of human blood coagulation factor IX. *Blood* **101**(5): 1871-3

Angelov D, Bondarenko VA, Almagro S, Menoni H, Mongelard F, Hans F, Mietton F, Studitsky VM, Hamiche A, Dimitrov S, Bouvet P (2006) Nucleolin is a histone chaperone with FACT-like activity and assists remodeling of nucleosomes. *Embo J* **25**(8): 1669-1679

Argyros O, Wong SP, Harbottle RP (2011) Non-viral episomal modification of cells using S/MAR elements. *Expert opinion on biological therapy* **11**(9): 1177-91

Argyros O, Wong SP, Niceta M, Waddington SN, Howe SJ, Coutelle C, Miller AD, Harbottle RP (2008) Persistent episomal transgene expression in liver following delivery of a scaffold/matrix attachment region containing non-viral vector. *Gene therapy* **15**(24): 1593-605

Ashburner M, Ball CA, Blake JA, Botstein D, Butler H, Cherry JM, Davis AP, Dolinski K, Dwight SS, Eppig JT, Harris MA, Hill DP, Issel-Tarver L, Kasarskis A, Lewis S, Matese JC, Richardson JE, Ringwald M, Rubin GM, Sherlock G (2000) Gene ontology: tool for the unification of biology. The Gene Ontology Consortium. *Nature genetics* **25**(1): 25-9

Atchison RW, Casto BC, Hammon WM (1965) Adenovirus-Associated Defective Virus Particles. *Science* **149**(3685): 754-6

Auten J, Agarwal M, Chen J, Sutton R, Plavec I (1999) Effect of scaffold attachment region on transgene expression in retrovirus vector-transduced primary T cells and macrophages. *Human gene therapy* **10**(8): 1389-99

Baiker A, Maercker C, Piechaczek C, Schmidt SB, Bode J, Benham C, Lipps HJ (2000) Mitotic stability of an episomal vector containing a human scaffold/matrix-attached region is provided by association with nuclear matrix. *Nature cell biology* **2**(3): 182-4

Bailey TL, Williams N, Misleh C, Li WW (2006) MEME: discovering and analyzing DNA and protein sequence motifs. *Nucleic acids research* **34**(Web Server issue): W369-73

Bainbridge JW, Smith AJ, Barker SS, Robbie S, Henderson R, Balaggan K, Viswanathan A, Holder GE, Stockman A, Tyler N, Petersen-Jones S, Bhattacharya SS, Thrasher AJ, Fitzke FW, Carter BJ, Rubin GS, Moore AT, Ali RR (2008) Effect of gene therapy on visual function in Leber's congenital amaurosis. *The New England journal of medicine* **358**(21): 2231-9

Bank A (1996) Human somatic cell gene therapy. *BioEssays : news and reviews in molecular, cellular and developmental biology* **18**(12): 999-1007

Bantel-Schaal U, zur Hausen H (1984) Characterization of the DNA of a defective human parvovirus isolated from a genital site. *Virology* **134**(1): 52-63

- Barski A, Zhao K (2009) Genomic location analysis by ChIP-Seq. *J Cell Biochem* **107**(1): 11-8
- Bartel M, Schaffer D, Buning H (2011) Enhancing the Clinical Potential of AAV Vectors by Capsid Engineering to Evade Pre-Existing Immunity. *Frontiers in microbiology* **2**: 204
- Bartlett JS, Samulski RJ, McCown TJ (1998) Selective and rapid uptake of adeno-associated virus type 2 in brain. *Human gene therapy* **9**(8): 1181-6
- Ben-Asher E, Bratosin S, Aloni Y (1982) Intracellular DNA of the parvovirus minute virus of mice is organized in a minichromosome structure. *Journal of virology* **41**(3): 1044-54
- Benham C, KohwiShigematsu T, Bode J (1997) Stress-induced duplex DNA destabilization in scaffold/matrix attachment regions. *J Mol Biol* **274**(2): 181-196
- Berezney R, Coffey DS (1974) Identification of a nuclear protein matrix. *Biochemical and biophysical research communications* **60**(4): 1410-7
- Berezney R, Mortillaro MJ, Ma H, Wei X, Samarabandu J (1995) The nuclear matrix: a structural milieu for genomic function. *International review of cytology* **162A**: 1-65
- Berger MF, Bulyk ML (2009) Universal protein-binding microarrays for the comprehensive characterization of the DNA-binding specificities of transcription factors. *Nature protocols* **4**(3): 393-411
- Berns KI, Linden RM (1995) The cryptic life style of adeno-associated virus. *BioEssays : news and reviews in molecular, cellular and developmental biology* **17**(3): 237-45
- Bernstein E, Caudy AA, Hammond SM, Hannon GJ (2001) Role for a bidentate ribonuclease in the initiation step of RNA interference. *Nature* **409**(6818): 363-6
- Bianchi ME, Agresti A (2005) HMG proteins: dynamic players in gene regulation and differentiation. *Current opinion in genetics & development* **15**(5): 496-506
- Biffi A, Montini E, Lorioli L, Cesani M, Fumagalli F, Plati T, Baldoli C, Martino S, Calabria A, Canale S, Benedicenti F, Vallanti G, Biasco L, Leo S, Kabbara N, Zanetti G, Rizzo WB, Mehta NA, Cicalese MP, Casiraghi M, Boelens JJ, Del Carro U, Dow DJ, Schmidt M, Assanelli A, Neduva V, Di Serio C, Stupka E, Gardner J, von Kalle C, Bordignon C, Ciceri F, Rovelli A, Roncarolo MG, Aiuti A, Sessa M, Naldini L (2013) Lentiviral hematopoietic stem cell gene therapy benefits metachromatic leukodystrophy. *Science* **341**(6148): 1233-1238
- Blackburn SD, Steadman RA, Johnson FB (2006) Attachment of adeno-associated virus type 3H to fibroblast growth factor receptor 1. *Archives of virology* **151**(3): 617-23

Blaese RM, Culver KW, Miller AD, Carter CS, Fleisher T, Clerici M, Shearer G, Chang L, Chiang Y, Tolstoshev P, Greenblatt JJ, Rosenberg SA, Klein H, Berger M, Mullen CA, Ramsey WJ, Muul L, Morgan RA, Anderson WF (1995) T lymphocyte-directed gene therapy for ADA-SCID: initial trial results after 4 years. *Science* **270**(5235): 475-80

Blankinship MJ, Gregorevic P, Allen JM, Harper SQ, Harper H, Halbert CL, Miller AD, Chamberlain JS (2004) Efficient transduction of skeletal muscle using vectors based on adeno-associated virus serotype 6. *Molecular therapy : the journal of the American Society of Gene Therapy* **10**(4): 671-8

Bode J, Benham C, Knopp A, Mielke C (2000) Transcriptional augmentation: modulation of gene expression by scaffold/matrix-attached regions (S/MAR elements). *Critical reviews in eukaryotic gene expression* **10**(1): 73-90

Bode J, Winkelmann S, Gotze S, Spiker S, Tsutsuil K, Bi CP, Prashanth AK, Benham C (2006) Correlations between scaffold/matrix attachment region (S/MAR) binding activity and DNA duplex destabilization energy. *J Mol Biol* **358**(2): 597-613

Boden M, Bailey TL (2008) Associating transcription factor-binding site motifs with target GO terms and target genes. *Nucleic acids research* **36**(12): 4108-17

Bostick B, Ghosh A, Yue Y, Long C, Duan D (2007) Systemic AAV-9 transduction in mice is influenced by animal age but not by the route of administration. *Gene therapy* **14**(22): 1605-9

Boulikas T (1993) Nature of DNA-Sequences at the Attachment Regions of Genes to the Nuclear Matrix. *J Cell Biochem* **52**(1): 14-22

Boutin S, Monteilhet V, Veron P, Leborgne C, Benveniste O, Montus MF, Masurier C (2010) Prevalence of serum IgG and neutralizing factors against adeno-associated virus (AAV) types 1, 2, 5, 6, 8, and 9 in the healthy population: implications for gene therapy using AAV vectors. *Human gene therapy* **21**(6): 704-12

Bulyk ML (2007) Protein binding microarrays for the characterization of DNA-protein interactions. *Advances in biochemical engineering/biotechnology* **104**: 65-85

Buske FA, Boden M, Bauer DC, Bailey TL (2010) Assigning roles to DNA regulatory motifs using comparative genomics. *Bioinformatics* **26**(7): 860-6

Cancio MI, Reiss UM, Nathwani AC, Davidoff AM, Gray JT (2013) Developments in the treatment of hemophilia B: focus on emerging gene therapy. *The application of clinical genetics* **6**: 91-101

Cartier N, Hacein-Bey-Abina S, Bartholomae CC, Veres G, Schmidt M, Kutschera I, Vidaud M, Abel U, Dal-Cortivo L, Caccavelli L, Mahlaoui N, Kiermer V, Mittelstaedt D, Bellesme C, Lahlou N, Lefrere F, Blanche S, Audit M, Payen E, Leboulch P, l'Homme B, Bougneres P, Von Kalle C, Fischer A, Cavazzana-Calvo M, Aubourg P (2009) Hematopoietic stem cell gene therapy with a lentiviral vector in X-linked adrenoleukodystrophy. *Science* **326**(5954): 818-23

Cavalli G (2012) Molecular biology. EZH2 goes solo. *Science* **338**(6113): 1430-1

Chao HJ, Liu YB, Rabinowitz J, Li CW, Samulski RJ, Walsh CE (2000) Several log increase in therapeutic transgene delivery by distinct adeno-associated viral serotype vectors. *Molecular Therapy* **2**(6): 619-623

Cheutin T, Cavalli G (2012) Progressive polycomb assembly on H3K27me3 compartments generates polycomb bodies with developmentally regulated motion. *PLoS genetics* **8**(1): e1002465

Choi VW, McCarty DM, Samulski RJ (2005) AAV hybrid serotypes: improved vectors for gene delivery. *Current gene therapy* **5**(3): 299-310

Cole A (2008) Child in gene therapy programme develops leukaemia. *BMJ* **336**(7634): 13

Conway JE, Zolotukhin S, Muzyczka N, Hayward GS, Byrne BJ (1997) Recombinant adeno-associated virus type 2 replication and packaging is entirely supported by a herpes simplex virus type 1 amplicon expressing Rep and Cap. *Journal of virology* **71**(11): 8780-9

Cremisi C, Pignatti PF, Croissant O, Yaniv M (1975) Chromatin-like structures in polyoma virus and simian virus 10 lytic cycle. *Journal of virology* **17**(1): 204-11

Czermin B, Melfi R, McCabe D, Seitz V, Imhof A, Pirrotta V (2002) Drosophila enhancer of Zeste/ESC complexes have a histone H3 methyltransferase activity that marks chromosomal Polycomb sites. *Cell* **111**(2): 185-96

Dang Q, Auten J, Plavec I (2000) Human beta interferon scaffold attachment region inhibits de novo methylation and confers long-term, copy number-dependent expression to a retroviral vector. *Journal of virology* **74**(6): 2671-8

Davidoff AM, Gray JT, Ng CY, Zhang Y, Zhou J, Spence Y, Bakar Y, Nathwani AC (2005) Comparison of the ability of adeno-associated viral vectors pseudotyped with serotype 2, 5, and 8 capsid proteins to mediate efficient transduction of the liver in murine and nonhuman primate models. *Molecular therapy : the journal of the American Society of Gene Therapy* **11**(6): 875-88

Davidoff AM, Ng CY, Sleep S, Gray J, Azam S, Zhao Y, McIntosh JH, Karimipoor M, Nathwani AC (2004) Purification of recombinant adeno-associated virus type 8 vectors by ion exchange chromatography generates clinical grade vector stock. *Journal of virological methods* **121**(2): 209-15

Davidoff AM, Ng CYC, Zhou JF, Spence Y, Nathwani AC (2003) Sex significantly influences transduction of murine liver by recombinant adeno-associated viral vectors through an androgen-dependent pathway. *Blood* **102**(2): 480-488

Davidson BL, Stein CS, Heth JA, Martins I, Kotin RM, Derksen TA, Zabner J, Ghodsi A, Chiorini JA (2000) Recombinant adeno-associated virus type 2, 4, and 5 vectors: transduction of variant cell types and regions in the mammalian central nervous system. *Proceedings of the National Academy of Sciences of the United States of America* **97**(7): 3428-32

Daya S, Berns KI (2008) Gene Therapy Using Adeno-Associated Virus Vectors. *Clin Microbiol Rev* **21**(4): 583-593

den Hollander AI, Koenekoop RK, Yzer S, Lopez I, Arends ML, Voeseke KE, Zonneveld MN, Strom TM, Meitinger T, Brunner HG, Hoyng CB, van den Born LI, Rohrschneider K, Cremers FP (2006) Mutations in the CEP290 (NPHP6) gene are a frequent cause of Leber congenital amaurosis. *American journal of human genetics* **79**(3): 556-61

Di Pasquale G, Davidson BL, Stein CS, Martins IS, Scudiero D, Monks A, Chiorini JA (2003) Identification of PDGFR as a receptor for AAV-5 transduction. *Nature medicine* **9**(10): 1306-1312

Dickinson LA, Dickinson CD, Kohwi-Shigematsu T (1997) An atypical homeodomain in SATB1 promotes specific recognition of the key structural element in a matrix attachment region. *Journal of Biological Chemistry* **272**(17): 11463-11470

Dickinson LA, Kohwi-Shigematsu T (1995) Nucleolin is a matrix attachment region DNA-binding protein that specifically recognizes a region with high base-unpairing potential. *Molecular and cellular biology* **15**(1): 456-65

Ding W, Zhang L, Yan Z, Engelhardt JF (2005) Intracellular trafficking of adeno-associated viral vectors. *Gene therapy* **12**(11): 873-80

Dover GJ, Brusilow S, Charache S (1994) Induction of fetal hemoglobin production in subjects with sickle cell anemia by oral sodium phenylbutyrate. *Blood* **84**(1): 339-43

Duan D, Yue Y, Engelhardt JF (2001) Expanding AAV packaging capacity with trans-splicing or overlapping vectors: a quantitative comparison. *Molecular therapy : the journal of the American Society of Gene Therapy* **4**(4): 383-91

Duan D, Yue Y, Yan Z, Engelhardt JF (2000) A new dual-vector approach to enhance recombinant adeno-associated virus-mediated gene expression through intermolecular cis activation. *Nature medicine* **6**(5): 595-8

Ehrhardt A, Haase R, Schepers A, Deutsch MJ, Lipps HJ, Baiker A (2008) Episomal vectors for gene therapy. *Current gene therapy* **8**(3): 147-61

Fagone P, Wright JF, Nathwani AC, Nienhuis AW, Davidoff AM, Gray JT (2011) Systemic Errors in Quantitative Polymerase Chain Reaction Titration of Self-Complementary Adeno-Associated Viral Vectors and Improved Alternative Methods. *Human gene therapy*

Fajardy I, Moitrot E, Vambergue A, Vandersippe-Millot M, Deruelle P, Rousseaux J (2009) Time course analysis of RNA stability in human placenta. *BMC molecular biology* **10**: 21

Fisher KJ, Gao GP, Weitzman MD, DeMatteo R, Burda JF, Wilson JM (1996) Transduction with recombinant adeno-associated virus for gene therapy is limited by leading-strand synthesis. *Journal of virology* **70**(1): 520-532

Flotte TR, Brantly ML, Spencer LT, Byrne BJ, Spencer CT, Baker DJ, Humphries M (2004) Phase I trial of intramuscular injection of a recombinant adeno-associated virus alpha 1-antitrypsin (rAAV2-CB-hAAT) gene vector to AAT-deficient adults. *Human gene therapy* **15**(1): 93-128

Flotte TR, Trapnell BC, Humphries M, Carey B, Calcedo R, Rouhani F, Campbell-Thompson M, Yachnis AT, Sandhaus RA, McElvaney NG, Mueller C, Messina LM, Wilson JM, Brantly M, Knop DR, Ye GJ, Chulay JD (2011) Phase 2 clinical trial of a recombinant adeno-associated viral vector expressing alpha1-antitrypsin: interim results. *Human gene therapy* **22**(10): 1239-47

Foust KD, Nurre E, Montgomery CL, Hernandez A, Chan CM, Kaspar BK (2009) Intravascular AAV9 preferentially targets neonatal neurons and adult astrocytes. *Nature biotechnology* **27**(1): 59-65

Gao G, Vandenberghe LH, Alvira MR, Lu Y, Calcedo R, Zhou X, Wilson JM (2004) Clades of Adeno-associated viruses are widely disseminated in human tissues. *Journal of virology* **78**(12): 6381-8

Gao GP, Alvira MR, Wang L, Calcedo R, Johnston J, Wilson JM (2002) Novel adeno-associated viruses from rhesus monkeys as vectors for human gene therapy. *Proceedings of the National Academy of Sciences of the United States of America* **99**(18): 11854-9

Garrick D, Fiering S, Martin DI, Whitelaw E (1998) Repeat-induced gene silencing in mammals. *Nature genetics* **18**(1): 56-9

Girod A, Ried M, Wobus C, Lahm H, Leike K, Kleinschmidt J, Deleage G, Hallek M (1999) Genetic capsid modifications allow efficient re-targeting of adeno-associated virus type 2. *Nature medicine* **5**(12): 1438

Gluch A, Vidakovic M, Bode J (2008) Scaffold/matrix attachment regions (S/MARs): relevance for disease and therapy. *Handbook of experimental pharmacology*(186): 67-103

Goetze S, Baer A, Winkelmann S, Nehlsen K, Seibler J, Maass K, Bode J (2005) Performance of genomic bordering elements at predefined genomic loci. *Molecular and cellular biology* **25**(6): 2260-72

Goncalves MA (2005) Adeno-associated virus: from defective virus to effective vector. *Virology journal* **2**: 43

Grieger JC, Samulski RJ (2005) Packaging capacity of adeno-associated virus serotypes: impact of larger genomes on infectivity and postentry steps. *Journal of virology* **79**(15): 9933-44

Haas J, Park EC, Seed B (1996) Codon usage limitation in the expression of HIV-1 envelope glycoprotein. *Current biology : CB* **6**(3): 315-24

Hacein-Bey-Abina S, von Kalle C, Schmidt M, Le Deist F, Wulffraat N, McIntyre E, Radford I, Villeval JL, Fraser CC, Cavazzana-Calvo M, Fischer A (2003a) A serious adverse event after successful gene therapy for X-linked severe combined immunodeficiency. *The New England journal of medicine* **348**(3): 255-6

Hacein-Bey-Abina S, Von Kalle C, Schmidt M, McCormack MP, Wulffraat N, Leboulch P, Lim A, Osborne CS, Pawliuk R, Morillon E, Sorensen R, Forster A, Fraser P, Cohen JI, de Saint Basile G, Alexander I, Wintergerst U, Frebourg T, Aurias A, Stoppa-Lyonnet D, Romana S, Radford-Weiss I, Gross F, Valensi F, Delabesse E, Macintyre E, Sigaux F, Soulier J, Leiva LE, Wissler M, Prinz C, Rabbitts TH, Le Deist F, Fischer A, Cavazzana-Calvo M (2003b) LMO2-associated clonal T cell proliferation in two patients after gene therapy for SCID-X1. *Science* **302**(5644): 415-9

Halbert CL, Allen JM, Miller AD (2001) Adeno-associated virus type 6 (AAV6) vectors mediate efficient transduction of airway epithelial cells in mouse lungs compared to that of AAV2 vectors. *Journal of virology* **75**(14): 6615-6624

Hamilton AJ, Baulcombe DC (1999) A species of small antisense RNA in posttranscriptional gene silencing in plants. *Science* **286**(5441): 950-2

Hauck B, Chen L, Xiao W (2003) Generation and characterization of chimeric recombinant AAV vectors. *Molecular therapy : the journal of the American Society of Gene Therapy* **7**(3): 419-25

Herzog RW, Fields PA, Arruda VR, Brubaker JO, Armstrong E, McClintock D, Bellinger DA, Couto LB, Nichols TC, High KA (2002) Influence of vector dose on factor IX-specific T and B cell responses in muscle-directed gene therapy. *Human gene therapy* **13**(11): 1281-91

Herzog RW, Hagstrom JN, Kung SH, Tai SJ, Wilson JM, Fisher KJ, High KA (1997) Stable gene transfer and expression of human blood coagulation factor IX after intramuscular injection of recombinant adeno-associated virus. *Proceedings of the National Academy of Sciences of the United States of America* **94**(11): 5804-9

Herzog RW, Yang EY, Couto LB, Hagstrom JN, Elwell D, Fields PA, Burton M, Bellinger DA, Read MS, Brinkhous KM, Podsakoff GM, Nichols TC, Kurtzman GJ, High KA (1999) Long-term correction of canine hemophilia B by gene transfer of blood coagulation factor IX mediated by adeno-associated viral vector. *Nature medicine* **5**(1): 56-63

High K, Manno C, Sabatino D, Hutchison S, Dake M, Razavi M, Kaye R, Aruda V, Herzog R, Rustagi P, Rasko J, Hoots K, Blatt P, Sommer J, Ragni M, Ozelo M, Konkle B, Lessard R, Luk A, Glader B, Pierce G, Couto L, Kay M (2004a) Immune responses to AAV and to Factor IX in a phase I study of AAV-mediated, liver-directed gene transfer for hemophilia B. *Molecular Therapy* **9**: S383-S384

High K, Tigges M, Manno C, Sabatino D, Arruda V, Herzog R, Rustagi P, Rasko J, Sommer J, Jaworski K, Ragni M, Glader B, Lessard R, Luk A, Couto L, Jiang HY, Pierce G, Kay M (2004b) Human immune responses to AAV-2 capsid may limit duration of expression in liver-directed gene transfer in humans with hemophilia B. *Blood* **104**(11): 121a-121a

High KA (2011) Gene therapy for haemophilia: a long and winding road. *Journal of thrombosis and haemostasis : JTH* **9 Suppl 1**: 2-11

Hoggan MD, Blacklow NR, Rowe WP (1966) Studies of small DNA viruses found in various adenovirus preparations: physical, biological, and immunological characteristics. *Proceedings of the National Academy of Sciences of the United States of America* **55**(6): 1467-74

Huttner NA, Girod A, Perabo L, Edbauer D, Kleinschmidt JA, Buning H, Hallek M (2003) Genetic modifications of the adeno-associated virus type 2 capsid reduce the affinity and the neutralizing effects of human serum antibodies. *Gene therapy* **10**(26): 2139-47

Inagaki K, Fuess S, Storm TA, Gibson GA, McTiernan CF, Kay MA, Nakai H (2006) Robust systemic transduction with AAV9 vectors in mice: efficient global cardiac gene transfer

superior to that of AAV8. *Molecular therapy : the journal of the American Society of Gene Therapy* **14**(1): 45-53

Jennings K, Miyamae T, Traister R, Marinov A, Katakura S, Sowders D, Trapnell B, Wilson JM, Gao G, Hirsch R (2005) Proteasome inhibition enhances AAV-mediated transgene expression in human synoviocytes in vitro and in vivo. *Molecular therapy : the journal of the American Society of Gene Therapy* **11**(4): 600-7

Jessup M, Greenberg B, Mancini D, Cappola T, Pauly DF, Jaski B, Yaroshinsky A, Zsebo KM, Dittrich H, Hajjar RJ (2011) Calcium Upregulation by Percutaneous Administration of Gene Therapy in Cardiac Disease (CUPID): a phase 2 trial of intracoronary gene therapy of sarcoplasmic reticulum Ca²⁺-ATPase in patients with advanced heart failure. *Circulation* **124**(3): 304-13

Jorgensen RA, Cluster PD, English J, Que Q, Napoli CA (1996) Chalcone synthase cosuppression phenotypes in petunia flowers: comparison of sense vs. antisense constructs and single-copy vs. complex T-DNA sequences. *Plant molecular biology* **31**(5): 957-73

Kadam P, Bhalerao S (2010) Sample size calculation. *International journal of Ayurveda research* **1**(1): 55-7

Kaludov N, Brown KE, Walters RW, Zabner J, Chiorini JA (2001) Adeno-associated virus serotype 4 (AAV4) and AAV5 both require sialic acid binding for hemagglutination and efficient transduction but differ in sialic acid linkage specificity. *Journal of virology* **75**(15): 6884-93

Kaplitt MG, Feigin A, Tang C, Fitzsimons HL, Mattis P, Lawlor PA, Bland RJ, Young D, Strybing K, Eidelberg D, During MJ (2007) Safety and tolerability of gene therapy with an adeno-associated virus (AAV) borne GAD gene for Parkinson's disease: an open label, phase I trial. *Lancet* **369**(9579): 2097-105

Kashiwakura Y, Tamayose K, Iwabuchi K, Hirai Y, Shimada T, Matsumoto K, Nakamura T, Watanabe M, Oshimi K, Daida H (2005) Hepatocyte growth factor receptor is a coreceptor for adeno-associated virus type 2 infection. *Journal of virology* **79**(1): 609-14

Kasper CK, Buzin CH (2009) Mosaics and haemophilia. *Haemophilia : the official journal of the World Federation of Hemophilia* **15**(6): 1181-6

Keats BJ, Corey DP (1999) The usher syndromes. *American journal of medical genetics* **89**(3): 158-66

Kocot FJ, Carter BJ, Garon CF, Rose JA (1973) Self-complementarity of terminal sequences within plus or minus strands of adenovirus-associated virus DNA. *Proceedings of the National Academy of Sciences of the United States of America* **70**(1): 215-9

Koeberl DD, Alexander IE, Halbert CL, Russell DW, Miller AD (1997) Persistent expression of human clotting factor IX from mouse liver after intravenous injection of adeno-associated virus vectors. *Proceedings of the National Academy of Sciences of the United States of America* **94**(4): 1426-31

Kohwi-Shigematsu T, deBelle I, Dickinson LA, Galande S, Kohwi Y (1998) Identification of base-unpairing region-binding proteins and characterization of their in vivo binding sequences. *Methods in cell biology* **53**: 323-54

Kurachi K, Davie EW (1982) Isolation and characterization of a cDNA coding for human factor IX. *Proceedings of the National Academy of Sciences of the United States of America* **79**(21): 6461-4

Kurre P, Morris J, Thomasson B, Kohn DB, Kiem HP (2003) Scaffold attachment region-containing retrovirus vectors improve long-term proviral expression after transplantation of GFP-modified CD34+ baboon repopulating cells. *Blood* **102**(9): 3117-9

Leger A, Le Guiner C, Nickerson ML, McGee Im K, Ferry N, Moullier P, Snyder RO, Penaud-Budloo M (2011) Adeno-associated viral vector-mediated transgene expression is independent of DNA methylation in primate liver and skeletal muscle. *PLoS one* **6**(6): e20881

Lienert F, Mohn F, Tiwari VK, Baubec T, Roloff TC, Gaidatzis D, Stadler MB, Schubeler D (2011) Genomic prevalence of heterochromatic H3K9me2 and transcription do not discriminate pluripotent from terminally differentiated cells. *PLoS genetics* **7**(6): e1002090

Ling C, Lu Y, Kalsi JK, Jayandharan GR, Li B, Ma W, Cheng B, Gee SW, McGoogan KE, Govindasamy L, Zhong L, Agbandje-McKenna M, Srivastava A (2010) Human hepatocyte growth factor receptor is a cellular coreceptor for adeno-associated virus serotype 3. *Human gene therapy* **21**(12): 1741-7

Ljung R, Petrini P, Nilsson IM (1990) Diagnostic symptoms of severe and moderate haemophilia A and B. A survey of 140 cases. *Acta paediatrica Scandinavica* **79**(2): 196-200

Ljung RC (1999) Prophylactic infusion regimens in the management of hemophilia. *Thrombosis and haemostasis* **82**(2): 525-30

Loiler SA, Conlon TJ, Song S, Tang Q, Warrington KH, Agarwal A, Kapturczak M, Li C, Ricordi C, Atkinson MA, Muzyczka N, Flotte TR (2003) Targeting recombinant adeno-associated virus vectors to enhance gene transfer to pancreatic islets and liver. *Gene therapy* **10**(18): 1551-8

Loiler SA, Tang Q, Clarke T, Campbell-Thompson ML, Chiodo V, Hauswirth W, Cruz P, Perret-Gentil M, Atkinson MA, Ramiya VK, Flotte TR (2005) Localized gene expression following administration of adeno-associated viral vectors via pancreatic ducts. *Molecular therapy : the journal of the American Society of Gene Therapy* **12**(3): 519-27

Lozier JN, Metzger ME, Donahue RE, Morgan RA (1999) Adenovirus-mediated expression of human coagulation factor IX in the rhesus macaque is associated with dose-limiting toxicity. *Blood* **94**(12): 3968-75

Lu F, Zhou J, Wiedmer A, Madden K, Yuan Y, Lieberman PM (2003) Chromatin remodeling of the Kaposi's sarcoma-associated herpesvirus ORF50 promoter correlates with reactivation from latency. *Journal of virology* **77**(21): 11425-35

Ma H, Siegel AJ, Berezney R (1999) Association of chromosome territories with the nuclear matrix. Disruption of human chromosome territories correlates with the release of a subset of nuclear matrix proteins. *The Journal of cell biology* **146**(3): 531-42

Mackus WJ, Frakking FN, Grummels A, Gamadia LE, De Bree GJ, Hamann D, Van Lier RA, Van Oers MH (2003) Expansion of CMV-specific CD8+CD45RA+CD27- T cells in B-cell chronic lymphocytic leukemia. *Blood* **102**(3): 1057-63

Maguire AM, High KA, Auricchio A, Wright JF, Pierce EA, Testa F, Mingozzi F, Bennicelli JL, Ying GS, Rossi S, Fulton A, Marshall KA, Banfi S, Chung DC, Morgan JI, Hauck B, Zeleniaia O, Zhu X, Raffini L, Coppieters F, De Baere E, Shindler KS, Volpe NJ, Surace EM, Acerra C, Lyubarsky A, Redmond TM, Stone E, Sun J, McDonnell JW, Leroy BP, Simonelli F, Bennett J (2009) Age-dependent effects of RPE65 gene therapy for Leber's congenital amaurosis: a phase 1 dose-escalation trial. *Lancet* **374**(9701): 1597-605

Maguire AM, Simonelli F, Pierce EA, Pugh EN, Jr., Mingozzi F, Bennicelli J, Banfi S, Marshall KA, Testa F, Surace EM, Rossi S, Lyubarsky A, Arruda VR, Konkle B, Stone E, Sun J, Jacobs J, Dell'Osso L, Hertle R, Ma JX, Redmond TM, Zhu X, Hauck B, Zeleniaia O, Shindler KS, Maguire MG, Wright JF, Volpe NJ, McDonnell JW, Auricchio A, High KA, Bennett J (2008) Safety and efficacy of gene transfer for Leber's congenital amaurosis. *The New England journal of medicine* **358**(21): 2240-8

Mann BS, Johnson JR, Cohen MH, Justice R, Pazdur R (2007) FDA approval summary: vorinostat for treatment of advanced primary cutaneous T-cell lymphoma. *The oncologist* **12**(10): 1247-52

Manno CS, Chew AJ, Hutchison S, Larson PJ, Herzog RW, Arruda VR, Tai SJ, Ragni MV, Thompson A, Ozelo M, Couto LB, Leonard DG, Johnson FA, McClelland A, Scallan C, Skarsgard E, Flake AW, Kay MA, High KA, Glader B (2003) AAV-mediated factor IX gene transfer to skeletal muscle in patients with severe hemophilia B. *Blood* **101**(8): 2963-72

Manno CS, Pierce GF, Arruda VR, Glader B, Ragni M, Rasko JJ, Ozelo MC, Hoots K, Blatt P, Konkle B, Dake M, Kaye R, Razavi M, Zajko A, Zehnder J, Rustagi PK, Nakai H, Chew A, Leonard D, Wright JF, Lessard RR, Sommer JM, Tigges M, Sabatino D, Luk A, Jiang H, Mingozzi F, Couto L, Ertl HC, High KA, Kay MA (2006) Successful transduction of liver in hemophilia by AAV-Factor IX and limitations imposed by the host immune response. *Nature medicine* **12**(3): 342-7

Marcus-Sekura CJ, Carter BJ (1983) Chromatin-like structure of adeno-associated virus DNA in infected cells. *Journal of virology* **48**(1): 79-87

Markusic DM, Herzog RW, Aslanidi GV, Hoffman BE, Li BZ, Li MX, Jayandharan GR, Ling C, Zolotukhin I, Ma WQ, Zolotukhin S, Srivastava A, Zhong L (2010) High-efficiency Transduction and Correction of Murine Hemophilia B Using AAV2 Vectors Devoid of Multiple Surface-exposed Tyrosines. *Molecular Therapy* **18**(12): 2048-2056

Martino AT, Basner-Tschakarjan E, Markusic DM, Finn JD, Hinderer C, Zhou S, Ostrov DA, Srivastava A, Ertl HC, Terhorst C, High KA, Mingozzi F, Herzog RW (2013) Engineered AAV vector minimizes in vivo targeting of transduced hepatocytes by capsid-specific CD8+ T cells. *Blood* **121**(12): 2224-33

Martins PADC, Bourajjaj M, Gladka M, Kortland M, van Oort RJ, Pinto YM, Molkentin JD, De Windt LJ (2008) Conditional Dicer gene deletion in the postnatal myocardium provokes spontaneous cardiac remodeling. *Circulation* **118**(15): 1567-1576

McCarty DM, Fu H, Monahan PE, Toulson CE, Naik P, Samulski RJ (2003) Adeno-associated virus terminal repeat (TR) mutant generates self-complementary vectors to overcome the rate-limiting step to transduction in vivo. *Gene therapy* **10**(26): 2112-8

McCarty DM, Monahan PE, Samulski RJ (2001) Self-complementary recombinant adeno-associated virus (scAAV) vectors promote efficient transduction independently of DNA synthesis. *Gene therapy* **8**(16): 1248-54

McLaughlin SK, Collis P, Hermonat PL, Muzyczka N (1988) Adeno-associated virus general transduction vectors: analysis of proviral structures. *Journal of virology* **62**(6): 1963-73

Miao CH, Nakai H, Thompson AR, Storm TA, Chiu W, Snyder RO, Kay MA (2000a) Nonrandom transduction of recombinant adeno-associated virus vectors in mouse hepatocytes in vivo: cell cycling does not influence hepatocyte transduction. *Journal of virology* **74**(8): 3793-803

Miao CH, Ohashi K, Patijn GA, Meuse L, Ye X, Thompson AR, Kay MA (2000b) Inclusion of the hepatic locus control region, an intron, and untranslated region increases and stabilizes hepatic factor IX gene expression in vivo but not in vitro. *Molecular therapy : the journal of the American Society of Gene Therapy* **1**(6): 522-32

Mingozzi F, Anguela XM, Pavani G, Chen Y, Davidson RJ, Hui DJ, Yazicioglu M, Elkouby L, Hinderer CJ, Faella A, Howard C, Tai A, Podsakoff GM, Zhou S, Basner-Tschakarjan E, Wright JF, High KA (2013) Overcoming preexisting humoral immunity to AAV using capsid decoys. *Science translational medicine* **5**(194): 194ra92

Mingozzi F, Liu YL, Dobrzynski E, Kaufhold A, Liu JH, Wang Y, Arruda VR, High KA, Herzog RW (2003) Induction of immune tolerance to coagulation factor IX antigen by in vivo hepatic gene transfer. *The Journal of clinical investigation* **111**(9): 1347-56

Mingozzi F, Maus MV, Hui DJ, Sabatino DE, Murphy SL, Rasko JE, Ragni MV, Manno CS, Sommer J, Jiang H, Pierce GF, Ertl HC, High KA (2007) CD8(+) T-cell responses to adeno-associated virus capsid in humans. *Nature medicine* **13**(4): 419-22

Mingozzi F, Meulenberg JJ, Hui DJ, Basner-Tschakarjan E, Hasbrouck NC, Edmonson SA, Hutnick NA, Betts MR, Kastelein JJ, Stroes ES, High KA (2009) AAV-1-mediated gene transfer to skeletal muscle in humans results in dose-dependent activation of capsid-specific T cells. *Blood* **114**(10): 2077-86

Mirkovitch J, Mirault ME, Laemmli UK (1984) Organization of the higher-order chromatin loop: specific DNA attachment sites on nuclear scaffold. *Cell* **39**(1): 223-32

Moazed D (2009) Small RNAs in transcriptional gene silencing and genome defence. *Nature* **457**(7228): 413-20

Monahan PE, Lothrop CD, Sun J, Hirsch ML, Kafri T, Kantor B, Sarkar R, Tillson DM, Elia JR, Samulski RJ (2010) Proteasome inhibitors enhance gene delivery by AAV virus vectors expressing large genomes in hemophilia mouse and dog models: a strategy for broad clinical application. *Molecular therapy : the journal of the American Society of Gene Therapy* **18**(11): 1907-16

Moreno R, Martinez I, Petriz J, Nadal M, Tintore X, Gonzalez JR, Gratacos E, Aran JM (2011) The beta-interferon scaffold attachment region confers high-level transgene expression and avoids extinction by epigenetic modifications of integrated provirus in adipose tissue-derived human mesenchymal stem cells. *Tissue engineering Part C, Methods* **17**(3): 275-87

Mori S, Wang L, Takeuchi T, Kanda T (2004) Two novel adeno-associated viruses from cynomolgus monkey: pseudotyping characterization of capsid protein. *Virology* **330**(2): 375-83

Mount JD, Herzog RW, Tillson DM, Goodman SA, Robinson N, McClelland ML, Bellinger D, Nichols TC, Arruda VR, Lothrop CD, Jr., High KA (2002) Sustained phenotypic correction of hemophilia B dogs with a factor IX null mutation by liver-directed gene therapy. *Blood* **99**(8): 2670-6

Mueller C, Flotte TR (2008) Clinical gene therapy using recombinant adeno-associated virus vectors. *Gene therapy* **15**(11): 858-63

Murphy SL, High KA (2008) Gene therapy for haemophilia. *British journal of haematology* **140**(5): 479-87

Muskens MW, Vissers AP, Mol JN, Kooter JM (2000) Role of inverted DNA repeats in transcriptional and post-transcriptional gene silencing. *Plant molecular biology* **43**(2-3): 243-60

Nakai H, Fuess S, Storm TA, Muramatsu S, Nara Y, Kay MA (2005) Unrestricted hepatocyte transduction with adeno-associated virus serotype 8 vectors in mice. *Journal of virology* **79**(1): 214-24

Nakai H, Storm TA, Kay MA (2000) Increasing the size of rAAV-mediated expression cassettes in vivo by intermolecular joining of two complementary vectors. *Nature biotechnology* **18**(5): 527-32

Nakai H, Thomas CE, Storm TA, Fuess S, Powell S, Wright JF, Kay MA (2002) A limited number of transducible hepatocytes restricts a wide-range linear vector dose response in recombinant adeno-associated virus-mediated liver transduction. *Journal of virology* **76**(22): 11343-11349

Nakai H, Yant SR, Storm TA, Fuess S, Meuse L, Kay MA (2001) Extrachromosomal recombinant adeno-associated virus vector genomes are primarily responsible for stable liver transduction in vivo. *Journal of virology* **75**(15): 6969-76

Namciu SJ, Blochlinger KB, Fournier RE (1998) Human matrix attachment regions insulate transgene expression from chromosomal position effects in *Drosophila melanogaster*. *Molecular and cellular biology* **18**(4): 2382-91

Napoli C, Lemieux C, Jorgensen R (1990) Introduction of a Chimeric Chalcone Synthase Gene into *Petunia* Results in Reversible Co-Suppression of Homologous Genes in trans. *The Plant cell* **2**(4): 279-289

Narayanan A, Ridilla M, Yernool DA (2011) Restrained expression, a method to overproduce toxic membrane proteins by exploiting operator-repressor interactions. *Protein science : a publication of the Protein Society* **20**(1): 51-61

Nathwani AC, Cochrane M, McIntosh J, Ng CY, Zhou J, Gray JT, Davidoff AM (2009) Enhancing transduction of the liver by adeno-associated viral vectors. *Gene therapy* **16**(1): 60-9

Nathwani AC, Davidoff A, Hanawa H, Zhou JF, Vanin EF, Nienhuis AW (2001) Factors influencing in vivo transduction by recombinant adeno-associated viral vectors expressing the human factor IX cDNA. *Blood* **97**(5): 1258-65

Nathwani AC, Davidoff AM, Hanawa H, Hu Y, Hoffer FA, Nikanorov A, Slaughter C, Ng CY, Zhou J, Lozier JN, Mandrell TD, Vanin EF, Nienhuis AW (2002) Sustained high-level expression of human factor IX (hFIX) after liver-targeted delivery of recombinant adeno-associated virus encoding the hFIX gene in rhesus macaques. *Blood* **100**(5): 1662-9

Nathwani AC, Gray JT, McIntosh J, Ng CY, Zhou J, Spence Y, Cochrane M, Gray E, Tuddenham EG, Davidoff AM (2007) Safe and efficient transduction of the liver after peripheral vein infusion of self-complementary AAV vector results in stable therapeutic expression of human FIX in nonhuman primates. *Blood* **109**(4): 1414-21

Nathwani AC, Gray JT, Ng CY, Zhou J, Spence Y, Waddington SN, Tuddenham EG, Kembball-Cook G, McIntosh J, Boon-Spijker M, Mertens K, Davidoff AM (2006) Self-complementary adeno-associated virus vectors containing a novel liver-specific human factor IX expression cassette enable highly efficient transduction of murine and nonhuman primate liver. *Blood* **107**(7): 2653-61

Nathwani AC, Tuddenham EG, Rangarajan S, Rosales C, McIntosh J, Linch DC, Chowdary P, Riddell A, Pie AJ, Harrington C, O'Beirne J, Smith K, Pasi J, Glader B, Rustagi P, Ng CY, Kay MA, Zhou J, Spence Y, Morton CL, Allay J, Coleman J, Sleep S, Cunningham JM, Srivastava D, Basner-Tschakarjan E, Mingozzi F, High KA, Gray JT, Reiss UM, Nienhuis AW, Davidoff AM (2011) Adenovirus-associated virus vector-mediated gene transfer in hemophilia B. *The New England journal of medicine* **365**(25): 2357-65

Ng R, Govindasamy L, Gurda BL, McKenna R, Kozyreva OG, Samulski RJ, Parent KN, Baker TS, Agbandje-McKenna M (2010) Structural Characterization of the Dual Glycan Binding Adeno-Associated Virus Serotype 6. *Journal of virology* **84**(24): 12945-12957

Nicklin SA, Buening H, Dishart KL, de Alwis M, Girod A, Hacker U, Thrasher AJ, Ali RR, Hallek M, Baker AH (2001) Efficient and selective AAV2-mediated gene transfer directed to human vascular endothelial cells. *Molecular therapy : the journal of the American Society of Gene Therapy* **4**(3): 174-81

Nonnenmacher M, Weber T (2012) Intracellular transport of recombinant adeno-associated virus vectors. *Gene therapy* **19**(6): 649-58

Okada T, Uchibori R, Iwata-Okada M, Takahashi M, Nomoto T, Nonaka-Sarukawa M, Ito T, Liu Y, Mizukami H, Kume A, Kobayashi E, Ozawa K (2006) A histone deacetylase inhibitor enhances recombinant adeno-associated virus-mediated gene expression in tumor cells. *Molecular therapy : the journal of the American Society of Gene Therapy* **13**(4): 738-46

Okulski H, Druck B, Bhalerao S, Ringrose L (2011) Quantitative analysis of polycomb response elements (PREs) at identical genomic locations distinguishes contributions of PRE sequence and genomic environment. *Epigenetics & chromatin* **4**: 4

Opie SR, Warrington KH, Agbandje-McKenna M, Zolotukhin S, Muzyczka N (2003) Identification of amino acid residues in the capsid proteins of adeno-associated virus type 2 that contribute to heparan sulfate proteoglycan binding. *Journal of virology* **77**(12): 6995-7006

Ostermeier M, Shim JH, Benkovic SJ (1999) A combinatorial approach to hybrid enzymes independent of DNA homology. *Nature biotechnology* **17**(12): 1205-9

Pal-Bhadra M, Bhadra U, Birchler JA (1997) Cosuppression in Drosophila: gene silencing of Alcohol dehydrogenase by white-Adh transgenes is Polycomb dependent. *Cell* **90**(3): 479-90

Pal-Bhadra M, Bhadra U, Birchler JA (2002) RNAi related mechanisms affect both transcriptional and posttranscriptional transgene silencing in Drosophila. *Molecular cell* **9**(2): 315-27

Palmer TD, Thompson AR, Miller AD (1989) Production of human factor IX in animals by genetically modified skin fibroblasts: potential therapy for hemophilia B. *Blood* **73**(2): 438-45

Pang JJ, Dai XF, Boye SE, Barone I, Boye SL, Mao S, Everhart D, Dinculescu A, Liu L, Umino Y, Lei B, Chang B, Barlow R, Strettoi E, Hauswirth WW (2011) Long-term Retinal Function and Structure Rescue Using Capsid Mutant AAV8 Vector in the rd10 Mouse, a Model of Recessive Retinitis Pigmentosa. *Molecular Therapy* **19**(2): 234-242

Penaud-Budloo M, Le Guiner C, Nowrouzi A, Toromanoff A, Cherel Y, Chenuaud P, Schmidt M, von Kalle C, Rolling F, Moullier P, Snyder RO (2008) Adeno-associated virus vector genomes persist as episomal chromatin in primate muscle. *Journal of virology* **82**(16): 7875-85

Petrus-Silva H, Dinculescu A, Li Q, Min SH, Chiodo V, Pang JJ, Zhong L, Zolotukhin S, Srivastava A, Lewin AS, Hauswirth WW (2009) High-efficiency transduction of the mouse retina by tyrosine-mutant AAV serotype vectors. *Molecular therapy : the journal of the American Society of Gene Therapy* **17**(3): 463-71

Phiel CJ, Zhang F, Huang EY, Guenther MG, Lazar MA, Klein PS (2001) Histone deacetylase is a direct target of valproic acid, a potent anticonvulsant, mood stabilizer, and teratogen. *The Journal of biological chemistry* **276**(39): 36734-41

Piechaczek C, Fetzter C, Baiker A, Bode J, Lipps HJ (1999) A vector based on the SV40 origin of replication and chromosomal S/MARs replicates episomally in CHO cells. *Nucleic acids research* **27**(2): 426-8

Pien GC, Basner-Tschakarjan E, Hui DJ, Mentlik AN, Finn JD, Hasbrouck NC, Zhou S, Murphy SL, Maus MV, Mingozi F, Orange JS, High KA (2009) Capsid antigen presentation flags human hepatocytes for destruction after transduction by adeno-associated viral vectors. *The Journal of clinical investigation* **119**(6): 1688-95

Qing K, Mah C, Hansen J, Zhou S, Dwarki V, Srivastava A (1999) Human fibroblast growth factor receptor 1 is a co-receptor for infection by adeno-associated virus 2. *Nature medicine* **5**(1): 71-7

Rabinowitz JE, Bowles DE, Faust SM, Ledford JG, Cunningham SE, Samulski RJ (2004) Cross-dressing the virion: the transcapsidation of adeno-associated virus serotypes functionally defines subgroups. *Journal of virology* **78**(9): 4421-32

Rabinowitz JE, Rolling F, Li C, Conrath H, Xiao W, Xiao X, Samulski RJ (2002) Cross-packaging of a single adeno-associated virus (AAV) type 2 vector genome into multiple AAV serotypes enables transduction with broad specificity. *Journal of virology* **76**(2): 791-801

Ramezani A, Hawley TS, Hawley RG (2003) Performance- and safety-enhanced lentiviral vectors containing the human interferon-beta scaffold attachment region and the chicken beta-globin insulator. *Blood* **101**(12): 4717-4724

Rose JA, Maizel JV, Jr., Inman JK, Shatkin AJ (1971) Structural proteins of adenovirus-associated viruses. *Journal of virology* **8**(5): 766-70

Rutledge EA, Halbert CL, Russell DW (1998) Infectious clones and vectors derived from adeno-associated virus (AAV) serotypes other than AAV type 2. *Journal of virology* **72**(1): 309-19

Rutledge EA, Russell DW (1997) Adeno-associated virus vector integration junctions. *Journal of virology* **71**(11): 8429-36

Schaarschmidt D, Baltin J, Stehle IM, Lipps HJ, Knippers R (2004) An episomal mammalian replicon: sequence-independent binding of the origin recognition complex. *Embo J* **23**(1): 191-201

Schnepp BC, Clark KR, Klemanski DL, Pacak CA, Johnson PR (2003) Genetic fate of recombinant adeno-associated virus vector genomes in muscle. *Journal of virology* **77**(6): 3495-504

Schnepp BC, Jensen RL, Chen CL, Johnson PR, Clark KR (2005) Characterization of adeno-associated virus genomes isolated from human tissues. *Journal of virology* **79**(23): 14793-803

Schubeler D, Mielke C, Maass K, Bode J (1996) Scaffold/matrix-attached regions act upon transcription in a context-dependent manner. *Biochemistry-Us* **35**(34): 11160-11169

Schuettrumpf J, Herzog RW, Schlachterman A, Kaufhold A, Stafford DW, Arruda VR (2005) Factor IX variants improve gene therapy efficacy for hemophilia B. *Blood* **105**(6): 2316-23

Selker EU (1999) Gene silencing: Repeats that count. *Cell* **97**(2): 157-160

Senapathy P, Carter BJ (1984) Molecular cloning of adeno-associated virus variant genomes and generation of infectious virus by recombination in mammalian cells. *The Journal of biological chemistry* **259**(7): 4661-6

Sharp PA (2001) RNA interference--2001. *Genes & development* **15**(5): 485-90

Shaw JE, Levinger LF, Carter CW, Jr. (1979) Nucleosomal structure of Epstein-Barr virus DNA in transformed cell lines. *Journal of virology* **29**(2): 657-65

Shen S, Bryant KD, Brown SM, Randell SH, Asokan A (2011) Terminal N-linked galactose is the primary receptor for adeno-associated virus 9. *The Journal of biological chemistry* **286**(15): 13532-40

Sikkel MB, Hayward C, MacLeod KT, Harding SE, Lyon AR (2014) SERCA2a gene therapy in heart failure: an anti-arrhythmic positive inotrope. *British journal of pharmacology* **171**(1): 38-54

Smith LM, Shortreed MR, Olivier M (2011) To understand the whole, you must know the parts: unraveling the roles of protein-DNA interactions in genome regulation. *The Analyst* **136**(15): 3060-5

Smith RH (2008) Adeno-associated virus integration: virus versus vector. *Gene therapy* **15**(11): 817-22

Stedman H, Wilson JM, Finke R, Kleckner AL, Mendell J (2000) Phase I clinical trial utilizing gene therapy for limb girdle muscular dystrophy: alpha-, beta-, gamma-, or delta-sarcoglycan gene delivered with intramuscular instillations of adeno-associated vectors. *Human gene therapy* **11**(5): 777-90

Stedman W, Kang H, Lin S, Kissil JL, Bartolomei MS, Lieberman PM (2008) Cohesins localize with CTCF at the KSHV latency control region and at cellular c-myc and H19/Igf2 insulators. *Embo J* **27**(4): 654-66

Stormo GD (2000) DNA binding sites: representation and discovery. *Bioinformatics* **16**(1): 16-23

Stroes ES, Nierman MC, Meulenberg JJ, Franssen R, Twisk J, Henny CP, Maas MM, Zwinderman AH, Ross C, Aronica E, High KA, Levi MM, Hayden MR, Kastelein JJ, Kuivenhoven JA (2008) Intramuscular administration of AAV1-lipoprotein lipase S447X lowers triglycerides in lipoprotein lipase-deficient patients. *Arteriosclerosis, thrombosis, and vascular biology* **28**(12): 2303-4

Summerford C, Bartlett JS, Samulski RJ (1999) AlphaVbeta5 integrin: a co-receptor for adeno-associated virus type 2 infection. *Nature medicine* **5**(1): 78-82

Summerford C, Samulski RJ (1998) Membrane-associated heparan sulfate proteoglycan is a receptor for adeno-associated virus type 2 virions. *Journal of virology* **72**(2): 1438-45

Sun L, Li J, Xiao X (2000) Overcoming adeno-associated virus vector size limitation through viral DNA heterodimerization. *Nature medicine* **6**(5): 599-602

Sykes RC, Lin D, Hwang SJ, Framson PE, Chinault AC (1988) Yeast ARS function and nuclear matrix association coincide in a short sequence from the human HPRT locus. *Molecular & general genetics : MGG* **212**(2): 301-9

Takeda S, Takahashi M, Mizukami H, Kobayashi E, Takeuchi K, Hakamata Y, Kaneko T, Yamamoto H, Ito C, Ozawa K, Ishibashi K, Matsuzaki T, Takata K, Asano Y, Kusano E (2004) Successful gene transfer using adeno-associated virus vectors into the kidney: comparison among adeno-associated virus serotype 1-5 vectors in vitro and in vivo. *Nephron Experimental nephrology* **96**(4): e119-26

Taymans JM, Vandenberghe LH, Haute CV, Thiry I, Deroose CM, Mortelmans L, Wilson JM, Debyser Z, Baekelandt V (2007) Comparative analysis of adeno-associated viral vector serotypes 1, 2, 5, 7, and 8 in mouse brain. *Human gene therapy* **18**(3): 195-206

van der Krol AR, Mur LA, Beld M, Mol JN, Stuitje AR (1990) Flavonoid genes in petunia: addition of a limited number of gene copies may lead to a suppression of gene expression. *The Plant cell* **2**(4): 291-9

Vandenberghe LH, Wang L, Somanathan S, Zhi Y, Figueredo J, Calcedo R, Sanmiguel J, Desai RA, Chen CS, Johnston J, Grant RL, Gao G, Wilson JM (2006) Heparin binding directs activation of T cells against adeno-associated virus serotype 2 capsid. *Nature medicine* **12**(8): 967-71

Vandendriessche T, Thorrez L, Acosta-Sanchez A, Petrus I, Wang L, Ma L, L DEW, Iwasaki Y, Gillijns V, Wilson JM, Collen D, Chuah MK (2007) Efficacy and safety of adeno-associated viral vectors based on serotype 8 and 9 vs. lentiviral vectors for hemophilia B gene therapy. *Journal of thrombosis and haemostasis : JTH* **5**(1): 16-24

VanderMolen KM, McCulloch W, Pearce CJ, Oberlies NH (2011) Romidepsin (Istodax, NSC 630176, FR901228, FK228, depsipeptide): a natural product recently approved for cutaneous T-cell lymphoma. *The Journal of antibiotics* **64**(8): 525-31

Vizlin-Hodzic D, Runnberg R, Ryme J, Simonsson S, Simonsson T (2011) SAF-A forms a complex with BRG1 and both components are required for RNA polymerase II mediated transcription. *PloS one* **6**(12): e28049

Wang C, Wang CM, Clark KR, Sferra TJ (2003) Recombinant AAV serotype 1 transduction efficiency and tropism in the murine brain. *Gene therapy* **10**(17): 1528-34

Wang Z, Zhu T, Qiao C, Zhou L, Wang B, Zhang J, Chen C, Li J, Xiao X (2005) Adeno-associated virus serotype 8 efficiently delivers genes to muscle and heart. *Nature biotechnology* **23**(3): 321-8

Weber M, Rabinowitz J, Provost N, Conrath H, Folliot S, Briot D, Cherel Y, Chenuaud P, Samulski J, Moullier P, Rolling F (2003) Recombinant adeno-associated virus serotype 4 mediates unique and exclusive long-term transduction of retinal pigmented epithelium in rat, dog, and nonhuman primate after subretinal delivery. *Molecular therapy : the journal of the American Society of Gene Therapy* **7**(6): 774-81

Weller ML, Amornphimoltham P, Schmidt M, Wilson PA, Gutkind JS, Chiorini JA (2010) Epidermal growth factor receptor is a co-receptor for adeno-associated virus serotype 6. *Nature medicine* **16**(6): 662-4

Wolffe AP, Matzke MA (1999) Epigenetics: regulation through repression. *Science* **286**(5439): 481-6

Wreggett KA, Hill F, James PS, Hutchings A, Butcher GW, Singh PB (1994) A Mammalian Homolog of Drosophila Heterochromatin Protein-1 (Hp1) Is a Component of Constitutive Heterochromatin. *Cytogenet Cell Genet* **66**(2): 99-103

Wu CH, Chen S, Shortreed MR, Kreitinger GM, Yuan Y, Frey BL, Zhang Y, Mirza S, Cirillo LA, Olivier M, Smith LM (2011) Sequence-specific capture of protein-DNA complexes for mass spectrometric protein identification. *PloS one* **6**(10): e26217

Wu Z, Miller E, Agbandje-McKenna M, Samulski RJ (2006) Alpha2,3 and alpha2,6 N-linked sialic acids facilitate efficient binding and transduction by adeno-associated virus types 1 and 6. *Journal of virology* **80**(18): 9093-103

Wu Z, Sun J, Zhang T, Yin C, Yin F, Van Dyke T, Samulski RJ, Monahan PE (2008) Optimization of self-complementary AAV vectors for liver-directed expression results in sustained correction of hemophilia B at low vector dose. *Molecular Therapy* **16**(2): 280-289

Wu Z, Yang H, Colosi P (2010) Effect of genome size on AAV vector packaging. *Molecular therapy : the journal of the American Society of Gene Therapy* **18**(1): 80-6

Xia X (2007) The +4G site in Kozak consensus is not related to the efficiency of translation initiation. *PloS one* **2**(2): e188

Yan C, Boyd DD (2006) Histone H3 acetylation and H3 K4 methylation define distinct chromatin regions permissive for transgene expression. *Molecular and cellular biology* **26**(17): 6357-71

Yan Z, Zhang Y, Duan D, Engelhardt JF (2000) Trans-splicing vectors expand the utility of adeno-associated virus for gene therapy. *Proceedings of the National Academy of Sciences of the United States of America* **97**(12): 6716-21

Yan ZY, Zak R, Luxton GWG, Ritchie TC, Bantel-Schaal U, Engelhardt JF (2002) Ubiquitination of both adeno-associated virus type 2 and 5 capsid proteins affects the transduction efficiency of recombinant vectors. *Journal of virology* **76**(5): 2043-2053

Yang CC, Xiao X, Zhu X, Ansardi DC, Epstein ND, Frey MR, Matera AG, Samulski RJ (1997) Cellular recombination pathways and viral terminal repeat hairpin structures are sufficient for adeno-associated virus integration in vivo and in vitro. *Journal of virology* **71**(12): 9231-47

Yasui D, Miyano M, Cai S, Varga-Weisz P, Kohwi-Shigematsu T (2002) SATB1 targets chromatin remodelling to regulate genes over long distances. *Nature* **419**(6907): 641-5

Yla-Herttuala S (2012) Endgame: glybera finally recommended for approval as the first gene therapy drug in the European union. *Molecular therapy : the journal of the American Society of Gene Therapy* **20**(10): 1831-2

Yue Y, Shin JH, Duan D (2011) Whole body skeletal muscle transduction in neonatal dogs with AAV-9. *Methods Mol Biol* **709**: 313-29

Zincarelli C, Soltys S, Rengo G, Koch WJ, Rabinowitz JE (2010) Comparative cardiac gene delivery of adeno-associated virus serotypes 1-9 reveals that AAV6 mediates the most efficient transduction in mouse heart. *Clinical and translational science* **3**(3): 81-9